TECHNISCHE UNIVERSITÄT MÜNCHEN

Lehrstuhl für Verkehrstechnik

Data Fusion in Sporadic Connected Environments for Urban Traffic Control

Eftychios Papapanagiotou

Vollständiger Abdruck der von der Ingenieurfakultät Bau Geo Umwelt der Technischen Universität München zur Erlangung des akademischen Grades eines Doktor-Ingenieurs genehmigten Dissertation.

Vorsitzender: Prof. Dr.-Ing. Klaus Bogenberger

Prüfer der Dissertation:

1. Prof. Dr.-Ing. Fritz Busch
2. Prof. Larry Head Ph.D.
3. Prof. Dr.-Ing. Constantinos Antoniou

Die Dissertation wurde am 19.11.2020 bei der Technischen Universität München eingereicht und durch die Ingenieurfakultät Bau Geo Umwelt am 22.04.2021 angenommen.

Για τον Αλέξανδρο

Munich, June 2020

Acknowledgments

I will never forget the time working at the Chair of Traffic Engineering and Control of the Technical University of Munich under Univ.-Prof. Dr.-Ing. Fritz Busch for 4,5 years. Antonios, Nihan, Heather, Jakob, Sasan, Gabriel, Florian, Sabine and the rest of the team, thanks for all the great ideas and hilarious exchanges. This work has been supported by SWARCO AG in a collaborative research project. I would like to thank especially Laura Coconea, Gino Franco, Maurizio Pasquero and Gianni Canepari for sharing knowledge and ideas with me, with such generosity. Two colleagues that were vital for this research contribution must be separately mentioned: Dr.-Ing. Jakob Kaths and Florian Noack. Jakob, thanks for welcoming me as your brother at the chair, and for recommending me for this position – not a bad idea. Florian, thanks for working with me, day and night, to get this prototype working with real data. I hope I will work with all of you again in the future. However, it all started with my Master Thesis, under the supervision of Prof. Dr.-Ing. Andreas Poschinger. Thank you Andreas, for putting me in the path of Research & Development in adaptive traffic signal control.

This thesis is dedicated to my brilliant son Alexandros. I have finally finished the little blue book you were asking for, every weekend the last year. My wholehearted adoration goes to my wonderful wife Katerina for putting up with me. And of course, I could not have done this without the priceless support from our dedicated companions, our two dogs, Didi and Dexter. My deepest gratitude goes to my beloved parents Aggeliki and Panagiotis and to my role model, my big brother Konstantinos, for teaching me everything in life. Except football.

This year I lost my father. You were always proud of me, with or without a Dr. title, as young football captain or as part-time waiter. Thank you Dad, for everything. On the other hand, this year I might earn a new (doctoral) father. Thank you Fritz, for giving me a chance, for inspiring me and for changing my life forever. Your authenticity, passion and leadership have not only marked me as a researcher and professional, but most importantly as a father. I will do my best to inspire students, young professionals, colleagues, and my son, to pursue the things they love, with enthusiasm. Alex is already building lovely formations with his train tracks next to me as I write.

A proper dissertation must start with a quote from a Greek philosopher and a note to the reader. So, here they come: The reader is advised to note that, “it is the mark of an educated person to search for that amount of precision in each class of things, to the extent that the nature of the subject admits” (πεπαιδευομένου γάρ ἐστιν ἐπὶ τοσοῦτον τἀκριβὲς ἐπιζητεῖν καθ’ ἕκαστον γένος) [Aristotle, Nicomachean Ethics, A. 1094α24].

Eftychios Papapanagiotou

Abstract

Urban Traffic Control Systems are an essential part of Dynamic Traffic Management, and vital to the success of future Smart City concepts. Current systems rely heavily on infrastructure-based sensors, such as inductive loop detectors, to adjust signal timings. The emergence of connected vehicles, with the ability to communicate with traffic signals, opens new sensing possibilities. However, measurements from isolated connected vehicles, such as vehicle speed and positioning, are currently sporadic, and thus difficult to exploit by existing systems. In this thesis, a methodology that enables cycle-to-cycle traffic data fusion of diverse measurements is presented. Overall, this dissertation sheds light on the potential benefits from enhancing limited measurements from connected vehicles, to contribute immediately to current systems and accelerate their transition to fully connected Urban Traffic Control Systems.

To achieve that goal, a prototypical data fusion module for state estimation and prediction at signalized intersections is introduced. The developed Extended Observer is a discrete-time, variable-dimension, implementation of multiple Extended Kalman Filters. It is independent of the type of signal control and does not require infrastructure sensors. Furthermore, it allows the fusion of diverse measurements from connected vehicles, such as instant vehicle speed, vehicle positioning, average section speeds and travel times. An adaptive fusion, according to the estimated penetration rate of connected vehicles and the respective queue length at the traffic signal, is proposed. The developed algorithms are analyzed and evaluated with the help of microscopic traffic flow simulations under different low penetration rates. Moreover, the Extended Observer is validated for its real-world applicability as a Proof of Concept with a state-of-the-art Urban Traffic Control System.

The simulation results show that, in oversaturated conditions, the proposed formulation improves the measurements from connected vehicles for all penetration rates. The highest benefit is observed for the lowest penetration rates. For low penetration rates (2-20%), isolated connected vehicles show their largest errors and therefore the potential for improvements in queue length estimation through fusion is the highest (16-30%). The fusion with aggregated section data from connected vehicles, such as section speeds and travel times improves the estimation even further. This leads to respective reduction of average vehicle delays (23-34%) and number of stops (19-45%), in comparison to signal control based solely on measurements from isolated connected vehicles. The impact of the enhanced fusion on the traffic flow starts from very low penetration rates, by recognizing oversaturation. The Extended Observer facilitates faster clearing of queues, in comparison to infrastructure-based detection.

The results of this thesis indicate that data fusion techniques capture long queues consistently, even in low penetration rates. The regular correction of the traffic state estimation, at the beginning of every signal cycle, has the potential to improve traffic signal control in oversaturation immediately, even with scarce measurements from connected vehicles.

Table of Contents

1. Introduction

As urbanization continues to grow radically, traffic congestion and its several negative impacts remain one of the biggest challenges for cities all over the world. Intelligent Transportation Systems (ITS) help cities become more efficient, safer and environmentally friendly by applying various Information and Communication Technologies (ICT) [EUROPEAN COMMISSION, 2019B]. The latest developments in ICT, in terms of computational and communication capabilities (e.g. Big Data, Artificial Intelligence, Internet of Things and 5G), present new opportunities to build a smarter transportation network and therefore set the foundation for the Smart City of the future.

This thesis aims to contribute towards smarter infrastructure in traffic signal control and thus towards the vision of Smart City. Section 1.1 draws the general setting of the dissertation with some key statements and facts. The motivation of this work is presented in section 1.2. In section 1.3, the main goal and the research questions are stated. A brief description of the research approach is given in section 1.4, based on the typical control loop for signalized intersections (Figure 1.1). The structure of the thesis along with the main objectives of each chapter are described in section 1.5 (Figure 1.2).

1.1 Urban Environments

Urbanisation and Congestion

Urbanization is an unquestionable megatrend that affects the sustainability of cities worldwide. It refers both to the growth in the number of urban dwellers and the size of the cities and affects therefore greatly the urban mobility. The percentage of people living in areas globally was 55% in 2018 and is expected to reach 68% by 2050 with almost 90% of this growth in Asia and Africa. In Europe, the proportion of urban population will rise from 74.5% in 2018 to more than 80% in 2050. In North America, this percentage is projected to exceed 85% in 2050 from 80.7% in 2018 [UNITED NATIONS, 2019].

Congestion is likewise an undisputable global phenomenon. The INRIX 2018 Global Traffic Scoreboard [2019] lists the most congested cities in the world and the estimated associated costs per city and per citizen. Boston ranks first as the most congested city in the U.S. with 164 total number of hours lost in congestion during peak hours in 2018. The estimated cost of this congestion for the city is 4.1B$ and 2,291$ per driver. In London, which ranks third in Europe, the number of hours lost reached 227 with total cost for the city of 4.9B£ and 1,680£ per driver. In Munich, that ranks third in Germany, drivers experienced 140 lost hours in congestion. The total cost for the city was estimated to 618.5M€.

Dynamic Traffic Management and Urban Traffic Control Systems

Traffic Management aims to balance transport supply and traffic demand according to the city's goals and objectives with appropriate sets of measures at an operational, tactical and strategic level [FGSV, 2003; FGSV, 2011]. Dynamic Traffic Management (DTM) performs the tasks of traffic management in real-time based on all currently available information from sensors. Typically, traffic flow models are an essential part of these systems and facilitate traffic data fusion. Traffic state estimation and prediction precedes the optimization based on the goals of the objective function [LINT & DJUKIC, 2012]. The term Adaptive Traffic Management Systems (ATMS) refers to systems that apply the concept of DTM.

Adaptive Traffic Control Systems (ATCS) or Urban Traffic Control Systems (UTCS), adjust signal timings of traffic lights in real-time, based on current traffic conditions, traffic demand and system capacity [STEVANOVIC, 2010]. UTCS, as an essential part of ATMS, increase traffic safety and efficiency of the road network by optimizing signal timings at intersections, while at the same time aim to mitigate the environmental impacts of congestion [BUSCH & KRUSE, 2001; BRAUN ET AL., 2009].

The observed benefits from UTCS vary naturally between studies, since deployment sites and implementations are unique. Stevanovic [2010] reports, in his study "Adaptive Traffic Control Systems: Domestic and Foreign State of Practice", that 60% of operators observed a reduction in travel times after the deployment of the system, and 70% of users found that the UTCS is better than the previous traffic control. Additionally, 59% of the participants in the study report that the UTCS reduced the extent of the oversaturation period. Interestingly, only 3% state that the UTCS eliminated oversaturation completely. This shows that UTCS can only be one part of a holistic solution for smart urban mobility.

Cities and traffic operators invest in UTCS to deal with the increasing congestion in urban areas during peak hours. According to the Standing Committee on Traffic Signal Systems of the Transportation Research Board (TRB) [2019], the number of UTCS increased from 25 in 2009 to more than 350 systems in 2019, with more than 20 brands (15 commercially available) in North America. Considering that only less than 3% (around 11,200) of all traffic signals in the U.S. are controlled by UTCS, the potential for further implementations is considered high. Of course, the interest for UTCS differs from country to county, but the increasing data availability and technological developments raise the expectations worldwide for further developments and deployments.

Smart City

The term Smart City has been widely used the last years in scientific and business studies [ALBINO ET AL., 2015]. According to RUSSO ET AL. [2014] the term was introduced firstly by GIFFINGER ET AL. [2007], where "Smart City generally refers to the search and identification of intelligent solutions which allow modern cities to enhance the quality of the services provided

to citizens". The definition of Smart City has been extended, since its first introduction, to include the latest technological trends and typically varies slightly according to the audience.

However, there is complete consensus on the significance of smart urban transport systems in Smart City concepts. For the European Commission [EUROPEAN COMMISSION, 2019A] "Smart City […] means smarter urban transport networks, upgraded water supply and waste disposal facilities and more efficient ways to light and heat buildings". IBM urges cities to focus on four high-impact areas: reduce congestion, create education services, improve public safety and healthcare [IBM GLOBAL BUSINESS SERVICES, 2010]. Intel and Juniper Research [JUNIPER RESEARCH FOR INTEL, 2017] identify mobility as one of the 4 key indices to evaluate the quality of life for citizens, together with healthcare, public safety and productivity. The report makes the benefits of smart city technologies and services measurable by estimating the "time given back" to the citizens. The potential of ITS (including advanced UTCS) is estimated to 19.4 hours per year per citizen and the overall potential of Smart Mobility projects is estimated to 59.5 hours.

1.2 Motivation

UTCS help cities deal with their persistent congestion problems and contribute to smarter infrastructure along the path towards Smart Cities with the real-time sensor and signal data. The potential of the emerging technologies seems enormous for further development of these systems. This potential is however currently neutralized by the rigidness of legacy UTCS that are mainly built to rely on one type of sensor or data source (e.g. inductive loop detectors or cameras).

Emerging Technologies

The radical advancements in sensing, communication, and processing technologies, in combination with the hype on Smart Cities, has opened the traffic signal control sector to new players without the traditional traffic engineering background. Traffic signal control can be viewed as an ideal business case for many of these new technologies. Consequently, the terminology and technology around UTCS has grown accordingly. For example, edge computing can improve the local processing capabilities and relocate the intelligence from a central system to the field sensors. At the same time, Big Data (BD) enables the central processing of high volume and various data sets, while generating value in high velocity. Machine Learning (ML), as subset of Artificial Intelligence (AI), opens new horizons in pattern recognition that can boost image, video and data processing for monitoring and control. The convergence of these technologies will lead to the realization of the Internet of Things (IoT) at signalized intersections. This will result into a completely new data set for UTCS, with potentially contradicting measurements.

The transition to next generation traffic control systems is expected to bring together Connected Vehicles (CV) and Automated Vehicles (AV) and lead eventually to signal-free

intersections through infrastructure adaption [LIU, 2016]. But before the realization of a fully IoT-based UTCS, there is a need for extension of the current signal control systems. More specifically, the emergence of vehicle connectivity and automation is expected to revolutionize the future motorway and urban traffic systems. Connected and Automated Vehicles (CAV) become potentially new data sources that can deliver new measurements of high quality, such as individual speeds, accelerations, gaps between vehicles and their interaction with the surrounding environment. At the same time, these vehicles become potentially also new actuators considering the possibility to inform or even control the speed of individual vehicles [KATHS, 2017]. The communication between vehicles and infrastructure can be divided in two main categories: short-range communication based on Wireless Local Area Network (WLAN) and long-range communication based on mobile telecommunication. For the short-range communication, the installation of a roadside unit (RSU) is required to establish the connection between CV and Traffic Light Controller (TLC) and consequently between CV and the Traffic Light (TL) (Figure 1.1).

Without underestimating the power and momentum of these technologies, their application on UTCS has been until now limited and fragmented. The high software and hardware costs prevent cities from investing to completely new systems. Furthermore, these technologies typically do not offer the level of transparency that is expected in traffic signal control. Cities look for ways to make their legacy UTCS smarter, but there is currently limited understanding of the benefits and accuracy with current data availability.

Transition Phase

In contrast to the radical ICT developments, UTCS are systems with extremely longer life cycles. Each UTCS typically relies on specific infrastructure sensors, detection layouts (e.g. inductive loop detectors) and algorithms [STEVANOVIC, 2010]. This lack of flexibility makes the integration of UTCS in an ecosystem of a Smart City particularly challenging. Moreover, traffic operators search for alternative ways to obtain real-time measurements, to replace loop detectors and reduce the associated installation, operational and maintenance costs. The installation costs of an UTCS ranges approximately between 20,000$ and 60,000$ per intersection [STEVANOVIC, 2010]. Additionally, the average RSU equipment and installation cost per site, in order to facilitate short-range communication between CV and infrastructure, is estimated from the Federal Highway Administration of the U.S. Department of Transportation to be around 17,600$ [WRIGHT ET AL., 2014].

Besides, as the number of CV on the streets increases day by day, new players already emerge as possible traffic data providers for UTCS. For example, fleet operators find themselves owning historical and real-time Probe Vehicle Data (PVD) for many urban routes. Similarly, companies originally specialized in digital maps and route recommendations, own historical databases and real-time travel time information for large parts of the urban road network, through partnerships with the mobile and automobile industry. In many cases, this

traffic dataset can be used from third parties through an Application Programming Interface (API) to develop new services [NOACK ET AL., 2019].

Therefore, before reaching complete connectivity and automation at signalized intersections, a transition phase is expected where current UTCS should demonstrate benefits from the emerging connectivity. On one hand, methods that allow the integration of limited number of CV in current systems are needed. On the other hand, these new methods should be able to work with other potential sources as input. This twofold challenge motivates this thesis.

1.3 Goal and Research Questions

The role of UTCS as vital part of a Smart City ecosystem is expected to be boosted by the emergence of new technologies. The ability of UTCS to utilize new input data is considered of vital importance for their further evolution. The following sentence epitomizes the overarching goal of the thesis:

> *Goal of the thesis is, to analyze the potential of the combination of new data sources and emerging technologies, in current urban environments, for traffic signal control.*

To reach that goal, this thesis needs to answer the following main research questions:

> *How to utilize diverse measurements from different types of sensors with a practical and adaptive formulation?*
>
> *What is the accuracy of the enhanced traffic state estimation, and what is the possible benefit for Urban Traffic Control Systems?*

1.4 Research Approach

To reach the above stated goal and answer the research questions, the influence of the emerging connectivity on the typical control loop for Urban Traffic Control (UTC) is examined. Figure 1.1 shows how the typical control loop [PAPAGEORGIOU, 1998A] changes in the examined transition phase, where emerging technologies will have to work together with legacy systems. In the traditional UTC loop, inductive loop detectors are used as data sources. Typical traffic measurements consist of vehicle presence, vehicle counts, detector occupancies and time gaps between detector activations. In the future, traffic measurements are expected to come from Connected Environments, with varying availability and accuracy. The traffic disturbances (e.g. accidents, weather conditions) in the control loop can be measured but cannot be controlled. Their measurements are also expected to be enriched with the inclusion of new data in the UTC loop. The data fusion module allows for traffic state estimation and prediction at the signalized intersections, based on the new measurements. The signal control decides on the optimal signal timings, based on the policy goals, and communicates the control actions to the traffic light, through the TLC.

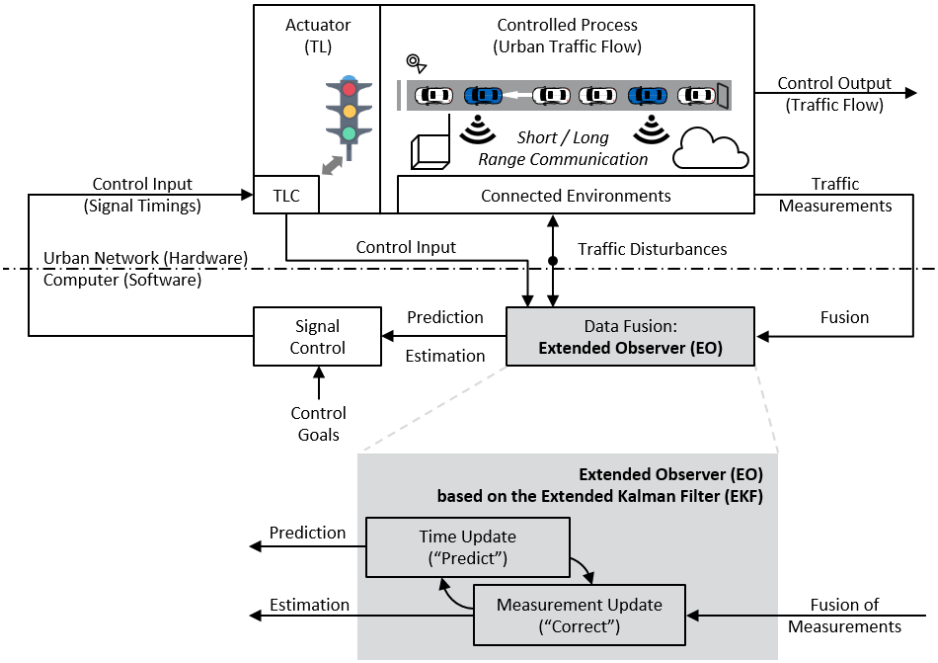

Figure 1.1 Connected Environments and the Extended Observer in the Urban Traffic Control loop

The development of new control and optimization algorithms is not in the scope of this thesis. However, the potential benefits from the enhanced estimation and prediction are examined by feeding two different control approaches: an example of rule-based intersection control and an example of model-based intersection control.

To examine and capitalize on the new data sources for adaptive traffic control, research approaches that consider dissimilar, contradictory, and faulty measurements from both infrastructure and mobile sensors, are necessary. In this thesis, a data fusion module that is called Extended Observer (EO) is proposed. The Extended Observer is the main development of this thesis. The typical UTC loop, as shown in Figure 1.1, is used as the basis for the technical and functional architecture. The algorithms of the well-established Extended Kalman Filter (EKF) are used as the foundation for the mathematical formulation. Traffic parameters that are considered essential in traffic signal control are estimated, such as queue length, departure rate, arrival rate, turning rates, and penetration rate.

1.5 Thesis Structure

Chapter 1 started by briefly presenting the urban congestion problems and the potential of UTCS, as part of the solution in a Smart City ecosystem. Then, the motivation to accelerate the anticipated transition phase, where emerging technologies must be integrated with legacy systems, is stated. The goal of analyzing the potential of the new data availability and connectivity, led to the selected research approach, as shown schematically in Figure 1.1. It shows how the main development of the thesis, a data fusion module that is called Extended Observer, fits in the UTC loop. Figure 1.2 gives an overview of the thesis structure, with the main objectives of each chapter.

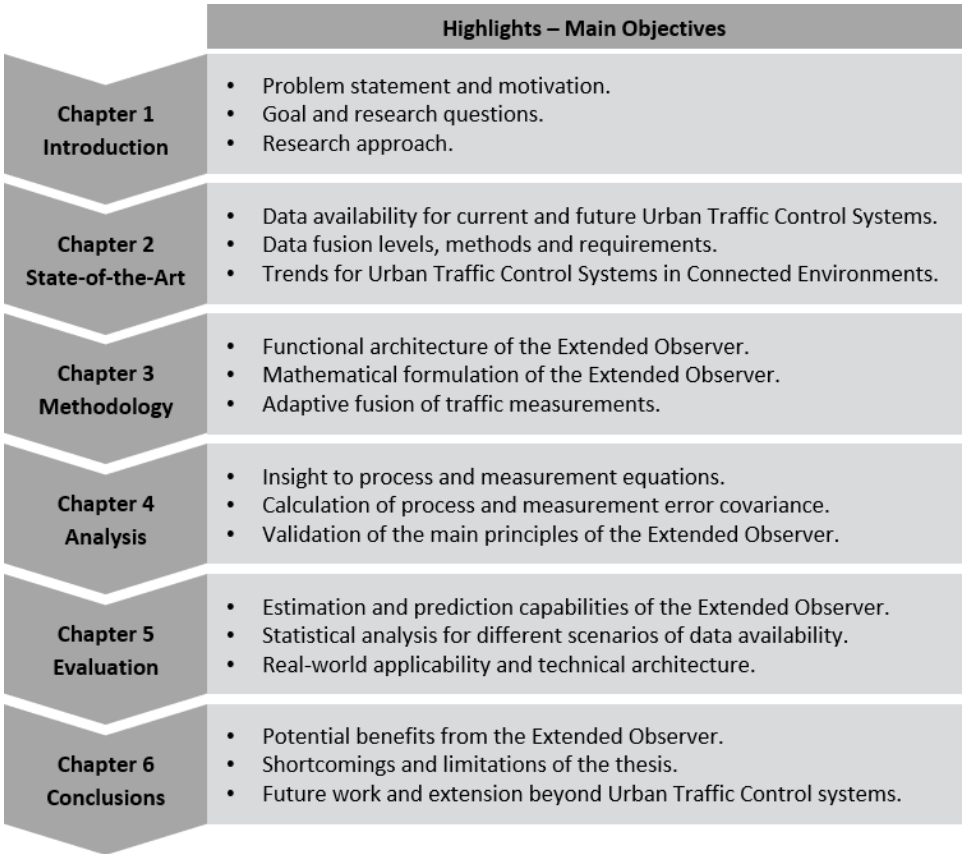

Figure 1.2 Thesis structure and main objectives of each chapter

Chapter 2 contains the state-of-the-art and the literature review, regarding Connected Environments, the respective traffic measurements, and data fusion methods. This chapter aims to highlight the different data availability possibilities, the research trends, and the emerging technologies for current and future UTCS. In chapter 3, the mathematical formulation of the Extended Observer is presented in detail, on a cycle-to-cycle basis for UTCS. The predictor-corrector type of filtering, based on the EKF, is presented. Traffic measurement equations for different types of data sources are exemplified. This chapter concludes by highlighting the adaptive fusion capabilities of the proposed methodology. Chapter 4 showcases the working principles of the developed algorithms. The analysis is done, based on microscopic simulations of a test intersection, with different signal control methods. The complete statistical evaluation of various scenarios is presented in chapter 5. In addition to the test intersection, the microscopic simulation of a real-world intersection aims to evaluate the algorithms in conditions closer to reality. Moreover, the prototypical developments are validated in the case of the UTCS Spot/Utopia. Chapter 6 summarizes the main contributions and limitations of the presented methodology and closes with the outlook of the thesis.

2. State-of-the-Art

ITS aim to utilize ICT to balance the demand and supply of the traffic network. UTCS is one of the most effective, prominent, and complex ITS applications. With the rapid increase of data diversity, complexity, and connectivity, the UTCS have a wide range of new data input possibilities at their disposal. In this thesis, the term Connected Environments is used to describe all the various connected sensors that are possibly available to UTCS.

Section 2.1 presents the most typical and the newest data sources that can be utilized in traffic signal control. Section 2.2 gives an overview of the data fusion methodologies in relation to UTCS. In section 2.3, the gap between research and practice in signal control is highlighted.

2.1 Connected Environments

As shown in Figure 1.1, Connected Environments can give traffic measurements and traffic disturbances. Both can be sensed (measured) but in terms of traffic control, they are fundamentally different. Traffic measurements give the output of the controlled process and therefore are directly affected from any change in the control. On the other hand, traffic disturbances are external factors that influence traffic flow but cannot be controlled by the traffic signals.

Figure 2.1 shows the range of sensors for traffic measurements and disturbances for traffic signal control, with the emerging sensing and communication technologies. This is a functional mapping of the data sources from the signal control perspective. It does not aim to provide an exhaustive list of all possibilities. The purpose is to give an overview of the types of sensors, that can provide certain type of data in the case of signal control. In Figure 2.1, the complexity of the algorithms for data fusion, increases generally from lower blocks to the upper ones per column. This is a qualitative assessment for a general overview. The complexity of each algorithm varies between implementations and use cases.

In the following, it is described, how mobile sensors are scarcely used in UTCS due to low penetration rates. They are considered key for accelerating the transition phase for UTCS from infrastructure sensors to mobile sensors. Algorithms are presented for Connected Sections, Connected Vehicles and Aggregated Section data in chapter 3, since they are considered crucial for the examined transition phase of UTCS.

Infrastructure sensors

Typically, infrastructure sensors are divided in intrusive and non-intrusive sensors, according to their placement in relation to the pavement (on the ground or over-head) [KLEIN, 2018]. In Figure 2.1, the infrastructure sensors are divided in point, point-to-point and area sensors that cover a complete section of the signalized approach.

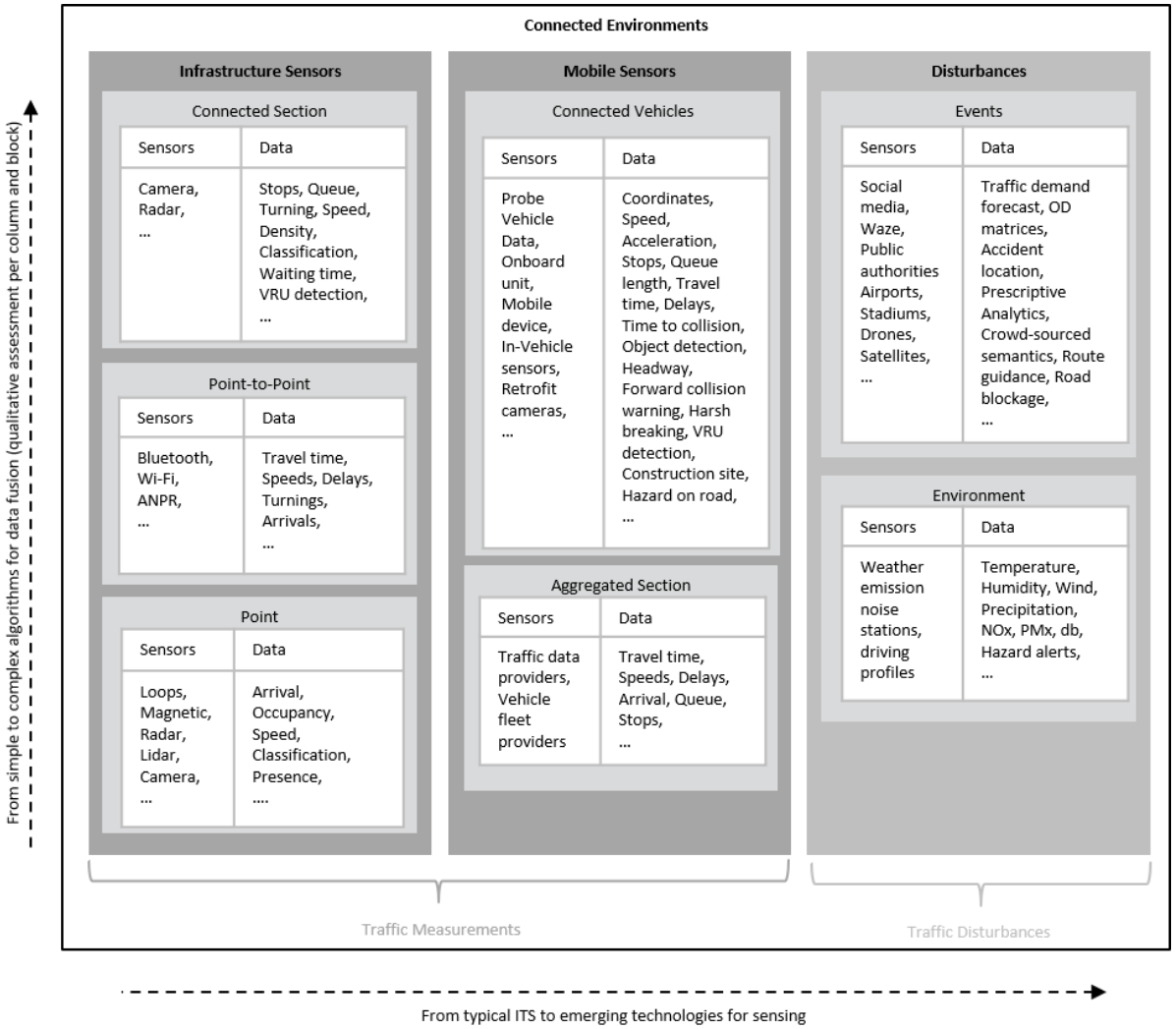

Figure 2.1 Data sources for Urban Traffic Control Systems

Some typical sensors used in UTCS are inductive loop detectors, magnetic sensors, cameras, microwave radar sensors, infrared sensors and lidar sensors. Overall, they can provide many data types with high accuracy such as counting, presence, classification, time gap, occupancy, density, arrival rate, turning rate, departure rate, queue length, number of stops, travel time and speed. Video Detection Systems (VDS) with the latest image processing technologies (e.g. see [SWARM ANALYTICS, 2020]), can be used for tracking vehicle trajectories and thus for enhanced data extraction. Point-to-point sensors on routes or sections allow the extraction of traffic information, such as travel times, delays, Origin-Destination (OD) matrices, turning rates etc. For example, Bluetooth readers and Automatic Number Plate Recognition (ANPR) cameras can be used for capturing travel time, and extract also average speed, and delay. A very detailed description of all types of ITS sensors can be found in the work of Klein [FHWA, 2006; KLEIN, 2018].

Mobile Sensors

The second part of the traffic measurements in the new era of connectivity consists of the mobile sensors. In Figure 2.1, they are divided in Connected Vehicles and Aggregated Section data. The former is used to describe measurements from individual CV and the latter to describe measurements from aggregated Floating Car Data (FCD). Theoretically, the sensors that provide this data are the same, namely ego vehicle data, in-vehicle sensors or retrofit sensors. However, the hands-on data analysis from traffic data and fleet providers shows that the format, data type and accuracy are quite different, due to low penetration rates, data privacy, data ownership. Moreover, they are fundamentally different in terms of resolution and coverage.

i) Connected Vehicles

The emerging Connected Vehicles environment promises transformation of mobility through wireless communication among vehicles and infrastructure [KLEIN, 2018]. In this thesis, the focus lies on the potential benefit for legacy UTCS systems from limited number of CV. The term CV is used in this thesis to describe vehicles that can send information to the UTCS in real-time (1-3 seconds) through Vehicle-to-Infrastructure (V2I) communication. This is a non-safety-critical application and therefore the technology and latency are not considered crucial. The transmission can be either from an onboard unit or from a mobile device. The communication can be either through a roadside unit or through the cellular network. Two main functionalities are vital for processing such geo-referenced data: the communication and the map matching.

The following standardized messages enable the integration of geo-location data from CV to the UTCS: the Basic Safety Message (BSM), the Cooperative Awareness Message (CAM) [ETSI, 2009A] and the Decentralized Environmental Message (DENM) [ETSI, 2009B]. BSM and CAM are the standards for continuous information through V2I for US and EU respectively. The second international Harmonization Task Group (HTG2) had the task to harmonize the two messages and allow sufficient cross-compatibility [FISCHER, 2015]. BAM and CAM are broadcasted continuously (multiple times per sec), as opposed to the DENM that is broadcasted only in case of an event (warning).

The Signal Phase And Timing (SPAT) and the MAP provide data towards the vehicle [ISO, 2017]. The SPAT message contains the (predicted) signal status, while the MAP provides detailed information about the intersection topology [MIUCIC, 2018]. The two messages are typically referred to as one service (SPAT/MAP) coming from intelligent Traffic Light Controllers.

The possible data available from individual CV, contain theoretically all the attributes from the ego vehicle and its surrounding in-range environment. Figure 2.1 indicates some of the possible data that can be extracted. In addition to all the conventional ego vehicle information (e.g. coordinates, speed, acceleration), the latest image processing advancements allow

moving vehicles to extract information from the surrounding environment, such as headways, time to collision, and Vulnerable Road Users (VRU) detection (e.g. see [MOBILEYE, 2020]). This kind of technology is certainly the forerunner of CAV integration in UTCS.

ii) Aggregated Section

In contrast to raw CV data, aggregated FCD are updated in longer intervals (30-60 seconds) and refer to sections (link-based or lane-based) of certain length ranging from 50 to 1000m. The currently available real-time traffic data providers differ in data format, location referencing methods, road coverage, accuracy, data collection and fusion methods. Accuracy varies not only between providers, but also between intersections within the same provider [NOACK, 2018; NOACK ET AL., 2019]. Like the raw CV, the two aspects that must be tackled are the communication and the map matching.

Most of the traffic data providers offer Representational State Transfer (REST) Application Programing Interfaces (API) for getting the traffic data. They are typically updated every minute, even though the values might remain unchanged for longer intervals where no vehicle information is available, depending on each proprietary underlying algorithm (that is not published). Typical data formats for the response are: Extensible Markup Language (.xml), JavaScript Object Notation (.json) and Protocol Buffers (.proto). The protocol buffers are a fast and efficient method developed by google for serializing structured data [GOOGLE DEVELOPERS, 2020].

Regarding the location referencing, even though Traffic Message Channel (TMC) is supported typically from all vendors, more detailed map location methods are needed. OpenLR is a method for map agnostic dynamic location referencing and enables systems with dissimilar maps to communicate independent of the channel, with minimum bandwidth. It was designed for information exchange between Traffic Management Centers and in-vehicle devices [TOMTOM INTERNATIONAL B.V., 2012]. Another emerging format for representing features and their spatial extent is GeoJSON [IETF, 2016]. Many traffic data providers, offer their data in GeoJSON format.

The basis for all traffic data provided is the travel time. Based on this, the free flow travel time, the free flow speed, the average current speed etc. are calculated. In some cases, even queue length, traffic flow (arrival) and stops are provided. In other cases, an estimation of the accuracy of these measurements is delivered from the traffic data providers. Furthermore, there is rarely an indication of the penetration rate (or number of probes) used for these measurements. Generally, it can be observed in the datasets that historical values are used when no probe vehicle is providing real-time information.

Usually, there are two approaches followed by the traffic data providers [JOHNSTON, 2017]: Publishing data after a certain number of probe vehicles available (e.g. >3) or publishing data even for lower number of vehicles. Even though the first approach is reasonable for consumer Cooperative ITS (C-ITS) applications, the second approach increases the spatial coverage.

Combined with transparent information of probe vehicle numbers, the second approach should be preferred for traffic management purposes.

Disturbances

Traffic disturbances influence greatly the urban traffic flow but are not controlled by the traffic signals. In Figure 2.1, two main sensor/data categories for disturbances are identified: data concerning events and the environment. They affect both traffic supply and traffic demand in the urban networks. Ideally, they must be included in the data fusion for UTCS but in practice, their inclusion in overarching ATMS is a priority. The state-of-the-art report for mobility platforms and ecosystems [PROJECT CONSORTIUM TUM LIVING LAB CONNECTED MOBILITY, 2016] underlines the importance of eco-sensitive traffic management [CELIKKAYA ET AL., 2016] and traffic management for major events [AMINI ET AL., 2016], as two of the four use cases examined. New low cost environmental sensors are lately gaining attention in the research and market community [BARTONOVA ET AL., 2019; CELIKKAYA ET AL., 2019]. Textual data extraction techniques [KINRA ET AL., 2019] and model-based Machine Learning approaches [PELED ET AL., 2019] start to enter the transportation field. Traffic disturbances are mainly exploited in UTCS in the form of reports (e.g. weather, roadworks) and predefined strategic plans (e.g. planned events) and are therefore not in the scope of this thesis.

2.2 Data Fusion

Data fusion has been a fundamental element of many applications for more than two decades. Nevertheless, it is still an emerging field in daily DTM operations [FAOUZI & KLEIN, 2016]. Data fusion is also a core function of the UTC control loop, as shown in Figure 1.1. Depending on the application and the exact input, the terms *data fusion* and *sensor fusion* are used in the literature for ITS [KLEIN, 2018]. Their difference lies on the level where the fusion takes place. At the device level, the term sensor fusion is used (e.g. vehicle classification, image processing, object tracking). At the central level, the term data fusion is more appropriate (e.g. Automatic Incident Detection, traffic flow prediction, decision support tools). This central fusion can be in a sub-center integrated in an overarching central traffic management system. Data fusion modules can be combined together, depending on the chosen ITS system architecture [VELOSO ET AL., 2009].

2.2.1 Data Fusion Levels

Fusion is always the means to an end, and not the end application. However, every ITS application needs almost certainly some level of data fusion. In DTM, fusion can support decision making for improved efficiency, safety, and sustainability of the transportation system through ITS applications at strategic, tactical, and operational level. The variety of definitions for data fusion stems naturally from the variety of applications that rely on it. One of the most highly cited definitions [KLEIN, 2018; UNIVERSITÄT BONN, 2020] is given by the Joint Directors

of Laboratories (JDL) from the U.S. Department of Defense. Data fusion is defined as: “a multilevel, multifaceted process dealing with the automatic detection, association, correlation, estimation, and combination of data and information from single and multiple sources to achieve refined position and identity estimates, and complete and timely assessments of situations and threats and their significance” [U.S. DEPARTMENT OF DEFENCE, 1991].

In [FAOUZI & KLEIN, 2016], the authors build on the six levels (Level 0 - Level 5) from the JDL to suggest the levels of data fusion in ITS. The fusion process extracts value from one or various data sources, refines the traffic situation, and gives insights about the possible causes and impacts of the observed events. The six levels are not supposed to describe a sequential process but provide a categorization of data fusion functions [KLEIN, 2018]. In Tab. 2.1, the six levels of data fusion are described for UTCS, with some input-output examples.

	Functional description	Example input	Example output
Level 0	**Pre-processing** of raw data from sensors connected to the UTCS.	It might include normalizing, formatting, batching of traffic and signal data.	Vehicle detection and classification with cameras, loop detectors or radar sensors.
Level 1	**Combination** of different data sources for refined traffic estimation in the urban network.	It might include information from infrastructure sensors, connected vehicles, public transport vehicles, emergency vehicles.	Travel time, speed estimation and short-term prediction. Queue length and traffic flow rates estimation and short-term prediction.
Level 2	**Identify the causes** for congestion at (groups of) intersections.	It might include information from construction schedules, signal configuration data, weather reports, police reports.	Identify low quality coordination of specific corridors. Recognize lane closures from construction or incidents.
Level 3	**Assess the impact** of recurring or non-recurring congestion at signals.	It might include historical database of similar events, signal data, FCD data, police reports, crowd-sourced data.	Calculate duration of congestion. Estimate delays and spillover effects.
Level 4	**Refine and evaluate** additional sources of information regarding the urban network.	It might include the assessment of all previous levels and additionally the integration of new sources.	Introduction of new data for testing and benchmarking. Cost/benefit analysis for justification of investments.
Level 5	**Enable human** interpretation and interaction with the UTCS.	It might include configurable data input and visualization techniques.	Appropriate human-machine interface for intuitive operation, such as changing weighting factors, using heatmaps and advanced plots.

Tab. 2.1 Levels of data fusion for Urban Traffic Control Systems

STEINBERG revised the JDL model and proposed a shorter definition: “Data fusion is the process of combining data or information to estimate or predict entity states” [STEINBERG & BOWMAN, 2001]. In the domain of Urban Traffic Control, this can be formulated as follows:

> *Data fusion in Urban Traffic Control is the process of combining traffic data or information to estimate and predict the traffic state at signalized intersections*.

This definition is in principle describing the Level 1 data fusion for UTCS and is in the scope of this thesis.

2.2.2 Data Fusion Requirements

The new data types from Connected Vehicles, Floating Car Data, in-vehicle sensors, Bluetooth readers, ANPR cameras, radar sensors and cameras promise to wider the short view of point sensors [FAOUZI & KLEIN, 2016]. Clearly, in such a complex environment, most of the traffic engineering challenges are a data fusion problem. KLEIN highlights the potential benefits from sensor fusion and the importance of complementing typical traffic flow sensors with additional data sources for DTM strategies. Especially for inductive loop detectors, that are predominately used for gathering point traffic flow data, two main challenges should be considered [KLEIN, 2018]:

- the high deployment and maintenance costs, especially for large scale UTCS
- the inability to capture spatial behavior of traffic flow

JOHNSTON reports the comparison of speed data from point sensors, point-to-point sensors, and GPS-tracked vehicles (in other words FCD or PVD) and shows that the there is no single ideal sensor for all traffic situations. Real data from a freeway section are collected and compared. The results indicate that the point measurements outperform all the others in no traffic and low traffic conditions. The FCD outperforms the others in heavy, jammed, and varying traffic conditions. The author suggests that each source has an inherent bias that stems from its measurement technology and the best estimate can only come from the fusion of multiple data sources of different type [JOHNSTON, 2017].

The optimal solution for the traffic management authority is to choose a combination of data sources to achieve the required accuracy and coverage with the available budget. Key factors for the selection of the data sources from the perspective of the traffic manager are [JOHNSTON, 2017]:

- Accuracy of the traffic measurements
- Spatial coverage of the traffic measurements
- Temporal coverage of the traffic measurements
- Latency of the data communication
- Quality index of the traffic measurements
- Transparency of the algorithms and technology behind the measurements

Detailed comparison of the advantages and disadvantages, in terms of traffic management operation, for different infrastructure-based sensor and emerging sensor technologies can be found in [KLEIN, 2018; JOHNSTON, 2017].

2.2.3 Data Fusion Methods

Data fusion can be utilized to create (or improve) a model of traffic parameters that describes the traffic phenomena of interest. In that sense, the state vector of the model might consist of a wide range of relevant traffic parameters, such as speeds, travel times, road surface state, weather state etc. [KLEIN, 2018]. If this model is updated in real-time, it can be the basis for dynamic traffic management and control applications [LINT & DJUKIC, 2012]. In the domain of UTCS, the underlying model for the data fusion might be an online traffic flow model. Microscopic traffic simulations have been used lately to play the role of the online traffic flow model. In that regard, they can also be used for data fusion.

Some examples for Level 1 central fusion algorithms that are used in DTM are: Fuzzy logic, Kalman Filter, Extended Kalman Filter, Kernel estimator, and Particle Filter. Data fusion algorithms originate from a variety of domains such as pattern recognition, statistical estimation, state estimation, artificial intelligence, and others [FAOUZI ET AL., 2011].

In the research community, the non-linear variations of Kalman filtering (Extended, Ensemble, Unscented) and particle filters have shown promising results in freeways, where the definition of a macroscopic traffic flow model is more convenient in comparison to urban networks. A great overview and introduction in Kalman filtering for DTM for freeways can be found in [LINT & DJUKIC, 2012].

For UTC however, the research community has put the focus on comparing new control methods based on Connected Vehicles and not so much on the fusion aspect of the UTC loop. Some examples of data fusion research approaches for UTC are: Probabilistic Methods [ROSTAMI SHAHRBABAKI ET AL., 2018], Kalman Filter [VIGOS ET AL., 2008] and Extended Kalman Filter [FRIEDRICH ET AL., 2002]. ROSTAMI utilizes input flow from single point measurements, speed, and location from connected vehicles. The output is a second-by-second estimation of queue length, vehicle accumulation and outflow [2018]. VIGOS utilizes the flow and occupancy from three loop detectors to estimate number of vehicles in the queue [2008]. FRIEDRICH utilizes MÜCK's loop-based queue length estimation [MÜCK, 2002] to estimate the average and maximum queue length [1999]. In [PAPAPANAGIOTOU & BUSCH, 2020], a data fusion method to estimate the cycle-to-cycle queue length is proposed, based on limited number of CV without any required loop detectors. The benefit from fusion of CV measurements in low penetration rates is demonstrated, as well as the benefit from fusion of CV and camera measurements. The proposed Extended Observer is presented in detail in this thesis and extended for adaptive data fusion and fusion with aggregated FCD.

FAOUZI proposes three major categories for data fusion techniques for ITS, from the traffic engineering perspective: statistical methods (e.g. weighted average), probabilistic methods (e.g. Bayesian approaches, state-space models) and artificial intelligence (e.g. genetic algorithms, neural networks) [2011]. KLEIN proposes that the Level 1 data fusion models for ITS can be generally divided in physical models (e.g. Kalman filtering), feature-based models (e.g. Bayesian inference, artificial neural networks, pattern recognition), and cognitive models

(e.g. knowledge-based expert systems, fuzzy logic) [2018]. Here the physical models refer to the modelling of the movement of an object (e.g. vehicle) and mainly to its identification, tracking and classification.

The domain of UTC is highly interconnected with many complex fields such as control theory, optimization algorithms, traffic flow models and traffic simulation. In addition, it is a very practical field that requires in many cases easy techniques and the knowledge of experts. In practice, a combination of techniques is used (e.g. weighted averages and if-then rules). The physical model in the case of signalized intersections can be formulated as state-space model, traffic flow model or simulation model (micro, meso or macro).

Each approach comes with an inherent bias. The estimation accuracy from the state-space model depends on the bias from the a priori estimation, while the accuracy from the traffic flow model is directly connected with the model assumptions. For the simulation models, the performance of the fusion relies on the online calibration of the simulation environment. The data fusion model for the UTCS can theoretically just be a feature-based model with no traffic (physical) relationship between the features (e.g. Deep Learning). The performance of the fusion lies in this case greatly on the quality of the training data.

To assist the selection of the data fusion method(s) in ITS, the following criteria are suggested [KLEIN, 2018]:

- Maximum effectiveness: maximum performance in presence of uncertainty or missing data.
- Resource efficiency: minimize computation resources
- Operational constraints: meet expectations from the operator(s) within time and budget constraints
- Operational flexibility: potential to include different needs, applications, sensor types
- Functional growth: functionalities of interfaces and algorithms must increase as system evolves

2.3 Urban Traffic Control Systems

Traffic signal control operations and guidelines are thoroughly defined all around the world due to the importance in efficiency and above all safety at urban intersections [FHWA, 2006; FHWA, 2015; FGSV, 2015]. In addition to the definitions found there, many researchers have proposed various valuable categorizations and descriptions of the existing UTCS, according to their data input and algorithmic principles. KATHS proposes a three dimension categorization based on the focus of the optimization (central or intersection), the degree of freedom of the phase sequence (free or fixed) and the logic behind the decision making (rule-based or model-based) [2017]. TISCHLER divides the UTCS in local responsive (rule-based or model-based) and network control (central, decentral or with two-level hierarchy) [2016]. LÄMMER focuses on

the optimization technique and divides the UTCS in incremental, rolling horizon approaches and two-level hierarchies [2007].

Examples of UTCS with intersection focus are: Ring-and-Barrier [FHWA, 2015], RiLSA [FGSV, 2015], LHOVRA [PETERSON ET AL., 1986], VS-PLUS [VERKEHRS-SYSTEME AG, 2020], Epics [MERTZ, 2001], Selbst-Steuerung [LÄMMER, 2007], Spot/Utopia [MAURO & TARANTO, 1989]. Spot is used as an UTCS example in this thesis for testing the proposed methodology. In combination with the area level control from Utopia offers a decentralized, model-based, rolling horizon, network control. Examples of network UTCS are: SCATS [SIMS & DOBINSON, 1980], SCOOT [ROBERTSON, 1886], RHODES [MIRCHANDANI & HEAD, 2001], MOTION [BUSCH & KRUSE, 2001], BALANCE [FRIEDRICH, 1999], ImFlow [DYNNIQ, 2020] and InSync [CHANDRA & GREGORY, 2011].

In this thesis, the term Urban Traffic Control System (UTCS) is used to simply describe systems that deal with the problem of adjusting signal timings to balance supply and demand at intersections without making any distinction between the typical classifications. Regarding data fusion for UTCS, the sensor type and the respective traffic data collected are mainly of interest. STEVANOVIC provides a detailed description of the different detection topologies and traffic data calculated for the most prominent UTCS in the world, while KLEIN focuses on the US market.

All known UTCS rely still on infrastructure-based sensors [STEVANOVIC, 2010; KLEIN, 2018] and particularly on point and area-wide sensors (see also Figure 2.1). The Inductive loop detectors are dominating the market with various topologies according to the needs of the specific system. Cameras and radars are used as point sensors increasingly in the last years. STEVANOVIC reports that 93% of the agencies that took part in his survey use loop detectors with an average of around 8-12 detectors per intersection [STEVANOVIC, 2010]. Typical traffic data measurements are vehicle counts, occupancy, speed, stops, queue length, and delays. The first two levels of data fusion, Level 0 and Level 1, are typical for all systems. They are used however mostly for measurements from individual sensors and not for multi-sensor fusion. A bright exception to the rule of point detection and absence of multi-sensor data fusion is InSync. InSync takes fully advantage of image processing and artificial intelligence advancements by using video cameras to capture the area in front of the stop-line (~75m) to derive queues and delays and optimize signal timings. Insync is the only UTCS that allows the real fusion of point detectors (inductive loops, radars) and area detectors (cameras) with a dedicated module (InSync:Fusion).

Even though existing (legacy) UTC systems were designed to utilize measurements coming mainly from point sensors, traffic operators search for alternative ways to obtain real-time measurements to avoid their high installation and maintenance costs [STEVANOVIC, 2010; KLEIN, 2018]. However, point-to-point (e.g. re-identification technology), aggregated FCD (e.g. aggregated section speeds) and raw CV (e.g. GPS probe vehicles) are mainly used for evaluation of the output of the signal control with Measures of Performance (MOP) or

Measures of Effectiveness (MOE). GPS probes have the advantage to provide link-specific data in comparison to point-to-point sensors. In addition the GPS probes have the advantage against aggregated FCD and point-to-point sensors in identifying more accurately incident locations [KLEIN, 2018]. For evaluating the traffic flow and the travel time reliability, the route and link travel time, delay, speed and number of stops can be used with GPS, tags and Bluetooth technology [FHWA, 2013].

2.3.1 Research Trends

Despite the limited practical applications of CV as new data sources for UTCS, there have been many simulation studies on the topic and several real-field demonstrations. Some common key points emerge from the existing work, such as the importance of the penetration rate in the effectiveness of the developed algorithms [ILGIN GULER ET AL., 2014; JING ET AL., 2017], the importance in estimating the position of unequipped vehicles [FENG ET AL., 2015], the significance of cycle-to-cycle queue length estimation [CHENG ET AL., 2011; PAPAPANAGIOTOU & BUSCH, 2020] and the implications from the coordination and public transport prioritization [HE ET AL., 2014; HEAD, 2016]. The benefits for traffic signal control start after the threshold of 25-40% of penetration rate and for queue length estimation above 30% [GOODALL, 2013; JING ET AL., 2017; ILGIN GULER ET AL., 2014]. For the calculation of MOP on an arterial the threshold of minimum penetration rate is typically around 10-50% [GOODALL, 2013] and can go as low as 1% [ARGOTE-CABAÑERO ET AL., 2015] for highly oversaturated conditions, where the number of available measurements increases.

Regarding queue length estimation, recent studies demonstrate the great potential of CV as new data source for improving the accuracy of established methodologies, such as shockwave theory and input-output (i.e. vehicle accumulation) models. In [CHENG ET AL., 2011], a method for cycle-to-cycle estimation is presented, which utilizes trajectory data to identify Critical Points on the time-space diagram, to reconstruct the queue dynamics based on shockwave theory. In [RAMEZANI & GEROLIMINIS, 2015], a method for cycle-to-cycle queue profile estimation is proposed based on shockwave theory and data mining of probe vehicle data. In [ROSTAMI SHAHRBABAKI ET AL., 2018], location and speed from CV are used to provide second-by-second estimations of the queue back-end with a probability-based error compensation to account for errors, especially in low penetration rates. COMERT [2013, 2016], presents analytical, cycle-to-cycle Queue Length Estimators (QLE), based on location and speed of CV, that perform very well in steady-state conditions.

Research Gap Statement

For low penetration rates and long periods of oversaturation, there might be several consequent cycles with no presence of CV that can lead to high estimation errors if no other sensor is available. Therefore, there is a need for robust data fusion methods that facilitate estimation and prediction to support UTC systems, even when no CV or other sensors are

present at the intersection, especially in varying saturation conditions and low penetration rates.

2.3.2 Industry Trends

Furthermore, the industry experts of traffic signal control see the fusion of aggregated FCD from low penetration data with inductive loop detectors as more realistic, as opposed to an abrupt change to full connectivity. Wide-range infrastructure sensors (e.g. cameras, radar), are already in use but are used mainly for conventional counting and classification measurements. Their role is expected to grow in the next future [SWARCO INTERNAL WORKSHOP, 2020].

Connected Vehicles (e.g. V2I with CAM messages) are expected to play a big role in the future UTCS independent of the communication technology. BRIGNOLO proposes a hybrid communication for C-ITS and places cooperative traffic lights in the middle of the spectrum between cellular (e.g. 4G/5G) and ad-hoc communication (e.g. ITS G5, DSRC) [2014]. However, the current very low penetration rates and limited deployments restrict their roll-out. CV data should enter the UTCS market faster in the next years with the introduction of C-ITS Day 1 and Day 1.5 services. Examples of C-ITS services that can boost the availability of CV measurements for UTCS based on V2I technology are: Traffic Jam ahead Warning (TJW), improved traffic state estimation from Probe Vehicle Data (PVD), Green Light Optimal Speed Advisory (GLOSA), Time To Green (TTG), Traffic Signal Priority Request (TSPR) [EUROPEAN COMMISSION, 2016].

Figure A.1, in the Appendix, presents the hype cycle of innovation drivers for UTCS based on relevant Gartner hype cycles [GARTNER, 2020], UTCS research trends, and UTCS industry trends. There are obviously numerous exciting R&D trends in UTCS that are not covered in this thesis, such as Automated Vehicles, multimodality, sustainability, smart city integration, deep learning, optimization, prescriptive analytics, micromobility and many more. Their significance is not underestimated by the focus of this thesis in data fusion. In fact, this multidimensionality of UTCS emphasizes the need for further research in multiple levels of data fusion.

Industry Gap Statement

For current and future UTCS, there might be several new sources available that can be used for improved signal control performance. Therefore, there is a need for robust data fusion methods that facilitate estimation and prediction to support UTC systems, independent of data availability and communication technology, especially in varying saturation conditions and low penetration rates.

2.4 Summary

Infrastructure sensors, and particularly inductive loop detectors, are the main source of information for UTCS. Mobile sensors are scarcely used in the control but mainly support the evaluation of UTCS or other C-ITS applications. The distinction between CV and Aggregated Section data from mobile sensors is necessary. These two types are fundamentally different and pinpoint the discrepancy between potential and real data availability. Moreover, low penetration rates are currently prohibiting the paradigm shift from legacy UTCS. The fusion of these profoundly different data sources should improve the traffic state estimation accuracy (section 2.1).

The different levels and definitions of data fusion are presented. The prototypical module of this thesis, the Extended Observer, covers the Level 1 data fusion, for traffic state estimation and prediction, from multiple sensors at signalized intersections. Criteria for selection of sensors and data fusion methods are presented to assist researchers and practitioners. The latter, emphasize the need not only for accuracy and coverage, but also for transparency and flexibility (section 2.2).

Legacy UTCS are hesitant to invest in algorithms that utilize CV, while the sensing possibilities from emerging technologies keep growing. Most research studies show that at least 25-40% penetration rates are needed, for improvements in traffic state estimation and traffic signal control. The gap between research and practice will grow, if the transition phase from legacy UTCS to connected UTCS is not accelerated (section 2.3).

To fill the research and industry gap, data fusion methods for varying penetration rates and traffic conditions are required. At the same time, the data and operational restrictions, as well as the future trends, must be taken into account. The widely used EKF is selected for the detailed formulation of the Extended Observer and is presented in chapter 3.

3. Methodology: The Extended Observer

The introduction of Connected Environments in the UTC loop calls for methodologies that can handle the variety of new traffic measurements. To answer that call, a module called Extended Observer is developed and proposed in this thesis for analysis, evaluation, and prototypical development. The Extended Observer aims for optimal traffic state estimation and prediction for traffic signal control by capitalizing on new data sources that might be faulty and sporadic.

A robust sensor and data fusion methodology is needed that offers the mathematical flexibility for extensions but is at the same time relatively easy to formulate for real world UTCS. The established Kalman filter is selected to be the foundation of the developed methodology and in particular its non-linear version, the EKF, that has found many applications in the field of dynamic traffic management and control [LINT & DJUKIC, 2012; LIU ET AL., 2006; LEE ET AL., 2015; LEE, 2013; TAMPÈRE & IMMERS, 2007].

One can certainly argue that different algorithms or methodologies, other than the EKF, could be used as foundation to answer the research questions and achieve the goal of the thesis. The decision to build on the EKF is principally justified by the consideration that the methodology should:

- utilize various types of measurements and ranges of measurement errors,
- exploit indirect measurements that come in different time intervals and
- take advantage of the system knowledge (i.e. signal timings).

These desired characteristics are covered in theory by the EKF algorithms, as is demonstrated in the rest of the chapter. They become however more evident in practice after the analysis and evaluation of the algorithms that are presented in chapter 4 and chapter 5 respectively. The rest of the chapter is structured as follows. Section 3.1 introduces the terminology and the algorithms of the EKF (Figure 3.1). It describes the general formulation of the Extended Observer and its role in the UTC loop with Connected Environments (Figure 3.2). The process and measurement equations are presented in detail in sections 3.2 and 3.3 respectively. Furthermore, measurement equations are proposed for different sensors based on the type of the incoming data. The ability to fuse measurements according to their error is highlighted in section 3.4.

3.1 Algorithmic Origins

State-Space Models

To describe dynamic controlled systems, *state-space* models are often used. According to ASTROM & MURRAY, the term *state-space* originates from mechanics and the attempts to describe planetary motions [2010]. The *state* of a dynamical system is defined as “a collection

of variables that completely characterizes the motion of a system for the purpose of predicting future motion". The set of all possible states is called *state-space*. Control theory further developed *state-space* models to include the *input-output* view of a dynamic system that resulted from the emergence of electrical engineering [ASTROM & MURRAY, 2010].

Kalman Filter

The state of a physical system can be described with a set of state variables that are linearly related to a set of inputs and outputs [MAU, 2005]. The Kalman filter addresses the general problem of trying to estimate the state of a controlled process that is governed by a linear stochastic difference equation. Kalman filter is an optimal recursive data processing algorithm [MAYBECK, 1979], named after Rudolph E. Kalman [KALMAN, 1960]. The term "filter" perhaps underestimates its capabilities and its wide-range applicability. It is one of the most widely used tools for stochastic estimation from noisy measurements. It has been used in many applications such as vision-based object tracking and vehicle navigation systems. The term recursive refers to the fact that there is no need to store and reprocess all previous data as new measurements become available. The Kalman filter in its linear, basic version provides an optimal estimator in the sense that it minimizes the estimated error covariance when some preconditions are met. Even though these preconditions are practically rarely met, the filter has found successful applications in many fields [WELCH & BISHOP, 2001; FARAGHER, 2012; MAU, 2005].

Extended Kalman Filter

The EKF is typically used if the process to be estimated and/or the measurement relationship to the process is non-linear. The EKF linearizes around the current mean and covariance and consequently the convergence to an optimal estimation is not guaranteed [WELCH & BISHOP, 2001]. Despite the loss of optimality, due to the local approximation, EKF has proven to work well in many applications in the field of dynamic traffic management and control [LINT & DJUKIC, 2012]. Figure 3.1 gives an overview of the operation and terminology of the EKF. The description and explanation of the algorithms in the rest of this chapter are based on the inspirational paper of WELCH & BISHOP [2001].

The filter applies each time step k a predictor-corrector type estimator. The result of the time update ("predict") is called a priori estimate ($\hat{x}_k^-$) and the result of the measurement update ("correct") is called a posteriori estimate ($\hat{x}_k$). Both estimates are in fact vectors that contain the variables to be estimated, but for the sake of simplicity and readability, the vector notation (e.g. $\overrightarrow{\hat{x}_k^-}$, $\overrightarrow{\hat{x}_k}$) is skipped in the formulas and figures. If n is the number of state variables that define that state to be estimated, then $\hat{x}_k^-$ and $\hat{x}_k$ are vectors of size n.

Two equations are needed in KF to define the mathematical models of the controlled process to be estimated: the process equation that defines the process model and the measurement

equation that defines the measurement model. In the case of EKF these two equations take the general form as shown in equations (3.1) and (3.2).

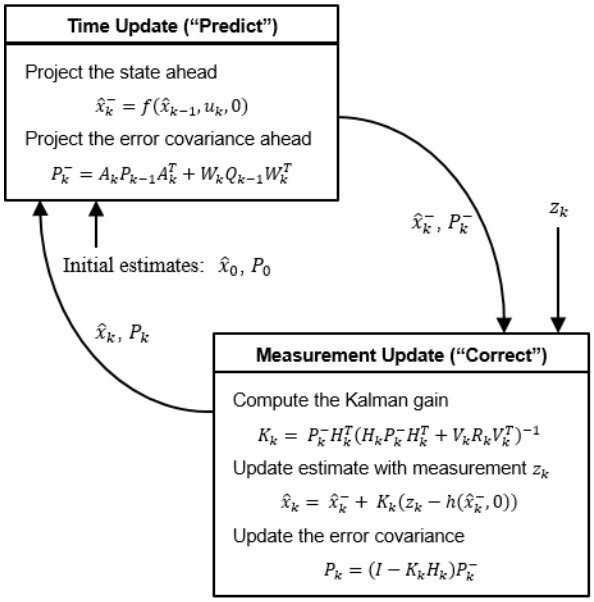

EKF Variable	Description	Dimension
$\hat{x}_k$	State vector	$n \times 1$
$f()$	Process vector function	$n \times 1$
$A_{k[i,j]}$	Jacobian matrix of $f()$ with respect to x	$n \times n$
Q_k	Process noise covariance	$n \times n$
P_k^-	*a priori* estimate error covariance	$n \times n$
z_k	Measurement vector	$m \times 1$
$h()$	Measurement vector function	$m \times 1$
$H_{k[i,j]}$	Jacobian matrix of $h()$ with respect to x	$m \times n$
R_k	Measurement noise covariance	$m \times m$
P_k	*a posteriori* estimate error covariance	$n \times n$
K_k	Kalman gain	$n \times m$

Figure 3.1 Step-by-step operation and equations of the Extended Kalman Filter

Process equation of EKF:

$$x_k = f(x_{k-1}, u_k, w_{k-1}) \tag{3.1}$$

Measurement equation of EKF:

$$z_k = h(x_k, v_k) \tag{3.2}$$

The vector x_k and vector z_k are the *actual* state and measurement vectors. That means that x_k is the number one is trying to estimate with the calculation of $\hat{x}_k$. In practice, one does not have access to the *actual* x_k. The vector z_k gives however the *actual* measurement that is used to estimate x_k (i.e. calculate $\hat{x}_k$). In practice, one indeed has access to z_k.

The non-linear function $f()$ relates the state at the previous time step k (x_{k-1}) to the state at the current time step k (x_k). The vector u_k is the (optional) control input and w_{k-1} is the zero-mean process noise (error in the model) with covariance Q_k.

The non-linear function $h()$ relates the vector of the measurements (z_k) at the current time step k to the state at the current time step k with v_k being the zero-mean measurement noise (error in the measurement) with covariance R_k. If m is the number of currently available measurements from the different sensors, the size of vector z_k is consequently m. In simple implementations, the m remains constant between filter steps. However, the number of available measurements might change every time step, because of different update intervals from sensors or possible loss of communication. To deal with the changing number of available

measurements, the filter must resize the vectors and matrices accordingly. In that case the filter can be characterized as a *variable-dimension EKF*.

The EKF needs the calculation of the Jacobians A_k, W_k, H_k and V_k to complete the update and correct steps (Figure 3.1). A_k is the Jacobian matrix of $f()$ with respect to x, whereas W_k is the Jacobian matrix of $f()$ with respect to w. H_k is the Jacobian matrix of $h()$ with respect to x and V_k is the Jacobian matrix of $h()$ with respect to v. The subscript k indicates that the Jacobians must be recomputed every time step. The subscript $[i,j]$ indicates the position of each calculated value in the matrix, where i and j indicate the respective elements of the vectors.

$$A_{k[i,j]} = \frac{\partial f_{[i]}}{\partial x_{[j]}}(\hat{x}_{k-1}, u_k, 0) \tag{3.3}$$

$$W_{k[i,j]} = \frac{\partial f_{[i]}}{\partial w_{[j]}}(\hat{x}_{k-1}, u_k, 0) \tag{3.4}$$

$$H_{k[i,j]} = \frac{\partial h_{[i]}}{\partial x_{[j]}}(\hat{x}_k^-, 0) \tag{3.5}$$

$$V_{k[i,j]} = \frac{\partial h_{[i]}}{\partial v_{[j]}}(\hat{x}_k^-, 0) \tag{3.6}$$

Q_k and R_k are the process noise covariance and the measurement noise covariance, respectively. The subscript k indicates that Q_k and R_k can be updated every step. In that case, the filter can be characterized as an *adaptive EKF*. In usual implementations, Q_k and R_k remain constant after initial tuning of the filter. Regarding the tuning requirements of the filter, the initial choices of $\hat{x}_0$ and P_0 should influence the performance only in the first filter steps and are thus not very critical for the overall performance. However, the initial choice and the possible adaptation of Q_k and R_k is decisive for the performance of the filter. They must be tuned before real-world implementations. More specifically, the ratio Q_k/R_k determines practically if the filter trusts the measurements or the process model more, since they are critical in the computations of the Kalman gain (K_k) at every filter step.

The role of K_k is to weight the difference $(z_k - h(\hat{x}_k^-, 0))$ for the calculation of the *a posteriori* state estimate ($\hat{x}_k$) during the correction step (Figure 3.1). This difference is called the measurement *innovation* or the *residual* and gives the difference between the predicted estimation $h(\hat{x}_k^-, 0)$, assuming zero measurement error, and the incoming measurement (z_k). If the *a priori* estimate error covariance (P_k^-) approaches zero, the Kalman gain also approaches zero, as shown in the computation of K_k in Figure 3.1. This means that the "corrected" estimate ($\hat{x}_k$) essentially ignores the measurement and trusts the "predicted" estimate ($\hat{x}_k^-$). Conversely, if the measurement noise covariance R_k approaches zero, K_k weights the residuals more heavily. In brief, the lower the expected error of a measurement, the more the filter trusts the specific measurement. This makes the filter particularly attractive for adaptive fusion of measurements with varying errors.

The Extended Observer is a predictor-corrector type estimator that enables fusion of a variable number of measurements depending on their error. Its algorithms are based on the algorithms of the EKF. Hence, it inherits the characteristics of EKF. More specifically, it is an implementation of multiple, variable-dimension, adaptive EKFs. Figure 3.2 illustrates the basic input-output variables.

The new data sources, be it infrastructure sensors or mobile sensors, allow a wide range of traffic measurements. In addition, a specific sensor can be the source for one or more measurements. For example, a camera could give a measurement of the turning rates and the departure rate. Or a traffic data provider might give an aggregated travel time measurement for the same road section. Furthermore, the update intervals of the incoming measurements can vary. In that case, as soon as a new measurement becomes available (i.e. every time step, i.e. every cycle), the size and the elements of the measurement vector are updated.

During the time update, the Extended Observer predicts the traffic state (e.g. $\hat{x}_k^{-queue\ length}$) based on the defined process equations. The process equations, in the form shown in equation (3.1), aim to capture the expected changes from the previous filter step to the next one. During the measurement update, the filter takes into account all available measurements in order to correct the prediction and estimate the new traffic state (e.g. $\hat{x}_k^{queue\ length}$).

The output of the Extended Observer for every signal at an intersection consists of queue length, arrival rate, departure rate, turning rate and penetration rate (Figure 3.2). The implementation is not one single filter but the parallel running of filters for each traffic state variable to be estimated. This makes tracking the performance for each state variable easier and therefore the analysis and evaluation more transparent. Additionally, this allows each filter to run independently in case only specific variables of the state vector are of interest for specific UTCS.

The theoretical disadvantage of this partition of the state vector is that the influence of one state variable to another is not modelled in one combined process equation. However, this is avoided by running the filters in parallel (i.e. consecutively in the same second) and feeding the relevant output of one filter to the appropriate next filter as input. For example, the process equation of the filter for the queue length utilizes the estimations from the filters for the arrival and departure rate as input (see also section 3.2 and Figure 3.3).

The filters for queue length, departure and arrival rate consist of the basic implementation of the Extended Observer for cycle-to-cycle traffic state estimation. They are introduced in [PAPAPANAGIOTOU & BUSCH, 2020]. The penetration and turning rate filters are additional filters for enhanced state estimation. Tab. 3.1 introduces the terminology for the elements of the state vector as possible output from the Extended Observer.

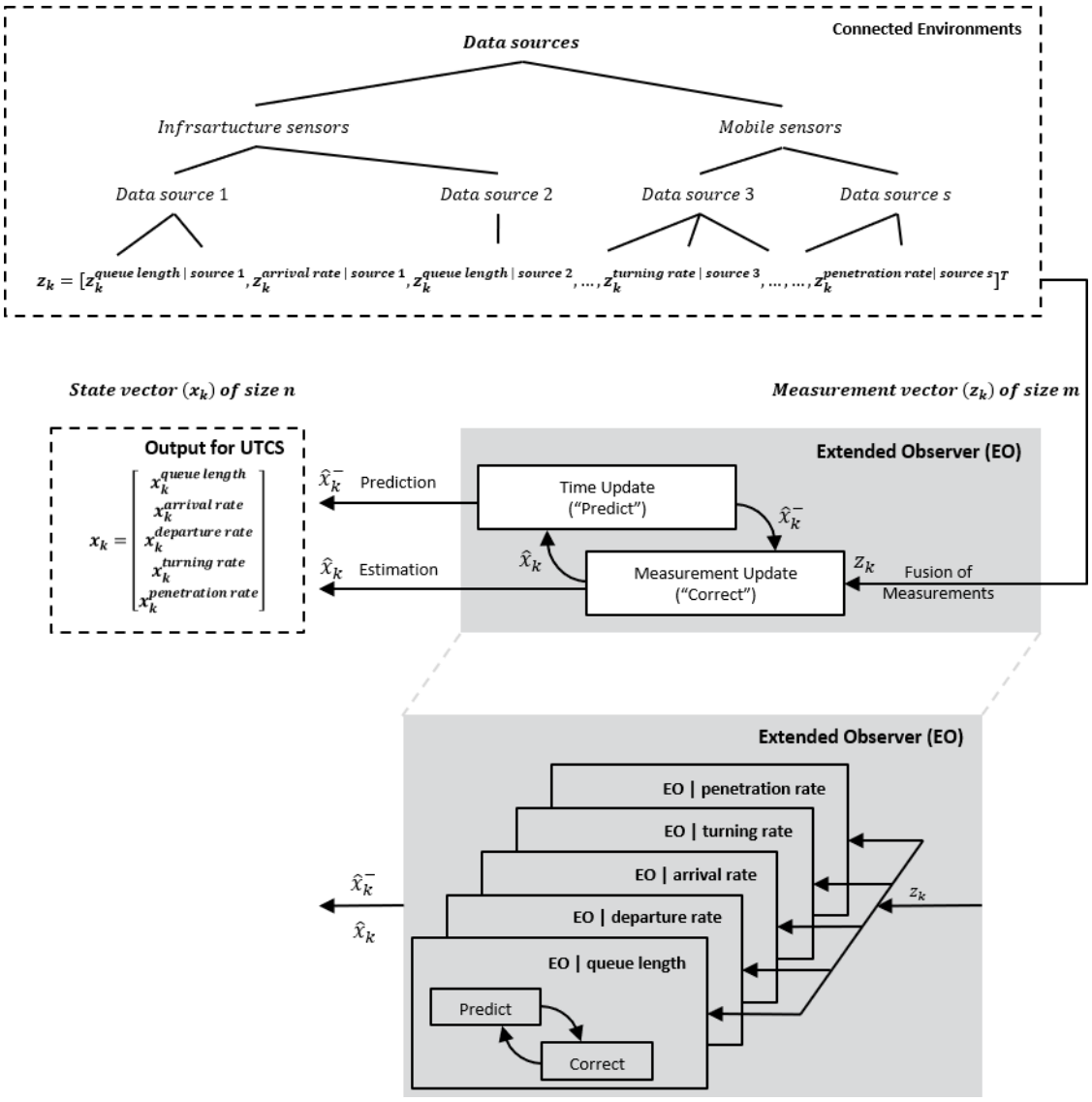

Figure 3.2 Overview of operation of the Extended Observer

Tab. 3.2 gives an overview of the examined input data and the notations that are used in the rest of the thesis (see also Tab. A.1). The potential of the proposed methodology is demonstrated by covering the types of data sources that are considered relevant to accelerate UTCS transition phase:

- Infrastructure sensors that can track vehicles for a certain "Connected Section" (z_k^{CS})
- Mobile sensors that send individual trajectory information (Connected Vehicles). The measurements (z_k^{CV}) become immediately (1-3 sec) available.
- Mobile sensors that deliver aggregated section data from FCD. The measurements become available in 1-minute aggregation intervals. Two options are examined: information on travel time (z_k^{TT}) and location of notable speed drops (z_k^{DV}). DV stands for "Difference in Velocities".

Notation	State to be estimated	Short description
x_k^{queue}	Queue length (veh)	The theoretical space between the back-end of the queue and the stop-line in number of vehicles.
x_k^{arr}	Arrival rate (veh/s)	The number of vehicles that join the queue per second.
x_k^{dep}	Departure rate (veh/s)	The number of vehicles that leave the queue per second.
x_k^{turn}	Turning rate (%)	Percentage of queued vehicles that choose a specific turning movement.
x_k^{pen}	Penetration rate (%)	Percentage of queued vehicles that can communicate their trajectory information.

Tab. 3.1 Output overview of the Extended Observer - state vector

Data source example	Measurement Vector from Connected Environments z_k					Data source description
	$z_k^{queue\|CE}$	$z_k^{arr\|CE}$	$z_k^{dep\|CE}$	$z_k^{turn\|CE}$	$z_k^{pen\|CE}$	
Connected Section measurements from camera, with real-time image processing (z_k^{CS})	$z_k^{queue\|CS}$	$z_k^{arr\|CS}$	$z_k^{dep\|CS}$	$z_k^{turn\|CS}$	–	Sensor type: Infrastructure Utilized information: Individual trajectories Challenge: Limited coverage
Connected Vehicles with short- or long-range communication (z_k^{CV})	$z_k^{queue\|CV}$	$z_k^{arr\|CV}$	$z_k^{dep\|CV}$	$z_k^{turn\|CV}$	$z_k^{pen\|CV}$	Sensor type: Mobile Utilized information: Individual trajectories Challenge: Limited vehicles
Aggregated Section speeds (z_k^{DV}) and travel times (z_k^{TT}) via cloud communication based on Application Programing Interfaces (API)	$z_k^{queue\|DV}$ $z_k^{queue\|TT}$	–	–	–	–	Sensor type: Mobile Utilized information: Aggregated trajectories Challenge: Limited vehicles, limited resolution
	State Vector from Extended Observer x_k					
	x_k^{queue}	x_k^{arr}	x_k^{dep}	x_k^{turn}	x_k^{pen}	

Tab. 3.2 Input overview of the Extended Observer - measurement vector

The rows of Tab. 3.2 give the measurements from each examined type of data source. The columns give the measurement vectors for each state to be estimated and thus the measurement vectors that are used from the respective filters. Different data availability scenarios result into different measurement vectors for each state to be estimated. Detailed explanation of each element of the state and measurement vectors, as well as the respective process and measurement equations, are given in sections 3.2 and 3.3.

3.2 Process Vector and Equations

For the sake of simplicity, the algorithms are presented based on one signal group that serves one lane. There is no assumption of fixed-time control. The green and cycle time may vary between cycles without restrictions. Each filter step k represents one signal cycle that begins with the start of the green phase of the relevant signal group and ends with the end of the red phase. The Extended Observer runs in discrete time steps, once per cycle. Since the control is adaptive, the time (in seconds) between consecutive filter steps varies accordingly. The complete state vector is:

$$x_k = \left[x_k^{queue}, x_k^{arr}, x_k^{dep}, x_k^{turn}, x_k^{pen}\right]^T \tag{3.7}$$

with:

x_k^{queue}: queued vehicles at the end of red time of signal cycle k (veh)

x_k^{arr}: vehicles that join the queue per second during signal cycle k (veh/s)

x_k^{dep}: vehicles that leave the queue per second during signal cycle k (veh/s)

x_k^{turn}: percentage of vehicles that turn during signal cycle k $(\%)$

x_k^{p}: percentage of queued Connected Vehicles $(\%)$

The process equations for each element of the state vector are presented separately.

Departure rate (x_k^{dep})

To model the cycle-to-cycle process of the departure rate, two main assumptions are made. The change between two consecutive cycles might be random and that during the day there might be an underlying daily traffic pattern. The process equation for the departure rate can be modelled by means of a random walk or with the consideration of a historical model.

Process equation of departure rate:

Random walk:

$$x_k^{dep} = x_{k-1}^{dep} + w_{k-1}^{dep} \tag{3.8}$$

Historical model:

$$x_k^{dep} = a_{k-1}^{dep} \times x_{k-1}^{dep} + w_{k-1}^{dep} \tag{3.9}$$

with:

$$a_{k-1}^{dep} = \frac{x_k^{dep\_hist}}{x_{k-1}^{dep}}$$

x_k^{dep}: queued vehicles that cross the stop line per second after the start of the green time of signal cycle k (veh/s).

x_{k-1}^{dep}: queued vehicles that cross the stop line per second after the start of the green time of signal cycle $k-1$ (veh/s).

a_{k-1}^{dep}: scaling factor according to the underlying historical model.

$x_k^{dep\_hist}$: expected departure rate according to the historical profile (veh/s).

w_{k-1}^{dep}: departure process noise (veh/s).

The scaling factor a_{k-1}^{dep} simply converts the last state (x_{k-1}^{dep}) to the expected historical value ($x_k^{dep\_hist}$), since the EKF model formulation demands that the current state is related to the previous state. In practice, the historical values might come from previous daily or peak hour observations. The process equation is not linear because a_{k-1}^{dep} changes every time step. The departure process noise (w_{k-1}^{dep}) refers to the expected error in the assumed process, be it the random walk or the historical model. It is defined by the process noise covariance for the departure rate (Q_{k-1}^{dep}). It's tuning and role in the performance of the filter is explained in section 3.4 and becomes evident in the analysis (chapter 4).

Arrival rate (x_k^{arr})

Similarly, the arrival rate can be modelled by means of a random walk or with the help of a historical model.

Process equation of arrival rate:

Random walk:

$$x_k^{arr} = x_{k-1}^{arr} + w_{k-1}^{arr} \tag{3.10}$$

Historical model:

$$x_k^{arr} = a_{k-1}^{arr} \times x_{k-1}^{arr} + w_{k-1}^{arr} \tag{3.11}$$

with:

$$a_{k-1}^{arr} = \frac{x_k^{arr\_hist}}{x_{k-1}^{arr}}$$

x_k^{arr}: vehicles that join the queue per second during signal cycle k (veh/s).

x_{k-1}^{arr}: vehicles that join the queue per second signal cycle $k-1$ (veh/s).

a_{k-1}^{arr}: scaling factor according to the underlying historical model.

$x_k^{arr\_hist}$: expected arrival rate according to the historical profile (veh/s).

w_{k-1}^{arr}: arrival process noise (veh/s).

As in the case of the departure rate, the scaling factor for arrival rate (a_{k-1}^{arr}) simply converts the last state (x_{k-1}^{arr}) to the expected historical value ($x_k^{\mathrm{arr}\_hist}$). Again, the historical values might come from previous historical observations. The arrival process noise (w_{k-1}^{arr}) refers to the expected error in the assumed process and is defined by the process noise covariance for the arrival rate (Q_{k-1}^{arr}) (see also sections 3.4 and 4).

Queue (x_k^{queue})

Due to the stochastic nature and dynamics of queue length at signalized intersections, a random walk or a historical model are not appropriate as process equations. To describe the queue formation at traffic signals, various approaches have been used, ranging from analytical formulas and shockwave theory for fixed-time control [MILLER, 1963; AKCELIK, 1980; ROUPHAIL ET AL., 2001; KUHNE & MICHALOPOULOS, 2001] to probabilistic approaches for actuated control [VITI, 2006; VITI & VAN ZUYLEN, 2009; VITI & VAN ZUYLEN, 2004].

Many methods build on the fundamental conservation equation [LINDLEY, 1952] for real-time queue length estimation [FU ET AL., 2001] in adaptive traffic signal control [MIRCHANDANI & HEAD, 2001]. The simplicity, applicability and robustness of the conservation equation make it very attractive for UTCS [LEE ET AL., 2015]. Moreover, according to PAPAGEORGIOU, the conservation equation is the only exact equation in traffic flow theory [1998B].

The Extended Observer builds on the conservation equation and the system knowledge (signal timings) to formulate the required process equation. The queue length at the end of red time of the current cycle is related to the queue length of the previous cycle. It considers the number of vehicles that enter and leave the queue during the examined cycle. The signal timings, as well as the arrival and departure rate estimation are utilized. Equation (3.12) gives the process equation for cycle-to-cycle queue length estimation.

Process equation of queue length:

$$x_k^{queue} = x_{k-1}^{queue} - u_k^{dep} + u_k^{arr} + w_{k-1}^{queue} \tag{3.12}$$

with:

x_k^{queue}: queued vehicles at the end of red time of signal cycle k (veh)

x_{k-1}^{queue} queued vehicles at the end of red time of signal cycle $k-1$ (veh)

u_k^{dep}: vehicles that departed during signal cycle k (veh)

u_k^{arr}: vehicles that arrived during signal cycle k (veh)

w_{k-1}^{queue}: queue process noise (veh).

The equation covers both undersaturated and oversaturated cycles. To calculate the number of vehicles that departed the queue during cycle k, the departure rate and the green time that is utilized from the queue are required. The vehicles that join the queue during signal cycle k are calculated using the red time and the arrival rate.

$$u_k^{dep} = u_k^{utilized\ green} \times x_k^{dep} \tag{3.13}$$

$$u_k^{arr} = u_k^{red} \times x_k^{arr} \tag{3.14}$$

$$u_k^{utilized\ green} = \min\left(\frac{x_{k-1}^{queue}}{x_k^{dep}}, u_k^{green}\right) \tag{3.15}$$

Using equations (3.13), (3.14) and (3.15), equation (3.12) becomes:

$$x_k^{queue} = x_{k-1}^{queue} - u_k^{utilized\ green} \times x_k^{dep} + u_k^{red} \times x_k^{arr} + w_{k-1}^{queue} \tag{3.16}$$

The term $u_k^{utilized\ green}$ refers to the green time that is utilized by the queued vehicles. It depends on the queued vehicles at the end of cycle $k-1$ (x_{k-1}^{queue}) and the departure rate during cycle k (x_k^{dep}). Its upper bound is the actual green time applied during signal cycle k (u_k^{green}). For high queues that cannot be dissolved during the green time, $u_k^{utilized\ green}$ equals u_k^{green}. For low queues that are completely dissolved, $u_k^{utilized\ green}$ becomes $\frac{x_{k-1}^{queue}}{x_k^{dep}}$. In practice, this prevents negative queue values at the end of green time. It models the fact that low queues need only a fraction of the green time. The remaining green time ($u_k^{green} - u_k^{utilized\ green}$) has no effect on the queue. The queue formation starts again with the beginning of the red time.

The knowledge of the departure (x_k^{dep}) and arrival rate (x_k^{arr}) of the current signal cycle is needed to get the queue length from the process equation (3.16). This issue is solved by running the prediction-correction filtering approach for the three parameters in parallel for signal cycle k. Additionally, the knowledge of the implemented signal timing (u_k^{green}, u_k^{red}) is

required. Since the Extended Observer is designed to be integrated within UTCS, it is assumed that this information becomes available immediately after the signal timing implementation.

Figure 3.3 shows how the three basic filters work together based on the process models and the incoming measurements ($z_k^{dep}, z_k^{arr}, z_k^{queue}$) in order to get the corrected estimations ($\hat{x}_k^{dep}, \hat{x}_k^{arr}, \hat{x}_k^{queue}$).

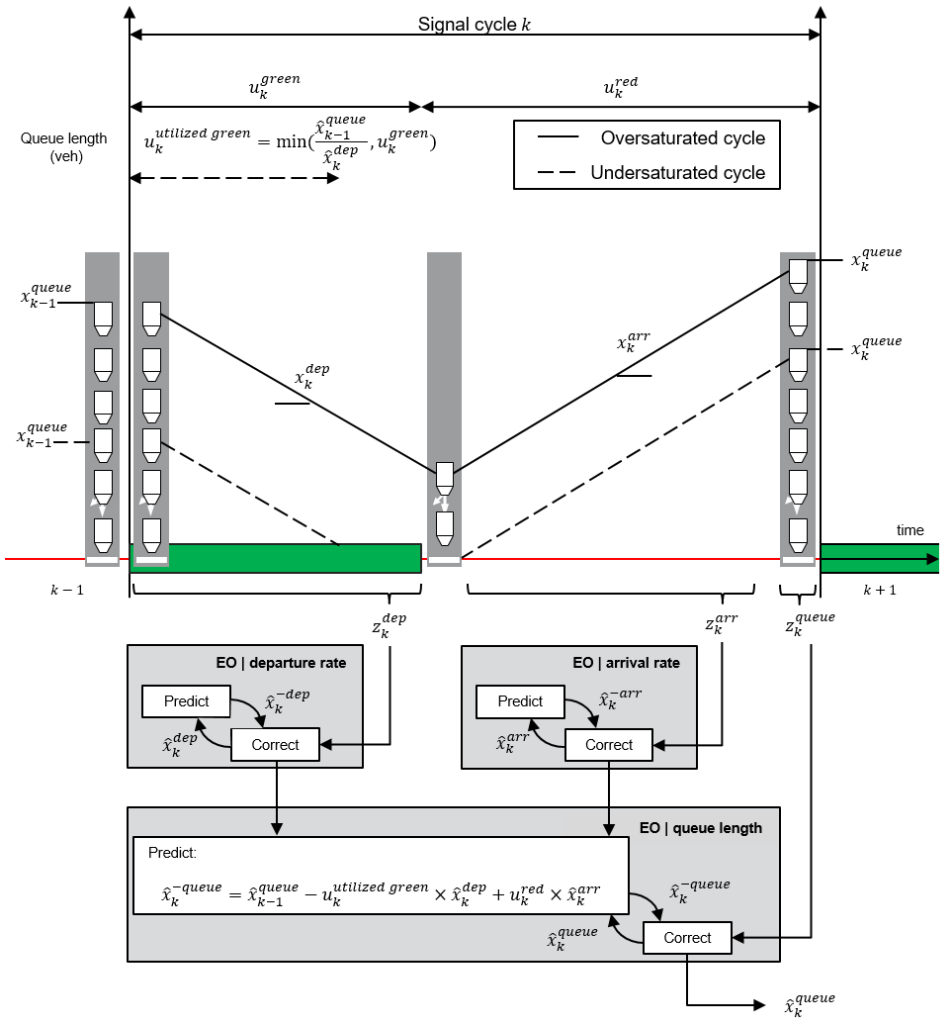

Figure 3.3 Queue process equation of the Extended Observer

The outcome of the filters for the departure and arrival rate can be used for the “predict” step for the queue. Based on the departure rate estimation ($\hat{x}_k^{dep}$) and the previous queue length estimation ($\hat{x}_{k-1}^{queue}$), the utilized green ($u_k^{utilized\ green}$) can be calculated based on equation (3.15). The “predict” step for the queue filter can run at the end of signal cycle k by taking into account the signal timings (u_k^{green}, u_k^{red}). The queue measurements are used to “correct” the estimation. The corrected queue length estimation is used for the next signal cycle $k-1$.

During signal cycle k, measurements for the departure, arrival and queue are gathered every second, to update the measurement vectors z_k^{dep}, z_k^{arr} and z_k^{queue}. At the end of signal cycle k, the three filters run successively. The computational time for each filter is trivial (<1 sec). The biggest computational effort (in the simulation environment) is updating the measurement vectors every second. If for one filter there is no new measurement for the current cycle, the "correct" step is skipped, and the updated estimation comes solely from the "predict" step.

Prediction

One of the main advantages of using the algorithms of the EKF is the inherent ability for prediction. The queue length "predict" step, as shown in Figure 3.3, takes place at the end of the signal cycle k and calculates the queued vehicles at the end of signal cycle k ($\hat{x}_k^{-queue}$). It takes advantage of the system knowledge (i.e. signal timings) and the process equation (i.e. conservation equation). Adding reliable measurements at the end of the cycle during the "correct" step allows for robust cycle-to-cycle estimation of the queue length.

Let $\hat{x}_{k|k-1}^{-queue}$ be the prediction of the queue at the end of signal cycle k that can only be based on information available at the beginning of signal cycle k (i.e. end of signal cycle $k-1$). At the beginning of signal cycle k there are no measurements available yet. Therefore, only the predicted (and not the corrected) arrivals and departures can be used (x_k^{-dep}, x_k^{-arr}) in equation (3.16) (see also Figure 3.3). The queue length prediction $x_{k|k-1}^{-queue}$ can be then calculated with the following formula:

$$\hat{x}_{k|k-1}^{-queue} = \hat{x}_{k-1}^{queue} - u_k^{-dep} + u_k^{-arr} \tag{3.17}$$

with:

$\hat{x}_{k|k-1}^{-queue}$: queued vehicles at the end of red time of signal cycle k, based on information only available at the end of signal cycle $k-1$ (veh)

$\hat{x}_{k-1}^{queue}$ queued vehicles at the end of red time of signal cycle $k-1$ (veh)

u_k^{-dep}: predicted number of vehicles that will depart during signal cycle k (veh)

u_k^{-arr}: predicted number of vehicles that will arrive during signal cycle k (veh)

$$u_k^{-dep} = u_k^{-utilized\ green} \times x_k^{-dep} \tag{3.18}$$

$$u_k^{-arr} = u_k^{-red} \times x_k^{-arr} \tag{3.19}$$

$$u_k^{-utilized\ green} = \min\left(\frac{x_{k-1}^{queue}}{x_k^{-dep}}, u_k^{-green}\right) \tag{3.20}$$

x_k^{-dep}: predicted departure rate for signal cycle k (veh)

x_k^{-arr}: predicted arrival rate for signal cycle k (veh)

u_k^{-green} predicted green time for signal cycle k (sec)

u_k^{-red} predicted red time for signal cycle k (sec)

Clearly, the total applied green and red time during cycle k are not known in the beginning of cycle k. In the case of fixed-time control, signal timings are known, and the predicted queue can be directly calculated with equation (3.21). Model-based adaptive traffic signal control systems have typically internal predictions for the green and red time of the cycle that has started. Rule-based signal control systems are sometimes more difficult to predict depending on the complexity of the control logic. Nevertheless, it can be assumed that even these systems have a certain knowledge of the signal timings (e.g. cycle time range, minimum and maximum green time). Prediction of signal timings in the case of UTCS (model-based or rule-based) is beyond the scope of this thesis. For the predicted red and green times, the signal timings of the previous cycle are used as simplification. In chapter 5 (section 5.2.1), it is shown that there is no statistically significant difference between prediction ($\hat{x}_{k|k-1}^{-queue}$) and a priori estimation ($\hat{x}_k^{-queue}$). The a priori estimation ($\hat{x}_k^{-queue}$) can be viewed as the best possible queue prediction ($\hat{x}_{k|k-1}^{-queue}$) with the Extended Observer. It must be emphasized that the accuracy of the filtered estimations ($\hat{x}_k^{queue}$) are not influenced by the prediction of the signal timings, since the applied signal timings of the current cycle are used.

Second-by-second implementation

The basic formulation of the Extended Observer considers cycle-to-cycle estimation and prediction. However, the developed algorithms are not limited to cycle-to-cycle implementation. Especially for the case of queue length, a second-by-second estimation could be considered of great value if the focus shifts from the beginning of the transition phase with low penetration rates to Connected Environments with high penetration rates. A slight adjustment of the process equation for the queue length allows a sec-by-second formulation.

The duration of each step becomes one second instead of the complete signal cycle. The green and red time are not referring to the complete cycle, but to the status of the signal during that second. The subscript t is used to indicate the second-by-second operation. Equation (3.12) becomes:

$$x_t^{queue} = x_{t-1}^{queue} - u_t^{dep} + u_t^{arr} + w_{t-1}^{queue} \tag{3.21}$$

with:

x_t^{queue}: queued vehicles at second t (veh)

x_{t-1}^{queue} queued vehicles at second $t-1$ (veh)

u_t^{dep}: vehicles that departed during second t (veh)

u_t^{dep}: vehicles that arrived during second t (veh)

w_{t-1}^{queue}: queue process noise (veh).

The term $u_k^{utilized\ green}$ from equation (3.15), for avoiding negative values and distinguishing between undersaturated and oversaturated cycles, becomes obsolete. To avoid negative queue values during green in cases of undersaturation, a lower limit of zero for the estimated queue (x_t^{queue}) is set. The arrival and departure process equations from equations (3.8), (3.9), (3.10) and (3.11) can be used without any changes for the second-by-second implementation. The subscript t is used as well to indicate their second-by-second implementation (x_t^{dep}, x_t^{arr}). Equations (3.13) and (3.14) become:

$$u_t^{dep} = u_t^{green} \times x_t^{dep} \qquad with \begin{cases} u_t^{green} = 1 & ,if\ green \\ u_t^{green} = 0 & ,if\ red \end{cases} \tag{3.22}$$

$$u_t^{arr} = u_t^{red} \times x_t^{arr} \qquad with \begin{cases} u_t^{red} = 0 & ,if\ green \\ u_t^{red} = 1 & ,if\ red \end{cases} \tag{3.23}$$

The process equation (3.16) becomes:

$$x_t^{queue} = \max(x_{t-1}^{queue} - u_t^{green} \times x_k^{dep} + u_k^{red} \times x_k^{arr} + w_{k-1}^{queue}, 0) \tag{3.24}$$

The second-by-second formulation does not give any added value for low penetration rates, where aggregated FCD and CV are only available sporadically. The analysis and evaluation focus therefore in the cycle-to-cycle formulation.

Turning rate (x_k^{turn}) and penetration rate (x_k^{pen})

To expand the applicability of the Extended Observer, the estimation of the turning (x_k^{turn}) and penetration (x_k^{pen}) rate can be added. There are two things to consider; how these new variables are estimated and how they influence the other states.

The process equations are similar to the arrival and departure rate process equations as described with (3.8), (3.9), (3.10) and (3.11). That means, the change from one cycle to the next is modelled with either a random walk or with the assistance of a historical model. The

repetition of the same equations for a different variable is considered redundant and is therefore skipped. The measurement equations are shown in section 3.3

Figure 3.4 shows schematically an example of the influence of the turning rate estimation on the arrival rate estimation. The left part of the figure shows that in case of a considerable number of “free” right-turners, the arrival rate at the back-end of the queue should be reduced accordingly. The right part shows that for queues that block the right-turning lane, the arrival at the back-end of the queue consists of the arrival for both turning movements. This can be expressed with the following equation:

$$x_k^{arr|turn} = \begin{cases} x_k^{arr} \times (1 - x_k^{turn}) & , if\ x_k^{queue} < N_{block} \\ x_k^{arr} & , else \end{cases} \tag{3.25}$$

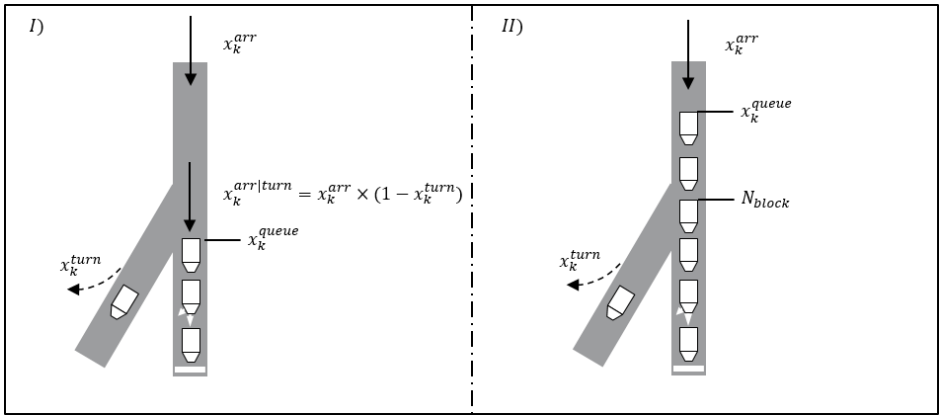

Figure 3.4 Extension of the Extended Observer for considering the influence of turning rates

The above consideration is not relevant for the simplified test intersection (section 5.2) but is included in the real-world intersection (section 5.3).

The percentage of CV currently at the queue (x_k^{pen}) is used to adjust the weighting of the measurement from CV. The basic principle for the penetration rate consideration in the Extended Observer is the following: for high penetration rates, the measurements from CV are expected to be more accurate. This intuitive principle can is included in the formulation, by adjusting the respective measurement error covariance (see also section 4.3.1)

3.3 Measurement Vector and Equations

After the definition of the state vector and process equations, the measurement vector and the measurement equations must be defined. The size of the measurement vector (z_k), unlike the state vector (x_k), varies depending on the availability of the data sources (see Tab. 3.2). Assuming that all the types of data sources shown in Tab. 3.2 are available, the measurement vector from all available Connected Environments (CE) becomes:

$$z_k = z_k^{queue|CE} + z_k^{arr|CE} + z_k^{dep|CE} + z_k^{turn|CE} + z_k^{pen|CE} \tag{3.26}$$

with:

$z_k^{queue|CE}$: queue measurements for signal cycle k coming from all CE (veh)

$z_k^{arr|CE}$: arrival measurements for signal cycle k coming from all CE (veh/s)

$z_k^{dep|CE}$: departure measurements for signal cycle k coming from all CE (veh/s)

$z_k^{turn|CE}$: turning measurements for signal cycle k coming from all CE $(\%)$

$z_k^{pen|CE}$: penetration measurements for signal cycle k coming from all CE $(\%)$

The rows of Tab. 3.2 give the measurements from each examined type of data source. For example, assuming that the only available data source is CV, the measurement vector becomes:

$$z_k^{CV} = \left[z_k^{queue|CV}, z_k^{arr|CV}, z_k^{dep|CV}, z_k^{turn|CV}, z_k^{pen|CV} \right]^T \tag{3.27}$$

with:

z_k^{CV}: all measurements for signal cycle k coming only from CV (veh)

$z_k^{queue|CV}$: queue measurements for signal cycle k coming only from CV (veh)

$z_k^{arr|CV}$: arrival measurements for signal cycle k coming only from CV (veh/s)

$z_k^{dep|CV}$: departure measurements for signal cycle k coming only from CV (veh/s)

$z_k^{turn|CV}$: turning measurements for signal cycle k coming only from CV $(\%)$

$z_k^{pen|CV}$: penetration measurements for signal cycle k coming only from CV $(\%)$

The columns of Tab. 3.2 represent the measurement vectors for each state to be estimated and thus the measurement vectors that are used from the respective filters. For example, assuming that all sources indicated in Tab. 3.2 are available, the measurement vector for the queue length estimation becomes:

$$z_k^{queue|CE} = \left[z_k^{queue|CS}, z_k^{queue|CV}, z_k^{queue|TT}, z_k^{queue|DV} \right]^T \tag{3.28}$$

with:

$z_k^{queue|CE}$: queue measurements for signal cycle k coming from all CE (veh)

$z_k^{queue|CS}$: queue measurements for signal cycle k coming from CS (veh)

$z_k^{queue|CV}$: queue measurements for signal cycle k coming from CV (veh)

$z_k^{queue|TT}$: travel time measurements for signal cycle k coming from TT (sec)

$z_k^{queue|DV}$: queue measurements for signal cycle k coming from DV (veh)

If a data source directly measures the state to be estimated, it is considered to give a *direct measurement*. An example of a direct measurement is, if a camera gives a measurement for queue length ($z_k^{queue|CS}$) in vehicles (i.e. as expected from the state to be estimated). In that case, the $h()$ function (3.2) that relates the single measurement to the specific state is $I = [1]$. For example:

$$z_k^{queue|CS} = x_k^{queue} + v_k^{queue|CS} \tag{3.29}$$

with:

$v_k^{queue|CS}$: queue measurement noise from CS with covariance $R_k^{queue|CS}$ (veh)

On the other hand, if a data source measures another variable, it is said to give an *indirect measurement*. In that case, $h()$ (3.2) needs to be defined for the specific measurement and respective state. An example of indirect measurement for queue is the travel time for the relevant road section. The rest of the chapter examines the individual elements of the measurement vector and the respective measurement equations for every type of data source.

Measurements from Connected Vehicles (z_k^{CV})

To formulate measurement equations from CV that could be immediately used in practice from UTCS, it is assumed that only basic information is available. Each CV i that is in queue during signal cycle k (CV_k^i) communicates the timestamp (T_k^i), its location (S_k^i) and its instant speed (V_k^i). It is distinguished between CV that are in the queue during cycle k (CV_k^q) and CV that are joining the queue during cycle k (CV_k^j). Figure 3.5 shows how the CV measurements ($z_k^{dep|CV}, z_k^{arr|CV}, z_k^{queue|CV}$) are correcting the predicted estimation. The information from the CV is communicated every second but the filters run once per cycle.

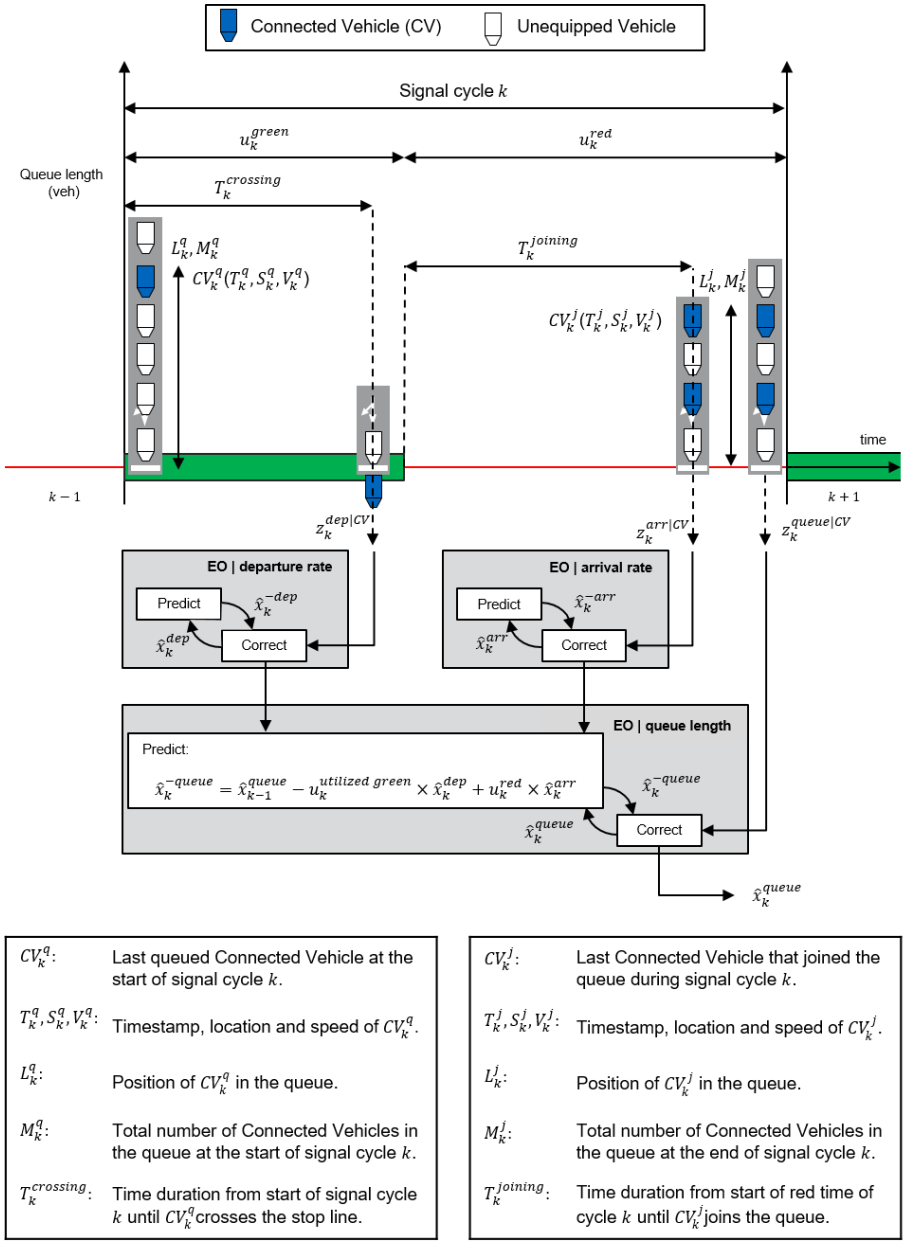

CV_k^q:	Last queued Connected Vehicle at the start of signal cycle k.
T_k^q, S_k^q, V_k^q:	Timestamp, location and speed of CV_k^q.
L_k^q:	Position of CV_k^q in the queue.
M_k^q:	Total number of Connected Vehicles in the queue at the start of signal cycle k.
$T_k^{crossing}$:	Time duration from start of signal cycle k until CV_k^q crosses the stop line.

CV_k^j:	Last Connected Vehicle that joined the queue during signal cycle k.
T_k^j, S_k^j, V_k^j:	Timestamp, location and speed of CV_k^j.
L_k^j:	Position of CV_k^j in the queue.
M_k^j:	Total number of Connected Vehicles in the queue at the end of signal cycle k.
$T_k^{joining}$:	Time duration from start of red time of cycle k until CV_k^j joins the queue.

Figure 3.5 Measurements from Connected Vehicles

From this basic trajectory information, the time $(T_k^{crossing})$ that the last queued CV (CV_k^q) crosses the stop-line, as well as the time $(T_k^{joining})$ that the last CV (CV_k^j) joined the queue can be calculated. The speeds (V_k^q, V_k^j) are used to determine if the CV is in queue or not. In the presented formulation, a vehicle is considered entering the queue if its speed is lower than 5 km/h and is considered leaving the queue if its speed becomes greater than 10 km/h. The speed (V_k^j) is used to determine the exact time joining the queue. In addition, the position in the queue (L_k^q, L_k^j) is calculated from the location (S_k^q, S_k^j) and the known location of the stop-line. An assumed average vehicle length of 6 meters is used for the conversion of meters to number of vehicles. The total number of CV in the queue (M_k^q, M_k^j) can be easily calculated assuming a working V2I communication.

The formulas for the measurements for arrival rate, penetration rate and queue length are based on the work of COMERT [2013, 2016]. In his work, expected values and estimation errors are presented in form of analytical expressions for different penetration rates and saturation degrees. COMERT proposes and analyses five penetration rate estimators, six arrival rate estimators and eight Queue Length Estimators (QLE). Two equations for each of these three variables (arrival rate, penetration rate and queue length) are selected for analysis with the Extended Observer. The detailed derivation of the formulas can be found in [COMERT, 2013; COMERT, 2016]. For the measurement equations of departure and turning rate, one new formula per variable is presented. Their derivation is based also only on basic trajectory information.

i. Departure rate ($z_k^{dep|CV}$)

For the calculation of the departure rate measurement ($z_k^{dep|CV}$), the position (L_k^q) of the last queued CV and the time needed to cross the stop-line ($T_k^{crossing}$) are used:

$$z_k^{dep|CV} = \frac{L_k^q}{T_k^{crossing}} \ (veh/s) \tag{3.30}$$

In the example of Figure 3.5, the CV_k^q is 5th in the queue. If after 10 seconds the position (S_k^q) shows that the CV_k^q has crossed the stop-line, then the departure rate measurement is:

$$z_k^{dep|CV} = \frac{5}{10} = 0.5 \ veh/s.$$

Remember that CV_k^q refers to the last queued CV. That means that if there are more than one CV in the queue, the last one is used for the measurement calculation of the departure rate. The measurement is valid only if it comes from a vehicle that is at least 4th in the queue for more representative measurements [HAMAD & ABUHAMDA, 2015].

ii. Arrival rate ($z_k^{arr|CV}$)

For the arrival rate measurements ($z_k^{arr|CV}$), two equations could be used based on information from the last CV that joined the queue (CV_k^j). The first one uses only the position (L_k^j) and the time joining the queue ($T_k^{joining}$). The second variation uses in addition the total number of queued CV (M_k^j).

$$z_k^{arr|CV} = \frac{L_k^j}{T_k^{joining}} \ (veh/s) \tag{3.31}$$

$$z_k^{arr|CV} = \frac{L_k^j - M_k^j}{T_k^{joining}} + \frac{M_k^j}{u_k^{red}} \ (veh/s) \tag{3.32}$$

In the example of Figure 3.5, the CV_k^j is 4th in the queue (i.e. $L_k^j = 4$) and there are two CV in the queue (i.e. $M_k^j = 2$). Assuming that the total red time (u_k^{red}) is 40 seconds and the CV joined the queue 30 seconds after red time started ($T_k^{joining}$), then the arrival rate measurement based on equation (3.31) is:

$$z_k^{arr|CV} = \frac{L_k^j}{30} = \frac{4}{30} = 0.13\ veh/s.$$

Using equation (3.32) for the same example, the arrival rate measurement is:

$$z_k^{arr|CV} = \frac{4-2}{30} + \frac{2}{40} = 0.117\ veh/s.$$

Equation (3.31) gives a good approximation in cases where the CV arrives close the end of red time. Equation (3.32) performs theoretically better by taking also into account the red duration and the total number of CV in the queue.

iii. Penetration rate ($z_k^{pen|CV}$)

For the penetration rate ($z_k^{pen|CV}$), two equations are examined, as possible measurement equations. The first one uses the number of CV in the queue (M_k^j) and the position (L_k^j) of the last CV. The second uses additionally the time joining the queue ($T_k^{joining}$) and the red time (u_k^{red}).

$$z_k^{pen|CV} = \frac{M_k^j}{L_k^j}\ (\%) \tag{3.33}$$

$$z_k^{pen|CV} = \frac{M_k^j \times T_k^{joining}}{M_k^j \times T_k^{joining} + (L_k^j - M_k^j) \times u_k^{red}}\ (\%) \tag{3.34}$$

In the example of Figure 3.5, the penetration rate measurement based on equation (3.33) is:

$$z_k^{pen|CV} = \frac{2}{4} = 50\ \%.$$

Using equation (3.34), the penetration rate measurement is:

$$z_k^{pen|CV} = \frac{2\times30}{2\times30+(4-2)\times40} = 43\ \%.$$

Equation (3.33) ignores the possibility that unequipped vehicles join the queue after the last CV. Equation (3.34) performs theoretically better by taking into account the timing information of $T_k^{joining}$ and u_k^{red}.

iv. Queue length ($z_k^{queue|CV}$)

The queue length can be calculated from CV based on the position of the last CV and the expected queue formation depending on the expected arrival and penetration rate [COMERT, 2016]. The queue grows theoretically after the last known CV joins the queue for $\left(u_k^{red} - T_k^{joining}\right)$ seconds.

$$z_k^{queue|CV} = L_k^j + \left(1 - z_k^{pen|CV}\right) \times z_k^{arr|CV} \times \left(u_k^{red} - T_k^{joining}\right) \tag{3.35}$$

Depending on which pair of the previously presented equations (equation (3.31) and (3.33) or (3.32) and (3.34)) is used for calculating the arrival and penetration rate, equation (3.35) can take the following forms:

$$z_k^{queue|CV} = L_k^j + \left(1 - \frac{M_k^j}{L_k^j}\right) \times \frac{L_k^j}{T_k^{joining}} \times \left(u_k^{red} - T_k^{joining}\right) \tag{3.36}$$

$$z_k^{queue|CV} = L_k^j + \left(1 - \frac{M_k^j \times T_k^{joining}}{M_k^j \times T_k^{joining} + \left(L_k^j - M_k^j\right) \times u_k^{red}}\right) \times \left(\frac{L_k^j - M_k^j}{T_k^{joining}} + \frac{M_k^j}{u_k^{red}}\right) \times \left(u_k^{red} - T_k^{joining}\right) \tag{3.37}$$

Equation (3.36) uses equations (3.31) and (3.33). Equation (3.37) uses the more elaborate equations (3.32) and (3.34). In any case, the queue length calculation requires in addition to the position of the CV (L_k^j) in the queue also the knowledge of the time joining the queue ($T_k^{joining}$) and the red time (u_k^{red}).

In the example of Figure 3.5, the queue length measurement based on (3.36) is:

$$z_k^{queue|CV} = 4 + (1 - 0.5) \times 0.13 \times (40 - 30) = 4.5\ veh$$

The queue length measurement based on (3.37) is:

$$z_k^{queue|CV} = 4 + (1 - 0.43) \times 0.117 \times (40 - 30) = 4.67\ veh$$

One can use only the position of the CV ($L_k^j = 4$) as queue length measurement. For the simple example of Figure 3.5 the differences are obviously insignificant. However, for high queues and low penetration rates, using only the position of the CV might lead to low quality queue measurements. The example of Figure 3.5 is only used for demonstration of main concepts of the algorithms.

v. Turning rate ($z_k^{turn|CV}$)

The measurements for the turning rates use the basic information from each CV (CV_k^i) that passes through the relevant signal to identify which turning movement is selected by the CV. Assuming that there are only two possible turning movements (e.g. right turn and straight), the tuning rate measurement is:

$$z_k^{turn|CV} = \frac{Number\ of\ CV\ that\ turn}{Total\ number\ of\ CV}\ (\%) \tag{3.38}$$

To avoid low quality measurements in cases of very low penetration rates and traffic volumes, the number of CV are summed not in a cycle-to-cycle basis but in bigger intervals (e.g. 5-15 minutes). For example, if only one CV passes through the intersection during cycle k und turns right, the measurement equation gives a value of 100% for right-turners in case the measurements are updated every cycle. If during the next cycle $k+1$ two CV go straight, the right-turners measurement would be 0%. Using the combined measurements from the two cycles gives a more moderate measurement calculation of 33% right-turners. This example does not prove the correctness of the one or the other possible measurement calculation, but it demonstrates the thought process behind choosing larger update intervals, especially for low penetration rates and low volumes.

It must be mentioned that the filter for the turning rate runs still every cycle (e.g. ca. every 60 seconds). The difference is that the measurement vector is updated in larger intervals (e.g. ca. every 300 seconds). For the cycles that have no new updated measurements, the filter uses only the process model and ignores the "correct" step. In other words, it is chosen to update the turning measurements less often, to avoid extreme values due to extremely low sample sizes.

The turning measurement is calculated only after crossing the stop-line and entering the next road section. One could include the intention of the driver (e.g. via activation of the turning signal or via chosen route in navigation device) to get the measurements earlier.

Measurements from Connected Section (z_k^{CS})

With the latest advancements in video analytics and computer vision, it is possible to track the trajectories of vehicles in real-time without the need of V2I communication. Hence, the thought process behind the formulation of the measurement equations from a Connected Section (e.g. camera) is equivalent to those from CV. However, there is a fundamental difference; the Connected Section is not limited by the penetration rate but it is limited by a certain detection range (Figure 3.6).

It is assumed that vehicles that are in range of the Connected Section can be tracked. From the trajectory information, the number of vehicles in the queue at the beginning of the signal cycle k (D_k^{CS}) and the number of queued vehicles that joined the queue during cycle k (A_k^{CS}) can be calculated. They are both limited by the maximum coverage (C_k^{CS}) of the Connected Section. Moreover, the time that the last queued vehicle (CSV_k^q) crossed the stop-line ($T_k^{crossing}$) and the time that the last vehicle (CSV_k^j) joined the queue ($T_k^{joining}$) can be derived. With this information, it is possible to formulate the necessary measurement equations.

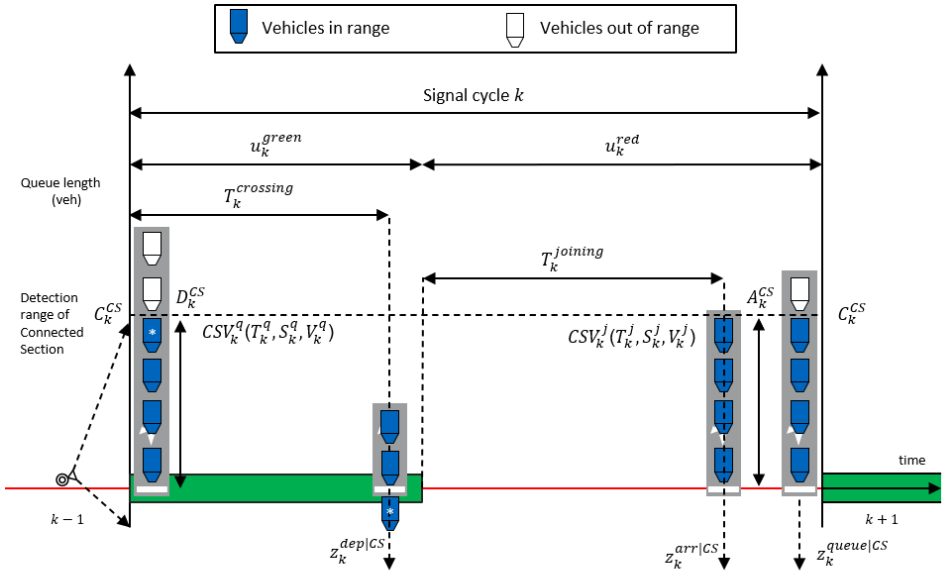

CSV_k^q:	Last queued vehicle detected by the Connected Section at the start of signal cycle k.	CSV_k^j:	Last vehicle detected by the Connected Section that joined the queue during signal cycle k.
T_k^q, S_k^q, V_k^q:	Timestamp, location and speed of CSV_k^q.	T_k^j, S_k^j, V_k^j:	Timestamp, location and speed of CSV_k^j.
D_k^q:	Total number of vehicles in range, departing the queue.	A_k^j:	Total number of vehicles in range, joining the queue.
C_k^{CS}:	Coverage (range) of Connected Section.		
$T_k^{crossing}$:	Time duration from start of signal cycle k until CSV_k^q crosses the stop line.	$T_k^{joining}$:	Time duration from start of red time of cycle k until CSV_k^j joins the queue.

Figure 3.6 Measurements from Connected Section

i. Departure rate ($z_k^{dep|CS}$)

The departure rate measurement ($z_k^{dep|CS}$) uses the number of queued vehicles (D_k^{CS}) detected and the time needed for the last detected vehicle to cross the stop-line ($T_k^{crossing}$):

$$z_k^{dep|CS} = \frac{D_k^{CS}}{T_k^{crossing}} \ (veh/s) \tag{3.39}$$

ii. Arrival rate ($z_k^{arr|CS}$)

The arrival rate measurement ($z_k^{arr|CS}$), uses the number of vehicles that joined the queue (A_k^{CS}) and the time that the last vehicle joined the queue ($T_k^{joining}$):

$$z_k^{arr|CS} = \frac{A_k^{CS}}{T_k^{joining}} \ (veh/s) \tag{3.40}$$

iii. Queue length ($z_k^{queue|CS}$)

Similarly to the queue measurement from CV, the queue length from CS can be calculated based on the position of the last detected vehicle (CSV_k^j) and the expected queue formation for the remaining $\left(u_k^{red} - T_k^{joining}\right)$ seconds of the cycle k:

$$z_k^{queue|CS} = A_k^{CS} + \frac{A_k^{CS}}{T_k^{joining}} \times \left(u_k^{red} - T_k^{joining}\right) \tag{3.41}$$

iv. Turning rate ($z_k^{turn|CS}$)

For the turning measurements it is assumed that the detection area covers also the beginning of the outgoing road section (i.e. after the stop-line) in order to distinguish between the turning movements of the vehicles. Practically, this can also be done by re-identification of the vehicles that enter the next road section if the next intersection is also equipped with similar sensors. Hence, the calculation of the turning measurement is simply:

$$z_k^{turn|CS} = \frac{Number\ of\ detected\ vehicles\ that\ turn}{Total\ number\ of\ detected\ vehicles}\ (\%) \tag{3.42}$$

Measurements from Aggregated Section ($z_k^{queue|DV}$, $z_k^{queue|TT}$)

In this thesis, the term Connected Vehicles refers to vehicles that can communicate their individual trajectory information to the infrastructure (traffic signal) in real-time. Traffic data providers (e.g. TomTom, Inrix, Here) do not offer individual trajectory information due to privacy or data ownership issues. Instead, only Aggregated Section measurements, such as travel times and speeds are available. Measurements for road sections und sub-sections are usually attainable through dedicated interfaces. This information can be considered of low resolution and in some cases even of low quality. However, both speeds and travel times can be used as indicators for congestion and therefore as rough measurements for queue length at intersections. The measurement equation based on difference in velocities (DV) between adjacent subsections is indicated with $z_k^{queue|DV}$ and the one based on travel times (TT) with $z_k^{queue|TT}$ (Figure 3.7).

The left part of Figure 3.7 depicts how from the aggregated speed information, a measurement for the queue length can be derived. Typically, traffic data providers, divide the road sections into subsections according to the speeds observed. The red subsection indicates very low speeds and thus congested sections. The green subsection indicates free flow speeds and thus sections that are unaffected from the congestion. Usually, between the green and the red subsections there can be one or two more shades of colouring that indicate congestion levels between complete congestion and free flow. This can vary between traffic providers but the main concept of red sections indicating congested areas is universal. The simple measurement equation for extracting a rough measurement of the queue length is in this case:

$$z_k^{queue|DV} = L_k^{DV}, \qquad if\ V_k^{subsection\ 1} < a_k^{DV} \times V_k^{freeflow} \tag{3.43}$$

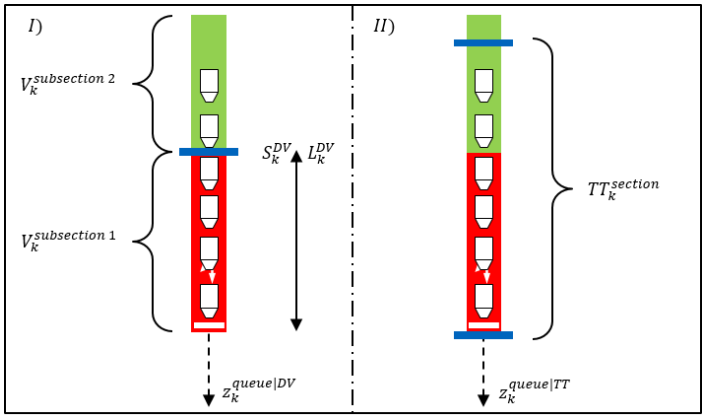

Figure 3.7 Measurements from Aggregated Section

The number of vehicles in queue (L_k^{DV}) is calculated from the distance (S_k^{DV}) between the end of the congested section and the stop line, assuming an average vehicle length of 6 meters. The parameter a_k^{DV} can be adjusted according to the data provider and/or the specific intersection. A typical value for a_k^{DV} is for example 0.65. That means, subsections with speed lower than 65% of the observed free flow speed are considered congested. The value for the free flow speed is given from all traffic data providers.

The most usual information from aggregated traffic data providers is the travel time. The travel time of a section is expected to variate even in free flow conditions. However, in highly congested signalized sections, high travel times can be related to the increase in queue. Hence, only travel times that are significantly higher than typical free flow travel times are considered:

$$z_k^{queue|TT} = TT_k^{section}, \qquad if\ TT_k^{section} > a^{TT} \times TT_k^{freeflow} \tag{3.44}$$

The factor a^{TT} can be set depending on the intersection and the road section. For example, it can be set to include the typical free flow travel time plus the typical red time. Assuming 30 seconds typical red time and 30 seconds typical travel time, factor a^{TT} can be set to 2. That means, according to (3.44), that only travel times higher than 60 seconds are considered.

Since this measurement is not a direct measurement, the definition of a the appropriate $h()$ is needed to relate the travel time to the queue length (3.2). For that, a simple power function is used:

$$z_k^{queue|TT} = \alpha \times (x_k^{queue})^{\beta} \tag{3.45}$$

The factors α and β of equation (3.45) can be set according to real observations, simulations or even by experience (see also chapter 4).

The measurements coming from aggregated traffic data are not expected to be very accurate, but they are a reliable indicator of congestion in urban areas. Especially in oversaturated conditions, these measurements give the possibility to detect very long queues that cannot be

detected by infrastructure sensors. The obvious drawback is that these measurements become available only after the congestion has occurred. Including late important information is considered in this thesis however better than ignoring the information. The key is to fuse all available information in a transparent and adaptive way.

3.4 Adaptive Fusion

Integrating all measurements in one *variable-dimension* vector is only the first step of the fusion process. The next crucial step is the "weighting" of each measurement according to how much each measurement should be "trusted" for the specific implementation. This "trust" is determined by choosing the appropriate measurement noise covariance (R_k) and process noise covariance (Q_k). If Q and R are constant and they refer to a steady-state process, the Kalman gain (K_k) and estimation error covariance (P_k) stabilize quickly. In this case, Q and R could be calculated off-line. Generally, the measurement noise covariance can be calculated easier by taking some sample off-line measurements. The process noise covariance is more difficult to define, since directly observing the *actual* process is not possible (the observation of the ground truth is in fact another measurement). However, in many real-world applications, neither the errors of the measurements nor of the process remain constant. Tuning a Kalman filter means mainly choosing the parameters Q and R. A first initial rational choice should be followed with off-line tuning before the real-time implementation [WELCH & BISHOP, 2001].

The Extended Observer deals with a process in which both the measurement and the process error change dynamically. For example, the measurement error from CV is expected to reduce for higher penetration rates. At the same time, the process error for the queue length is expected to increase for higher queues. The proposed formulation allows the updating and resizing of the measurement vector, for each filter step, depending on the data availability. It allows additionally the recalculation of the process and measurement error covariance (Q_k, R_k) at every filter step. Figure 3.8 shows how the adaptive fusion takes place in the operational diagram of the EKF algorithms. The adaptive fusion is described in detail only for the case of the queue length, which is the most challenging. The approach can be summarized with the following steps:

- Update the process error covariance Q_{k-1}^{queue} based on the last state estimation $\hat{x}_{k-1}^{queue}$, before the calculation of the *a priori* estimate error covariance P_k^{-queue}.
- Check the data availability from the Connected Environments for current filter step k before computing the Kalman gain $K_k^{queue|CE}$.
- Resize the matrices $H_k^{queue|CE}$, $V_k^{queue|CE}$, $R_k^{queue|CE}$ according to the number of measurements m from the Connected Environments.
- Update the measurement error covariance $R_k^{queue|CE}$ based on the available measurements $z_k^{queue|CE}$ and the *a priori* state estimation $\hat{x}_{k-1}^{-queue}$.

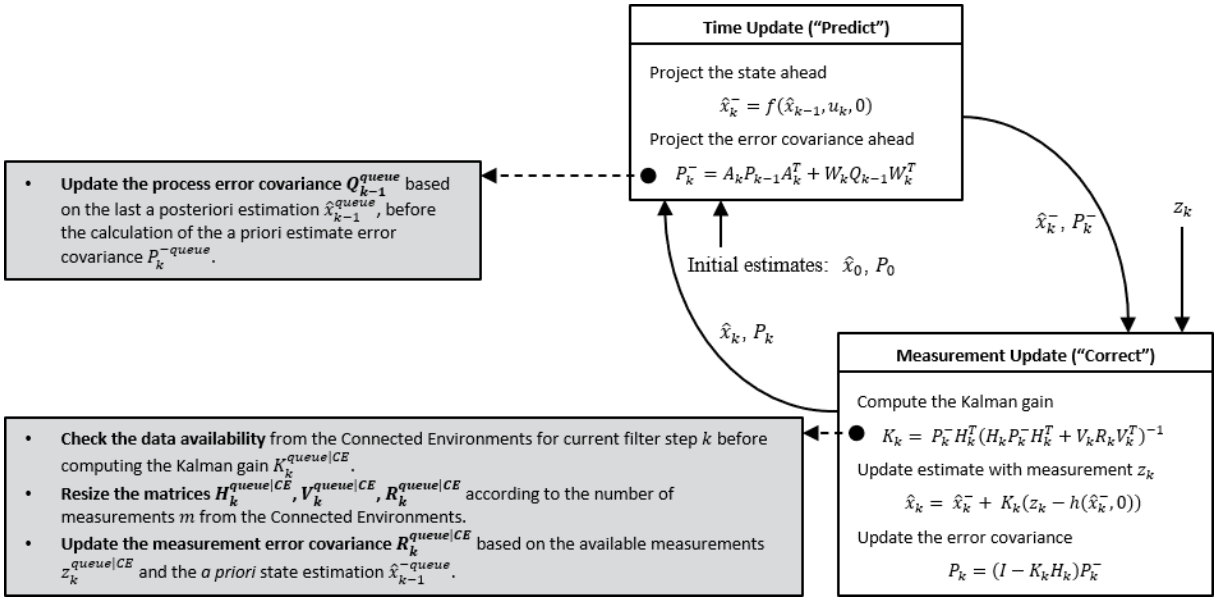

Figure 3.8 Adaptive traffic data fusion with the Extended Observer

Based on equations (3.2), (3.28), (3.29) and (3.44), the complete measurement equation for the queue length is:

Measurement equation for queue:

$$z_k^{queue|CE} = \begin{bmatrix} z_k^{queue|CV} \\ z_k^{queue|CS} \\ z_k^{queue|DV} \\ z_k^{queue|TT} \end{bmatrix} = \begin{bmatrix} x_k^{queue} \\ x_k^{queue} \\ x_k^{queue} \\ \alpha \times (x_k^{queue})^{\beta} \end{bmatrix} + \begin{bmatrix} v_k^{queue|CV} \\ v_k^{queue|CS} \\ v_k^{queue|DV} \\ v_k^{queue|TT} \end{bmatrix} \tag{3.46}$$

with:

$v_k^{queue|CS}$: queue measurement noise from CS (veh)

$v_k^{queue|CV}$: queue measurement noise from CV (veh)

$v_k^{queue|DV}$: queue measurement for noise from DV (veh)

$v_k^{queue|TT}$: travel time measurement noise from TT (sec)

Each measurement noise has its own error covariance. The complete measurement noise covariance $R_k^{queue|CE}$ is therefore a diagonal matrix of $m \times m$ dimensions, where m is the number of measurements.

$$R_k^{queue|CE} = \begin{bmatrix} R_k^{queue|CS} & 0 & 0 & 0 \\ 0 & R_k^{queue|CV} & 0 & 0 \\ 0 & 0 & R_k^{queue|DV} & 0 \\ 0 & 0 & 0 & R_k^{queue|TT} \end{bmatrix} \tag{3.47}$$

with:

$R_k^{queue|CS}$: queue measurement noise covariance from CS (veh)

$R_k^{queue|CV}$: queue measurement noise covariance from CV (veh)

$R_k^{queue|DV}$: queue measurement for noise covariance from DV (veh)

$R_k^{queue|TT}$: travel time measurement noise covariance from TT (sec)

The matrix is diagonal with the assumption that the measurement noises of the individual measurements are not correlated. The calculation of $R_k^{queue|CE}$ should involve off-line measurements for tuning of the filter. This effort however might be considered expensive for large scale deployments and might limit the real-world attractiveness of the proposed methodology. To avoid this limitation, the proposed algorithms allow the immediate implementation, without the need for extensive, off-line tuning. It must be however stressed that an optimal (in terms of minimum error) estimation can only be achieved with respective tuning efforts. On the other hand, for traffic engineers and operators of real-world systems, a less than optimal estimation might suffice, if the method is relatively easy to understand, implement and fine-tune.

3.5 Summary

EKF offers a robust and transparent data fusion method that exploits multiple direct and indirect measurements, with different errors, that arrive at different times. The Extended Observer uses multiple, variable-dimension, adaptive EKFs, to estimate the queue length, arrival, departure, turning and penetration rate. The process equation for the queue length utilizes the conservation law and the signal timings. It is presented in detail, with the help of Figure 3.3. In addition, the formulas for prediction and second-by-second formulation are presented for the queue length. The other states can be modeled with a random walk or with the help of a historical model.

Measurement equations are presented in detail for Connected Sections, Connected Vehicles and Aggregated Sections. The measurements for CV (Figure 3.5) build mostly on the algorithms of COMERT [2013, 2016], for steady state estimation in longer intervals. The proposed algorithms for Connected Section (Figure 3.6) and Aggregated Section (Figure 3.7)

are simple formulations with realistic assumptions. The information needed for all algorithms is basic trajectory information.

The adaptive formulation of the Extended Observer allows the update of number of measurements, the measurement errors, and the process error at every filter step. Figure 3.8 depicts the step-by-step formulation, based on the basic EKF formulation (Figure 3.1). The importance of the adaptive formulation, in the case of UTCS, is highlighted in the state-of the-art (chapter 2), and becomes even more evident in the analysis (chapter 4).

4. Analysis

The algorithms of the Extended Observer deal with queue dynamics at signalized intersections. Before evaluating the results of the developed module, it is important to analyze in detail the behavior of the filter in these highly unstable conditions. This chapter, combined with the methodology, aims to answer the first research question regarding the ability to use diverse measurements in a practical and adaptive way. The analysis aims to demonstrate:

- the traffic state and traffic measurements variability at signalized intersections
- the principles and limitations of the presented methodology

For that, time series diagrams on a cycle-to-cycle basis are mainly used for clarifications. The focus is on queue length which is the hardest to estimate and the easiest to relate. Example diagrams for arrival and departure rate are also provided. The diagrams represent typically 2-hour simulation runs, where the ground truth, the measurements, and the fused estimation can be compared. The current chapter is not aiming to examine different scenarios (e.g. increasing penetration rates) and perform sensitivity analysis (e.g. reduction in delays). This will take place in chapter 5. However, some statistical values, such as Root Mean Square Error (RMSE) are also here indicated to complement the diagrams of the analysis. Figure 4.1 shows the concept and structure of the analysis.

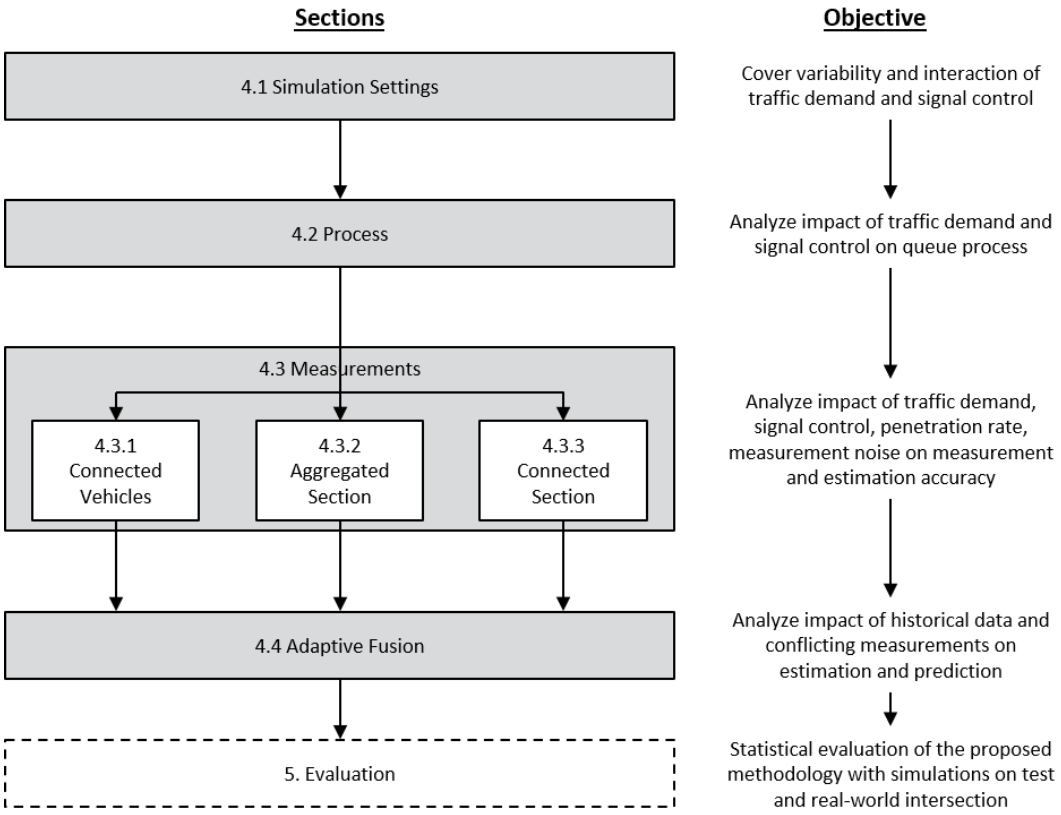

Figure 4.1 Analysis approach overview

First, the test intersection is introduced in order to cover not only the traffic demand variability but also the interaction with the signal control (section 4.1). In section 4.2, the impact of variable demand and control on the queue process is shown. Moreover, this section illustrates that the chosen simulation settings cover a wide range of traffic state dynamics for the analysis and later for the evaluation. The diversity of the measurements from Connected Vehicles, Aggregated Sections and Connected Sections are examined in 4.3. Some key elements of the of the proposed data fusion, considering the practical applicability are demonstrated in section 4.4.

4.1 Simulation Settings

A robust estimation should work not only independent of the traffic demand, but also independent of the underlying signal control and resulting saturation degree. Fixed-time control and steady traffic demand patterns are avoided for the analysis and evaluation. A simple four-legged intersection (one lane per leg) with two stages separating the conflicting streams is used as a test intersection for transparency. Figure 4.2 illustrates the traffic demand patterns, the traffic signal control configuration and the detector topology.

The traffic demands on the respective signals are chosen to cover different and changing saturation degrees to emulate the (transition to and from) peak hour. Signal Groups (SG) SG 1 and SG 3 are controlling the traffic streams in the minor traffic direction, with low traffic demand and reduced green split. SG 2 and SG 4 are controlling the traffic streams in the major traffic direction, with high traffic demand and higher green time share. Notice that for SG 4 there are two different traffic demand scenarios. A normal oversaturated peak and an extended oversaturated peak. The traffic demand from each direction is variable and stochastic around the values depicted in Figure 4.2.

The rule-based control is a simple second-by-second, time-gap control that uses detectors, placed approximately 50 meters away from the stop line. The model-based control (Spot/Utopia) uses the entry and exit detectors to update the queues for each signal every 3 seconds. The entry detectors are placed far away from the stop-line (300m) and provide very accurate queue length estimations.

4.2 Process

The queue process to be estimated is modelled with the help of equation (3.12). As described in section 3.4, the process noise covariance Q_k^{queue} is generally difficult to calculate. This becomes even more challenging in the case of queue length estimation, due to the stochastic nature of queues at signalized intersections. Figure 4.3 shows the queue length (average value vs. standard deviation) for multiple simulation runs of the test intersection with different control methods (fixed-time, rule-based, model-based). The fixed-time control is used to emulate adaptive control that has been outdated and runs constantly with maximum green times. It is

evident that the queue variance differs significantly between simulation runs because of stochastic arrivals and the influence from the signal control. For example, the standard deviation of the queue for SG 4 with identical rule-based control ranges between 5 and 50 vehicles between simulation runs.

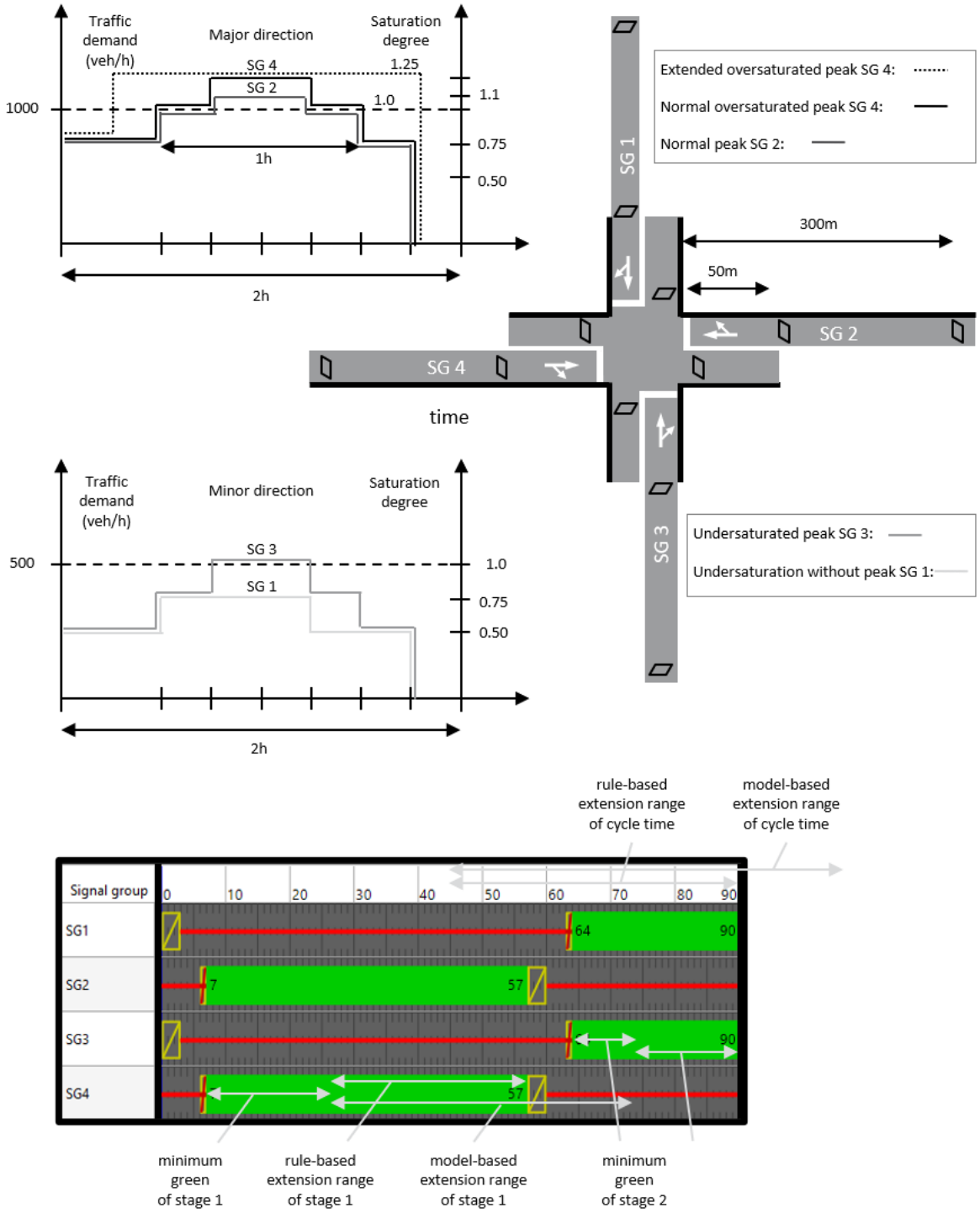

Figure 4.2 Traffic demand and traffic control settings for analysis and evaluation

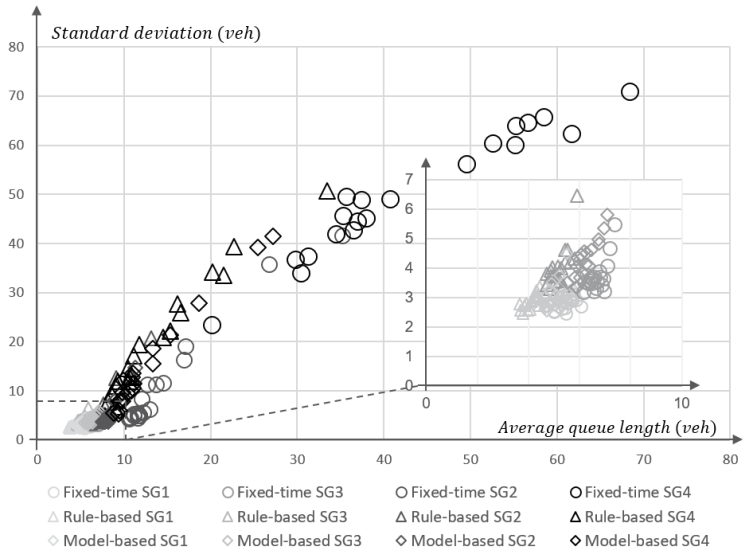

Figure 4.3 Average queue length and average standard deviation for multiple simulation runs

For mostly undersaturated conditions (see zoomed area in Figure 4.3 for SG1 and SG3), the standard deviation of the queue ranges from around 3 vehicles to 7 vehicles, whereas the average queue ranges from 4 to 8 vehicles for all signal control methods. Naturally, the average queue length is higher for fixed-time control than for rule-based and model-based control.

For mostly oversaturated conditions, the queue variance and average queue length ranges between from 10 to 70 vehicles. In general, oversaturation leads to larger variance. In addition, the model-based control leads to lower average queue but cannot limit so much the queue variance from the oversaturation. This shows that the process noise covariance for modelling the queue length should not be a constant value, even for this simple simulated test intersection.

The purpose of Figure 4.3 is not to derive one formula for correlating the average queue length and the standard deviation. However, it highlights the challenges when dealing with the queue process at signalised intersections. Furthermore, it suggests that the variance increases as the queue increases. Moreover, it shows that the chosen simulation configurations with different traffic demands for conflicting signals cover a wide range of traffic states and are therefore suitable for fundamental analysis of the algorithms.

In order to solve the issue of the high variability of the process error (and the difficulty of its calculation) the Extended Observer allows an adaptive calculation of Q_k^{queue} based on the following intuitive assumption: higher expected queue means higher expected uncertainty of the queue model. To avoid overfitting a formula to a simple test intersection and dismiss any need for extra tuning or calibration, it is assumed that the expected process error would be equal to the estimated queue. The following formula is used to update the queue process noise covariance:

$$Q_{k-1}^{queue} = \hat{x}_{k-1}^{queue} \tag{4.1}$$

This assumption can be easily integrated in the step-by-step formulation, by updating the Q_{k-1}^{queue} during the prediction step (Figure 3.8). Figure 4.4 shows schematically the concept of using an adaptive process noise covariance based on equation (4.1) instead of a constant process noise covariance based on average observed values. A constant error assumption means for example that the same error is expected in the estimation for 5 or 50 queued vehicles.

As discussed in chapter 3, the ratio Q/R defines the performance of the filter and not the actual Q and R values. The use of simple equality in (4.1) is not affecting the performance of the filter, if the measurement noise covariance R_k^{queue} is calculated based on Q_{k-1}^{queue}, without changing the $R_k^{queue}/Q_{k-1}^{queue}$ ratio (see also next section). The rest of the state variables are modelled either with a random walk or based on a historical model. Therefore, a constant process noise covariance from experience is considered sufficient for this thesis.

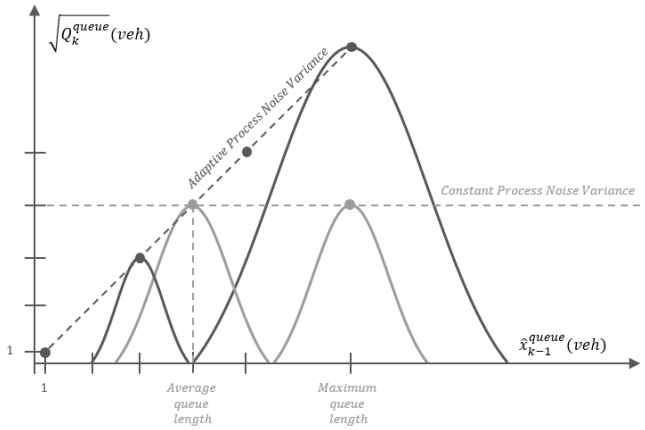

Figure 4.4 Adaptive and constant process noise covariance - schematic clarification

4.3 Measurements

The Extended Observer enables sensor and data fusion according to the expected measurement error, which is depicted with the measurement noise covariance matrix $R_k^{queue|CE}$, as shown in equation (3.47). If the ground truth can be observed, calculating the measurement noise covariance for a certain time is straightforward; it equals the Mean Square Error (MSE) of the measurement. In theory, the specifications of sensors (such as cameras) would give values for the expected errors. However, expected errors from Connected Vehicles or Aggregated Section data are in practice very hard to get. In addition, the errors vary greatly depending on the data provider, the city, the topology of the intersection and other external factors (i.e. disturbances).

The process noise covariance (Q_{k-1}^{queue}) is updated at every filter step, based on the last queue estimation (see section 4.2), during the "predict" step of the filter (Figure 3.8). During the "correct" step of the filter, the measurement noise covariance comes into play to compute the Kalman gain, that ultimately decides on the weighting between measurements and model. Instead of defining the measurement noise covariance (R_{k-1}^{queue}), it is proposed to define the noise covariance ratio $\frac{R_k^{queue}}{Q_{k-1}^{queue}}$. This allows a very straight forward tuning of the filter: increasing the noise ratio for one measurement means that this measurement is trusted less and therefore its impact on the estimation is lower.

Section 4.3.1 starts with the analysis for CV measurements. First, the process and noise covariance for different penetration rates is examined. The analysis of the measurement and estimation accuracy is presented with the help of cycle-to-cycle queue diagrams. The impact of the penetration rate and saturation degree is highlighted. The effect of changing the noise covariance ratio ($\frac{R_k^{queue|CV}}{Q_{k-1}^{queue}}$) is also demonstrated. Section 4.3.2 examines the utilization of travel time and speeds from Aggregated Sections for queue estimation. Section 4.3.3 examines the use of cameras for arrival and departure rate estimation.

The underlying signal control for the diagrams presented in the following sections of this chapter is a rule-based control to enable one to one comparison between diagrams. The reason is that a simulation run with rule-based control can be precisely repeated. A simulation run with model-based control cannot be perfectly duplicated, due to certain stochastic characteristics of the control (e.g. random arrivals before reaching the detector). The analysis focuses on mainly on signal groups SG 2 and SG 4 of the major direction (Figure 4.2).

4.3.1 Connected Vehicles

Using the simulation environment of the test intersection, the average RMSE of the CV measurements is calculated for different penetration rates and multiple simulation runs, to obtain the measurement noise covariance. In addition, the process noise covariance is calculated based on the cycle-to-cycle variance of the ground truth for the queue length. Figure 4.5 presents the ratio results for signals SG 1 (lowest demand) and SG 4 (highest demand). The 2-hour simulation runs shown in Figure 4.2 are repeated 10 times with different random seeds.

The results indicate a trend for the noise covariance ratio below one for low demand and above one for high demand. The higher error for higher demand (and consequently higher saturation degrees) can be explained by the higher queues and by the stop-and-go behaviour in oversaturation, that leads to slow-moving vehicles being recognized in and out of the queue in consecutive cycles. Moreover, the results, especially for low demands, indicate a reduction of the noise covariance ratio as the penetration rate increases. This is expected due to the higher possibility for the CV to be on the "write place" (i.e. close to queue back-end).

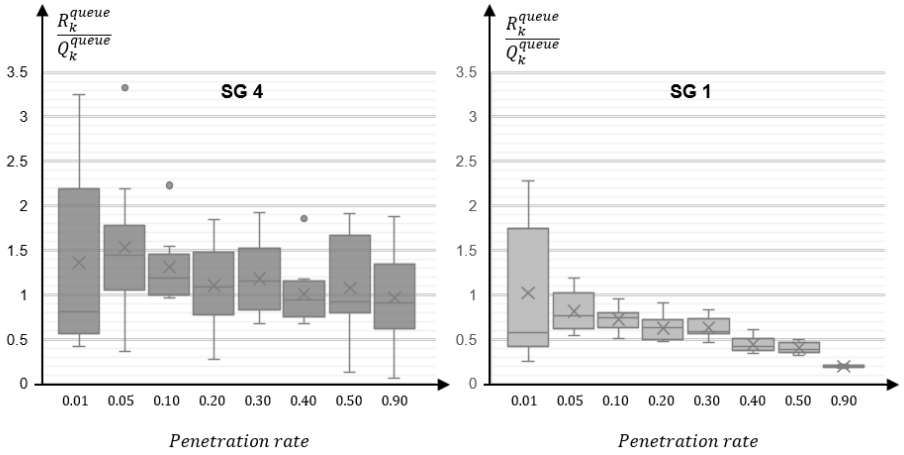

Figure 4.5 Ratio of measurement to process noise covariance for queue length

To capture these intuitive sensitivities of CV measurements, the $R_k^{queue|CV}$ is updated at every filter step (i.e. every cycle), based on the formula:

$$R_k^{queue|CV} = \begin{cases} Q_{k-1}^{queue} & ,EO\ basic\ formulation \\ Q_{k-1}^{queue}(1-\hat{x}_{k-1}^{pen}) & ,EO\ with\ penetration\ rate\ estimation \end{cases} \quad (4.2)$$

For very low (estimated) penetration rates, the ratio remains close to one and the filter trusts the CV measurements and the model equally. For high (estimated) penetration rates, the measurement error is reduced and thus the CV measurements are considered more trustworthy.

The analysis focuses mainly on demonstrating the filter in the challenging case of oversaturation with low penetration rates. Thus, signals SG 2 and SG 4 are mostly presented. A moderate filter tuning with constant and equal process and measurement noise covariance ($R_k^{queue|CV} = 10.00$, $Q_k^{queue} = 10.00$) is used. This reduces the performance of the filter, (as shown in the following sections) but makes the analysis easier to follow. A total number of 100 cycles ($k = 100$) is demonstrated in each diagram. The average penetration rate for the examined simulation run is 5 %.

First, the impact of variable traffic demand and saturation degree on the measurements is demonstrated with the help of Figure 4.6. Then, the impact of increased penetration rate is explained with the help of Figure 4.7. Figure 4.8 and Figure 4.9 showcase the impact of measurement noise on the estimation accuracy.

Impact of variable traffic demand and saturation degree on measurement accuracy

Traffic demand and thus saturation degree (i.e. volume to capacity ratio) can vary greatly during the day and even more importantly the changes might occur sharply. The ability to follow changes might be considered more essential than the estimation of a steady state in the case

of filtering for signal control. Hence, varying traffic demand scenarios are simulated for the analysis.

Figure 4.2 shows the configured inflows for the examined signals. The arrivals per cycle in the simulation vary around these values due to the stochastic nature of the simulation. The arrival and departure rate process equations follow a random walk. The parameters for the presented simulation run are shown in Tab. 4.1.

EO parameters for Figure 4.6 and Figure 4.7			
EKF Parameter	**Departure Rate (vehicles/sec)**	**Arrival Rate (vehicles/sec)**	**Queue Length (vehicles)**
$\hat{x}_0$	0.50	0.20	3.00
P_0	0.10^2	0.10^2	1.00^2
Q_k	0.10^2	0.10^2	10.00^2
R_k	0.10^2	0.10^2	10.00^2

Tab. 4.1 Intuitive tuning of the Extended Observer for chapter 4

An indicative simulation run of mostly undersaturated cycles (i.e. queue lower than 12 vehicles for SG 2) is presented in Figure 4.6. The crosses (x) indicate the ground truth, the blue circles (o) indicate the measurements coming from the CV and the filled gold circles (•) indicate the estimation coming from the Extended Observer. Cycles with no information from CV are depicted below the zero line. In other words, missing cycle measurements are plotted as circles with the value -1. Obviously, these values are excluded from the calculation of the RMSE from the CV. The queue measurement is calculated with equation (3.37) and is generally very close to the ground truth considering the average queue length and its standard deviation.

In Figure 4.6.a, two wrong low measurements jump out from the plots between simulation second 4000-5000, where oversaturated cycles with stop-and-go behavior appear. The incorrect measurements appear, because the CV is first in the queue and at the same time the arrival measurement part from equation (3.37) gives extremely low values.

Figure 4.6(b) shows however that the CV measurements might capture sudden peaks of queue length even for low penetration rates. Nevertheless, Figure 4.6.c shows clearly that the CV measurements in cases of oversaturation cannot be trusted uncritically. The large measurement errors appear where the number of oversaturated cycles increases. This can be explained by the stop-and-go behavior of the queued vehicles. For example, a slowly moving CV might not be viewed as queued vehicle depending on its speed at the end of red time. At the same time, another CV closer to the stop-line might be recognized as the last queued CV and thus trigger a wrong queue measurement calculation.

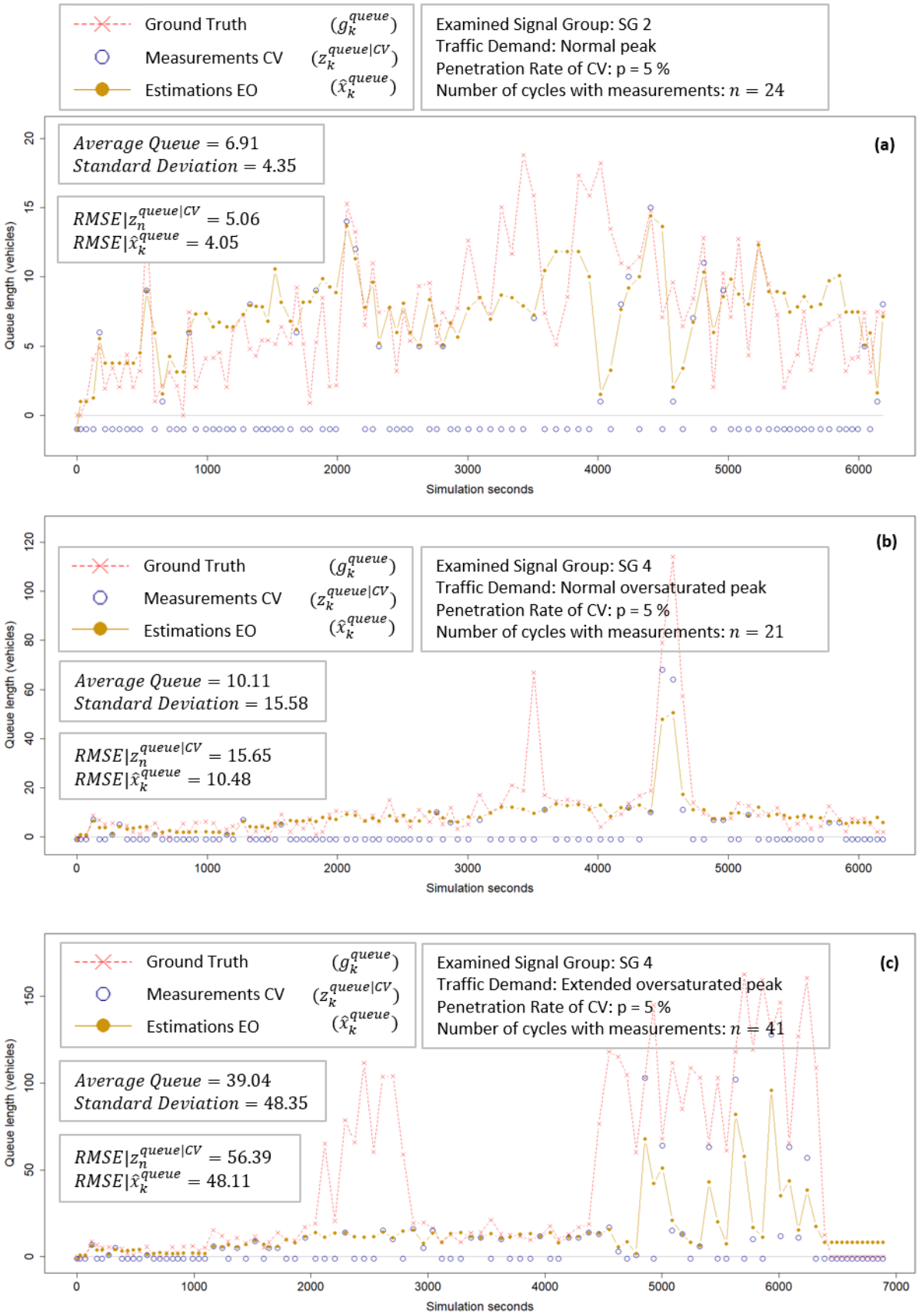

Figure 4.6 Impact of traffic demand on measurement accuracy

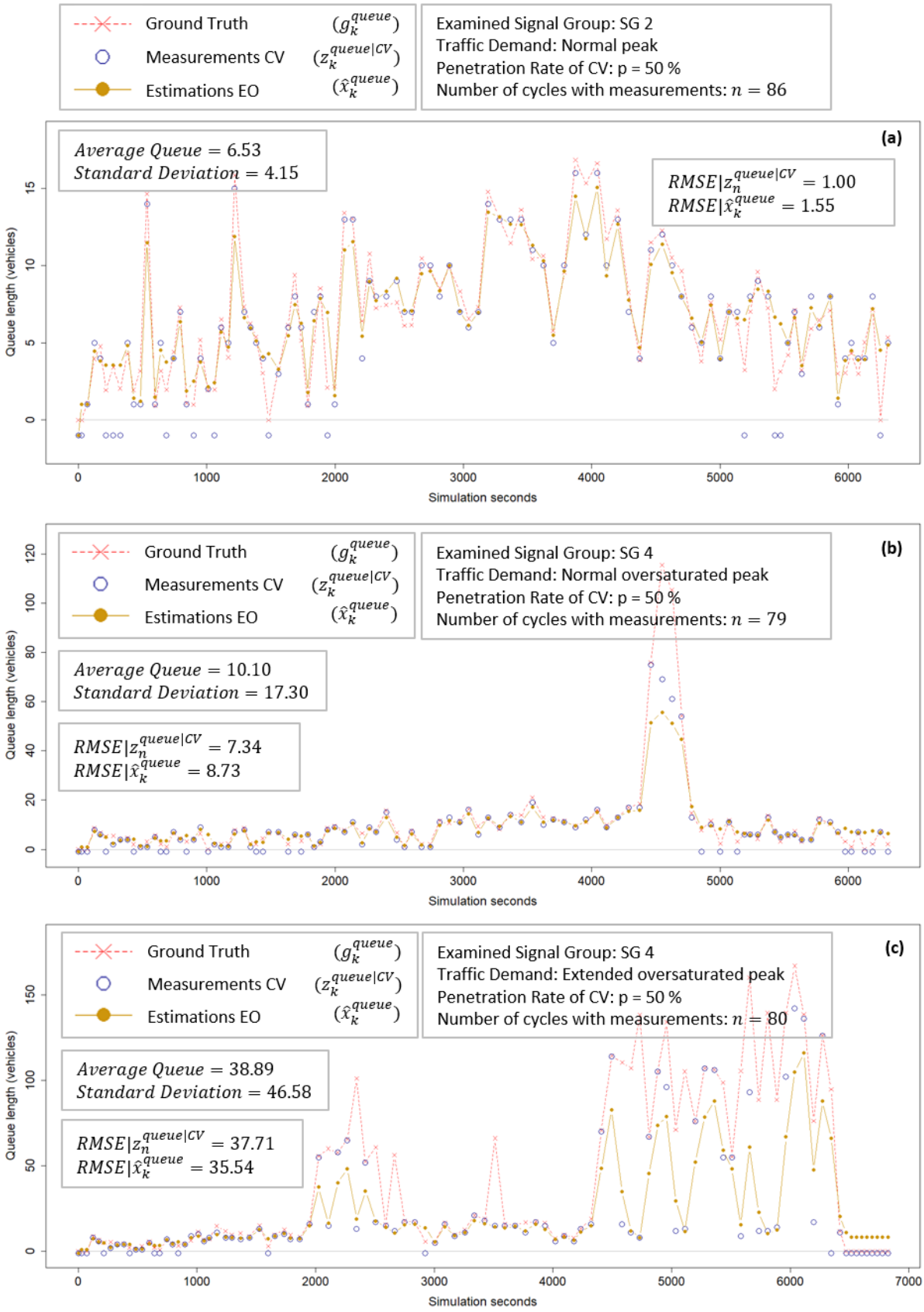

Figure 4.7 Impact of penetration rate on measurement accuracy

Impact of penetration rate on measurement accuracy

One might jump into the conclusion that the issue of large CV measurement errors is only due to the limited penetration rate of the presented example. This is partially true. For undersaturated conditions increasing penetration rates decrease the errors, since the probability of CV to be at the back-end of the queue is higher. However, in cases of oversaturation, the issue of stop-and-go is the main source of errors. Therefore, even extremely high penetration rates are bound to provide incorrect cycle-to-cycle measurements.

Figure 4.7 shows the results for the same random seed, traffic demand and control as before, but for 50% penetration rate of CV. Clearly, based on Figure 4.7.a and Figure 4.7.b, such a high penetration rate reduces dramatically the measurement and estimation error. However, Figure 4.7.c shows that the errors remain high during the long oversaturation period due to the instability of the CV measurements. Figure 4.6 and Figure 4.7 show that for the same random seed, the error from CV measurements can change drastically depending on saturation degree and penetration rate. This suggests the need for filtering even in high penetration rates.

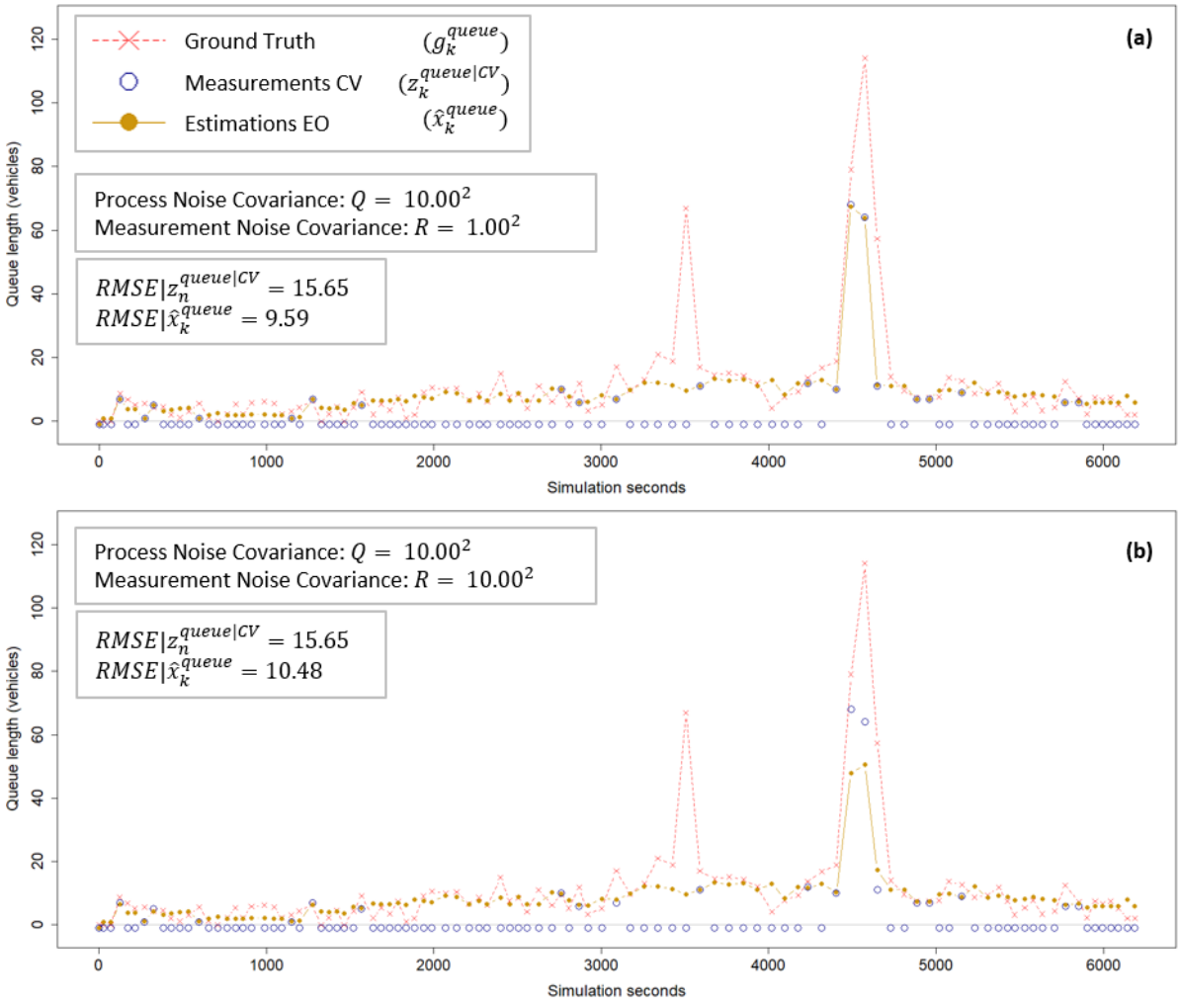

Figure 4.8 Impact of measurement noise on estimation accuracy - SG4 normal oversaturated peak

Impact of measurement noise covariance on estimation accuracy

The instability of the error of CV measurements makes choosing the measurement noise covariance very difficult. At the same time, the selected noise covariance ratio defines the behavior of the filter. To illustrate this change of behavior, Figure 4.9.a and Figure 4.9.b illustrate the results with different measurement noise covariance, for the same simulation run as shown in Figure 4.6.b and Figure 4.6.c. Figure 4.9 shows how the reduced noise covariance ratio allows the filter to follow the measurements extremely closely. The quality of the measurements remains the same, since the measurements are identical. On the one hand, the oversaturation peak in Figure 4.9.a is better captured by the filter with lower measurement noise covariance. On the other hand, the extended oversaturation peak in Figure 4.9.a leads to very unstable estimations. One way to deal with the instability of CV measurements is to include other types of measurements from Connected Environments in the fusion process, such as Aggregated Section data.

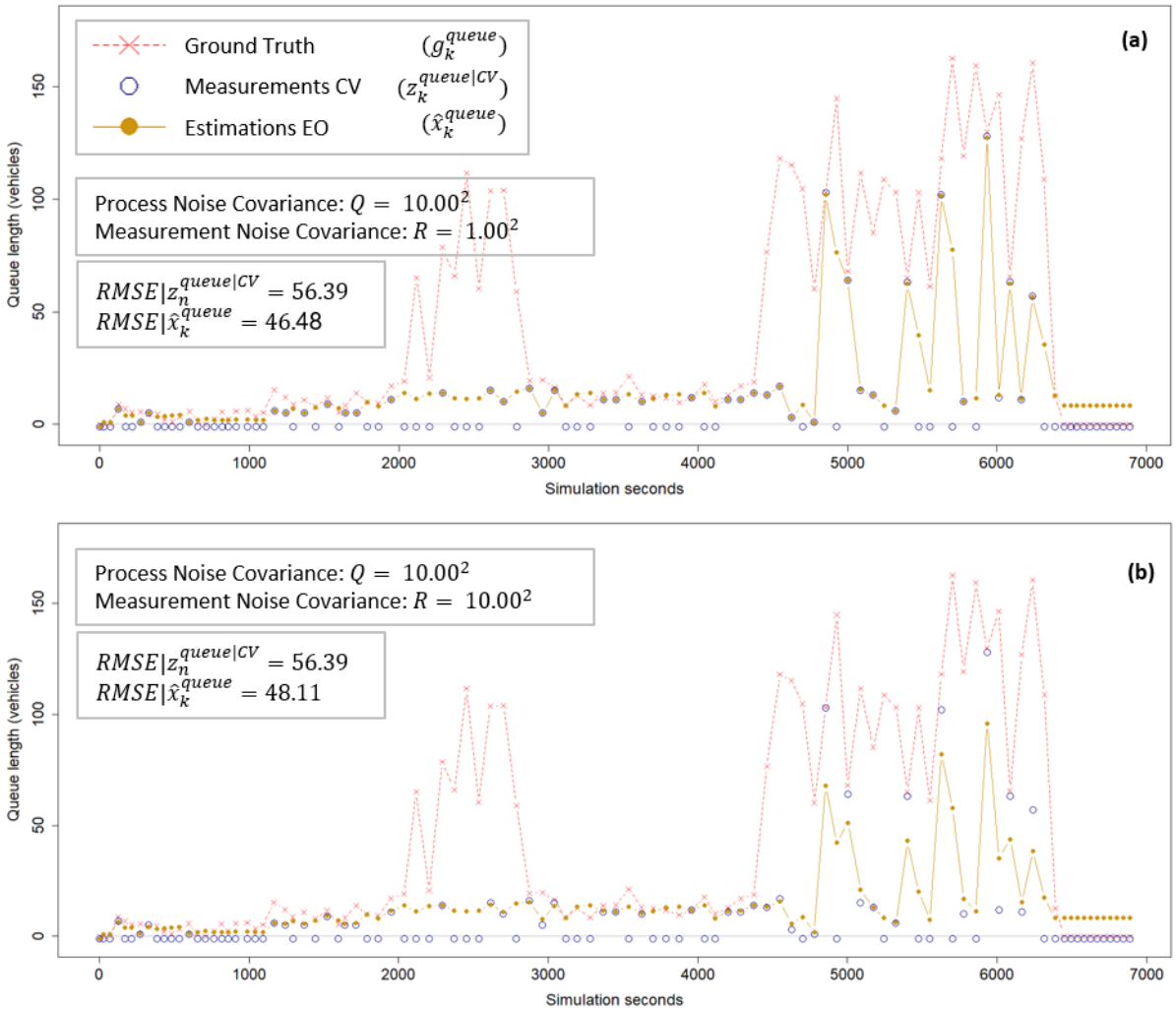

Figure 4.9 Impact of measurement noise on estimation accuracy - SG4 extended oversaturated peak

4.3.2 Aggregated Section

Traffic data providers typically do not give information from individual vehicles, but they provide instead aggregated traffic data, such as travel times for complete sections and speeds of sub-sections. This information is a rather macroscopic view of the traffic situation. These data sources have been ignored from UTCS due to their reduced granularity and questionable quality.

Despite the undeniable uncertainty of Aggregated Section data quality in comparison to infrastructure sensors, this dataset has certain valuable characteristics for UTCS:

- Aggregated Section data is available constantly and thus there are no signal cycles without information.
- Aggregated Section data is available from many data providers that have already large historical data bases and can be therefore used for identifying traffic patterns and abnormalities.

In addition to the uncertain quality, there are some other characteristics that make their integration in signal control challenging:

- No information about the real-time penetration rate.
- No information about the algorithms used for the calculations.

To emulate Aggregated Section data in the simulation environment, the travel time and speed measurements are not derived from the complete vehicle population, but instead only from the simulated CV according to the simulated penetration rate scenario.

Figure A.2.a shows the simulation results for the travel time and queue length for SG 4 (extended oversaturated peak). The travel time measurements (cyan squares) come from 5 % of CV and the ground truth comes from all vehicles (blue crosses). The ground truth of the queue length is also plotted (brown crosses). The (ground truth) travel time peaks follow the (ground truth) queue length peaks. In addition, the travel time measurements are very consistent with the ground truth travel time, despite the low penetration rate.

As mentioned in the methodology, a simple power function (3.45) is used to convert the measured travel times to queue length measurements. The calculation of the scaling factor (α) and exponent (β) can be done in simulations or real-world observations by measuring for certain period the travel time and the queue length. For real implementations, the related effort might be a prohibiting factor for the testing of new algorithms. Hence, a simple way to define the needed factors (α and b) based only on limited travel time measurements, which are nowadays easily obtainable from different data providers, is given here and used in the thesis.

Figure A.2(b) (see Appendix) depicts how an approximate power function can be obtained based on plain travel time measurements for the specific test intersection. The same simplified calculation can be used for any signalized approach based on limited travel time

measurements to avoid cumbersome tuning and overfitting. In any case, this function gives just an approximation of the queue length.

The free flow travel time is defined as the minimum observed travel time (in this case 60 seconds). For this travel time a minimum queue length is defined (in this case, 1 vehicle). This gives the first point to draw the power function. The scaling factor equals thus the free flow travel time (in this case, $\alpha = 60$). The maximum observed travel time (in this case, 160 seconds) and the maximum possible queue length (in this case, 150 vehicles) give the second point. With two points and scaling factor (α), the exponent (β) can be calculated (in this case, $\beta = 0.20$). This set of parameters means for example that an aggregated travel time measurement of around 100 seconds is converted to around 14 vehicles and aggregated travel time measurement of around 130 seconds is converted to around 50 vehicles.

This function naturally is not expected to be accurate, but it improves the overall estimation ability and stability, especially in oversaturated conditions. The filter takes advantage of the fact thar persistently high travel times (in comparison to free flow travel times) are very likely to be the result of oversaturation in front of the signal. To avoid that very low travel time measurements (just above free flow travel time) could pull the estimations unnecessarily down to low values, an extra limit can be defined as “minimum significant travel time” (Figure A.**2**(b)). For travel times below this value, the $R_k^{queue|TT}$ is set to a high value (square of the maximum queue length) to reduce the influence of the travel times in the estimation.

For the measurements based on speeds (and more precisely based on speed differences) according to equation (3.43), a factor of $a_k^{DV} = 0.65$ is used. This value is typical for real-world traffic data providers.

Figure 4.10 shows all measurements from CV and Aggregated Section for the same simulation run as before. The queue length measurements based on the travel time are indicated with squares and the queue length measurements based on speed drops are indicated with triangles. Notice that in many cases, the Aggregated Section measurements are repeated for some cycles. This happens when no new measurement is available, to emulate the experience from real-world traffic data providers.

In Figure 4.10.a it is interesting to notice how the very high incorrect measurement (after second 4000) does not pull the estimation accordingly, due to the presence of the other measurements and the process model. In Figure 4.10(b) and Figure 4.10(c), the Aggregated Section recognize the queue peaks also in cases where the CV failed. As expected, there is a lag in the measurements that leads to overestimation of the duration of the oversaturation.

Overall, the estimation accuracy improves in all cases and especially in oversaturation (compare Figure 4.10 and Figure 4.6). For the fusion, the same measurement noise covariance is used for all measurements ($R_k^{queue|CV} = R_k^{queue|TT} = R_k^{queue|DV} = 10.00$).

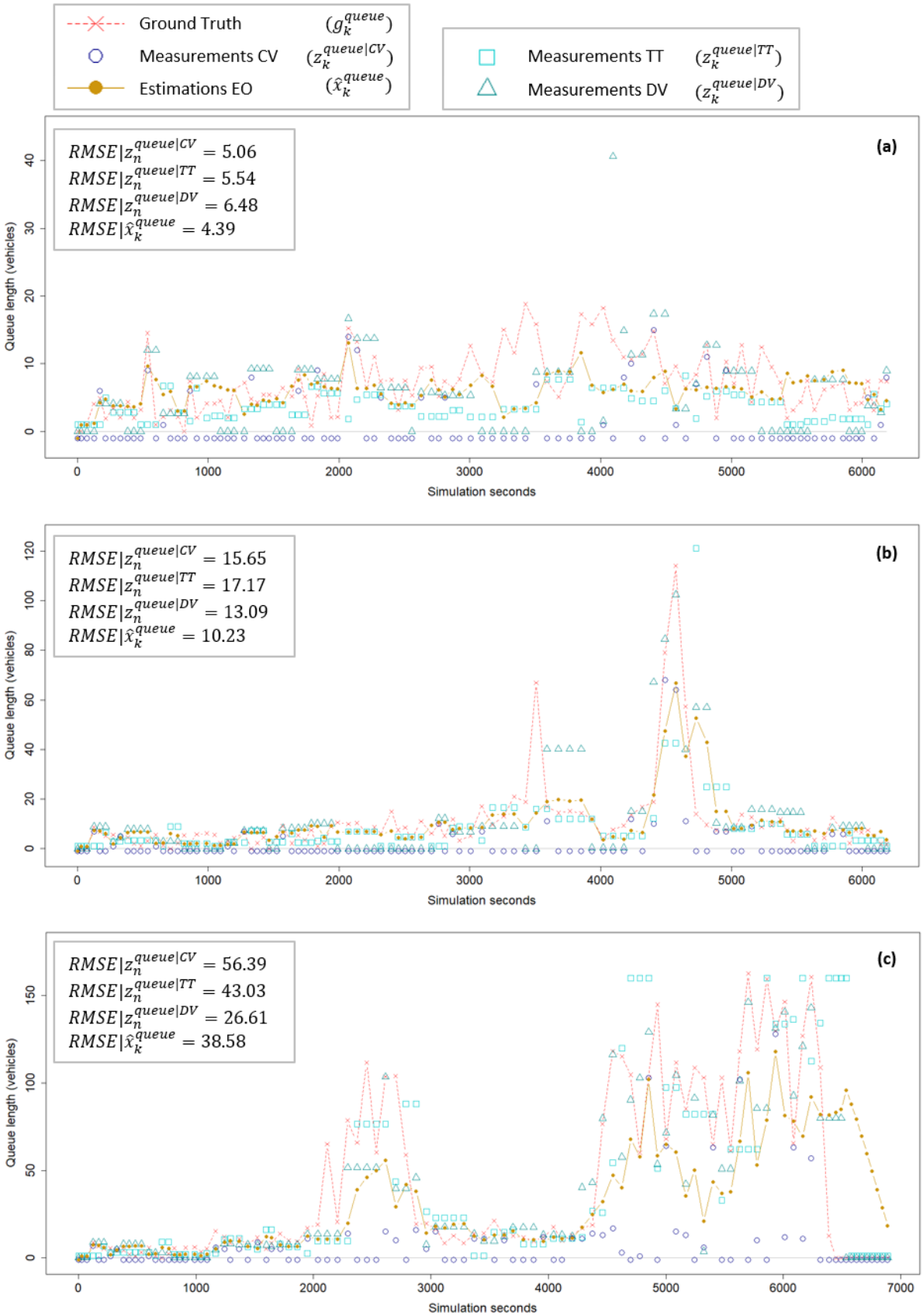

Figure 4.10 Measurements from Aggregated Section measurements

4.3.3 Connected Section

The Connected Section (CS) data is fundamentally different from the aggregated data presented before, in terms of granularity, accuracy and range. It is a microscopic point of view of the intersection that has the potential to give detailed information but for limited range. The ability to detect queues is limited to its line of sight (e.g. camera range). Arrival and departure rate can be accurately observed with the installation of wide-area sensors, such as cameras and radars.

Figure 4.11 and Figure 4.12 show the resulting measurements and estimation for the arrival rate and departure rate respectively. The CS measurements are indicated with a diamond shape and the CV measurements again with a circle. None of the previous results of this chapter assumed any camera measurements. The CV measurements in Figure 4.11 and Figure 4.12 are identical as in the previous presented results. The estimation results are however different, since now the CS and CV measurements are fused. For the fusion, the same measurement noise covariance (0.10) is used for all measurements for both CS and CV. The initial values for the arrival rate and departure rate estimation are 0.2 and 0.5, respectively.

Figure 4.11 shows that the CS measurements are more accurate than the CV measurements, using equation (3.40). This is expected, as the CS data is including the trajectories of all the incoming vehicles in its range. The range for the test intersection is set to 10 vehicles for the arrival rate. In Figure 4.11(b) and Figure 4.11(c), the maximum accepted measurement set in the simulation can be recognized in oversaturation. A value of 1500 vehicles per hour (0.42 vehicles/sec) is chosen as maximum value for the test intersection.

Figure 4.12 shows the results for the departure rate measurements for SG4 in normal oversaturated peak. To obtain a meaningful departure rate (measurements and estimations) a calculation is made only if there are more than 3 vehicles in the queue that are departing in the examined signal cycle. That means, that even though the CS data are delivering information every cycle, measurements are only valid if more than 3 vehicles are recognized. This explains also the partially steady estimation in the first 2000 seconds in Figure 4.12. Between the valid measurements (CV or CS) only the process model is in use. The random walk of equations (3.8) and (3.10) are used.

Keep in mind that the arrival and departure rate filters are running always in parallel and are feeding the queue length filter. In all previous results, the arrival and departure rate filters are running with random walk and only with the limited CV measurements. In the next section, the possibility to integrate historical models and use equations (3.9) and (3.11) is explained. However, the analysis and evaluation generally do not use the historical models, if not explicitly stated. The CS measurements have always lower error than the CV measurements. In the simple test intersection, the estimated departure rate is quite stable (low standard deviation) around 0.5-0.6 vehicles/sec, as expected.

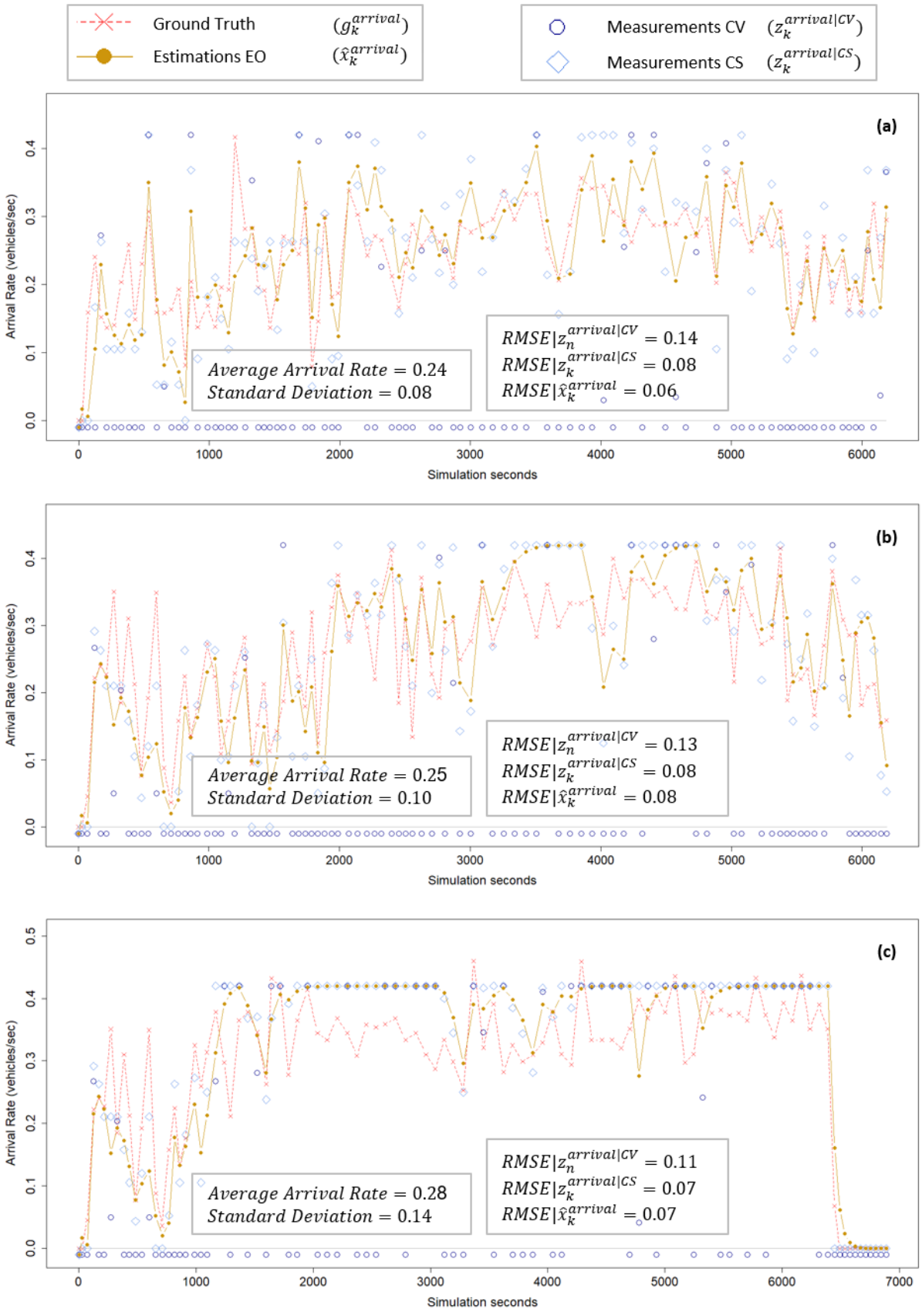

Figure 4.11 Arrival measurements from Connected Section and Connected Vehicles

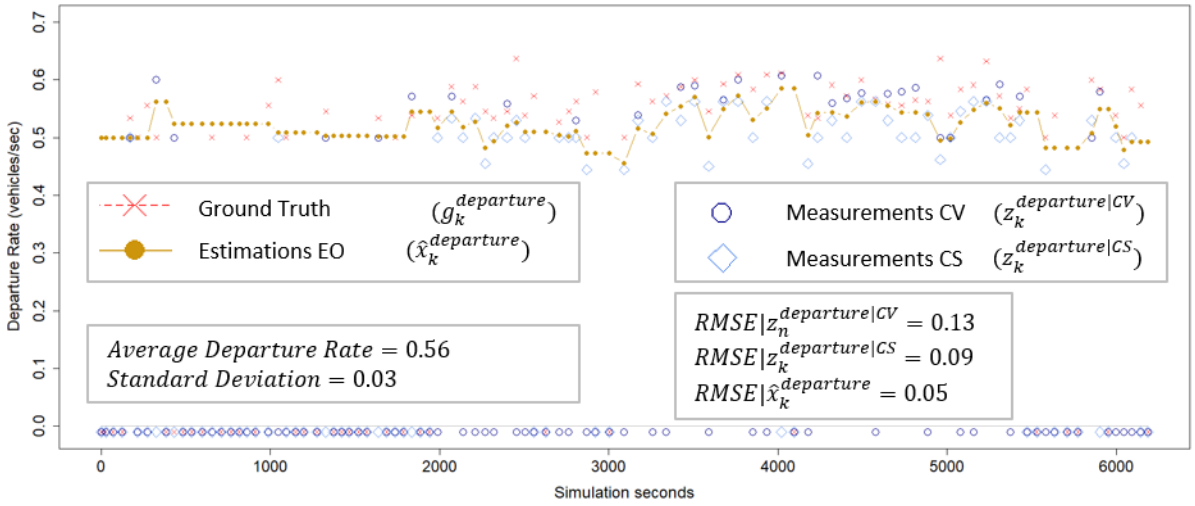

Figure 4.12 Departure measurements from Connected Section and Connected Vehicles

4.4 Data Fusion

The possible wide range of measurement errors from Connected Environments and the volatility of traffic flow at signalized intersections, call for flexible and adaptive fusion approaches. In case of EKF algorithms, this means a variable dimension measurement vector and an adaptive process and measurement noise covariance calculation. However, for UTCS, adaptivity needs to consider the operational requirements of applied traffic engineering. The term adaptive should refer also to the ability to switch easily between an automated fusion and a rather controlled fusion (e.g. including historical values). This is considered important for the method's applicability, due to two main traffic engineering aspects:

- The need of traffic engineers to understand and adjust their systems.
- The irregularity of new data from mobile sensors.

The prototypical formulation suggests intuitive starting values for the filtering that are updated automatically but can be also specified by the traffic engineers at any time. For example, if at a specific area of the city, the quality of data from Aggregated Section is considered very reliable (through observations, or experience), it should be easy to determine a higher weight on these measurements. On the other side, it should be possible to reduce the weighting of CV measurements if for example a city has low penetration rates.

4.4.1 Inclusion of Historical Data

There are many cases where a certain historical pattern of the traffic demand might be recognized at urban intersections. The proposed formulation allows the integration of historical data for the arrival and the departure rate by using the corresponding process equations (3.9) and (3.11). This might be useful in cases of very low penetration rates when for many cycles

no new information is coming. Because of the queue dynamics, there is no historical model consideration for the queue length process equation.

Figure 4.13 shows the results for SG 4 (normal oversaturated peak) with and without a historical model consideration. The historical model can be viewed as “perfect knowledge” of the historical pattern of the arrivals, as it fits the demand shown in Figure 4.2. Since the departure rate remains practically constant, only the impact of the historical model on the arrival rate estimation is shown. The CV measurements are the same but the underlying model for the arrival rate is different. The resulting filtered estimations differ because of the implemented process model. The error of the CV measurements remains naturally the same as in Figure 4.11(b). There are no CS (camera) measurements included but only CV.

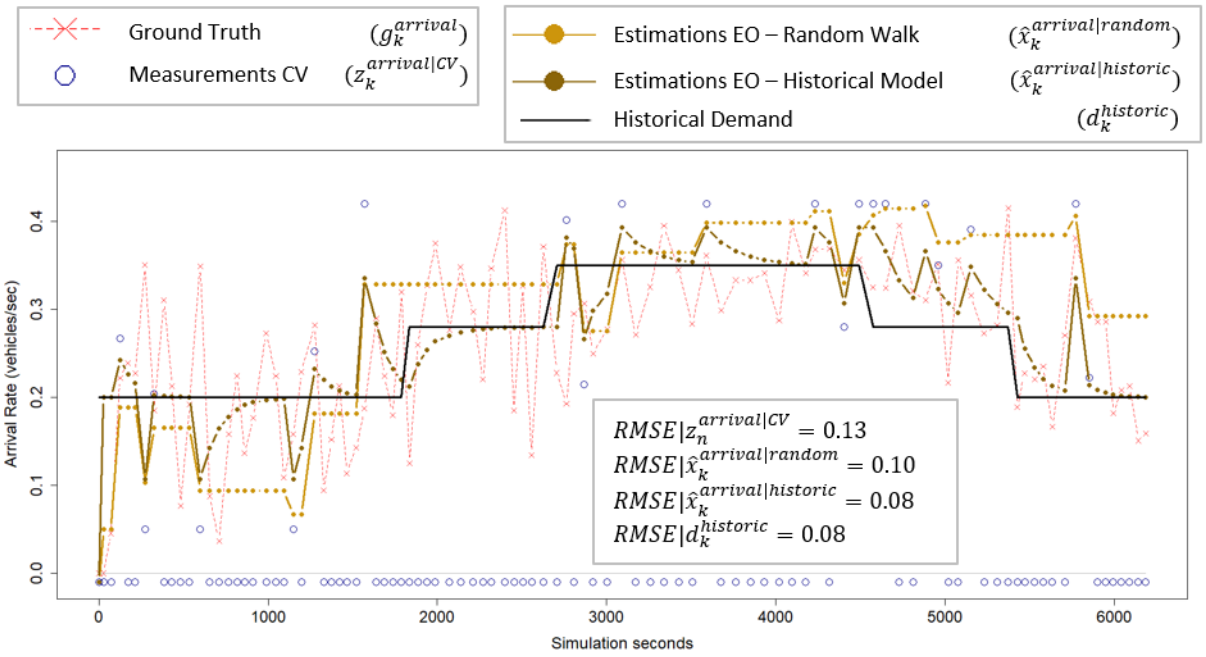

Figure 4.13 Arrival rate estimation - historical model and random walk

Notice how the behavior of the filter changes with the different process models. In the case of a random walk ($\hat{x}_k^{arrival|random}$), the estimation remains constant between CV measurements. If no measurement is available, the “time update” of the EKF algorithms is skipped and the predicted value (a priori estimation) is the final estimation (a posteriori). This explains the stepwise changes in the estimations as a measurement arrives. On the contrary, in the case of a historical model ($\hat{x}_k^{arrival|historic}$), the historical demand ($d_k^{historic}$) pulls the estimations between the sporadic CV measurements. The latest a posteriori estimation is used as a quasi-measurement and is fused with the historical demand. Consequently, the estimations between CV measurements shape a curve that is trying to “touch” the historical demand.

The performance of the arrival rate filter, in terms of reduced error, increases naturally with the inclusion of the historical model. It should be stressed though, that a historical model reduces the ability of the filter to follow sudden changes that go against the historical pattern.

Furthermore, a random walk process model is very attractive for intersections with no historical data or for the first implementation phase. The prior knowledge of historical patterns, process and measurement errors is expected to improve the performance. However, the basic formulation of the Extended Observer allows for a general and at the same time robust fusion, estimation, and prediction technique, with low necessity for tuning and maintenance.

Figure 4.14 shows the results for SG 4 (oversaturated extended peak hour). An overview of the used filter parameters is given in Tab. 4.2. The arrival and departure rate follow a random walk process. Only sporadic (5 %) CV measurements are available.

EKF Parameter	EO Parameters with Minimum Assumptions (Figure 4.14)		
	Departure Rate (vehicles/sec)	Arrival Rate (vehicles/sec)	Queue Length (vehicles)
	Figure 4.14(a)(b)(c)	Figure 4.14(a)(b)(c)	Figure 4.14(a)(b)(c)
$\hat{x}_0$	0.50	0.20	3.00
P_0	0.10^2	0.10^2	1.00^2
$\hat{x}_k$	$\hat{x}_{k-1}$	$\hat{x}_{k-1}$	$x_k^{queue} = x_{k-1}^{queue} - u_k^{dep} + u_k^{arr}$
Q_k	0.10^2	0.10^2	$\hat{x}_k$
R_k	0.10^2	0.10^2	Q_k

Tab. 4.2 Intuitive tuning of the Extended Observer with minimum assumptions

Figure 4.14 shows the potential of the Extended Observer even with limited input. The estimations follow the CV measurements, that point to the sudden (upward) jumps in the queue. A possible moderate behavior of the filter is avoided (compare with Figure 4.9.a). At the same time, the estimations in Figure 4.14 mitigate the possible unstable behavior of the filter (compare with Figure 4.9.b). This is possible due to the inherent step-by-step prediction.

4.4.2 Inherent Prediction

Figure 4.14 depicts in detail the a priori estimations from the Extended Observer. The prediction values are responsible for not following uncritically the CV measurements and for providing an estimation even when no CV measurements are available.

If there is a new measurement ($z_{69}^{queue} = 103$), the estimation ($\hat{x}_{69}^{queue} = 98$) lays between the prediction ($x_{69}^{-queue} = 7$) and the measurement, according to the measurement to noise covariance ratio. In cases where no new measurements are available (z_{70}^{queue}), the prediction ($x_{70}^{-queue} = 72$) equals the estimation ($\hat{x}_{70}^{queue} = 72$), since the measurement update of the EKF is skipped. Typically, the prediction has higher error than the estimation after the correction from the measurement. However, in some cases, the prediction might have lower error than

the “corrected” estimation, when a measurement with high error “misguides” the estimation. For example, the process equation predicts that the queue at the end of signal cycle 84 (x_{84}^{-queue}) will be 104 vehicles. However, because of the measurement (z_{84}^{queue}) that identifies only 12 queued vehicles, the corrected final estimation ($\hat{x}_{84}^{queue}$) is 55 vehicles. The ground truth (g_{84}^{queue}) according to the simulation is 146 vehicles.

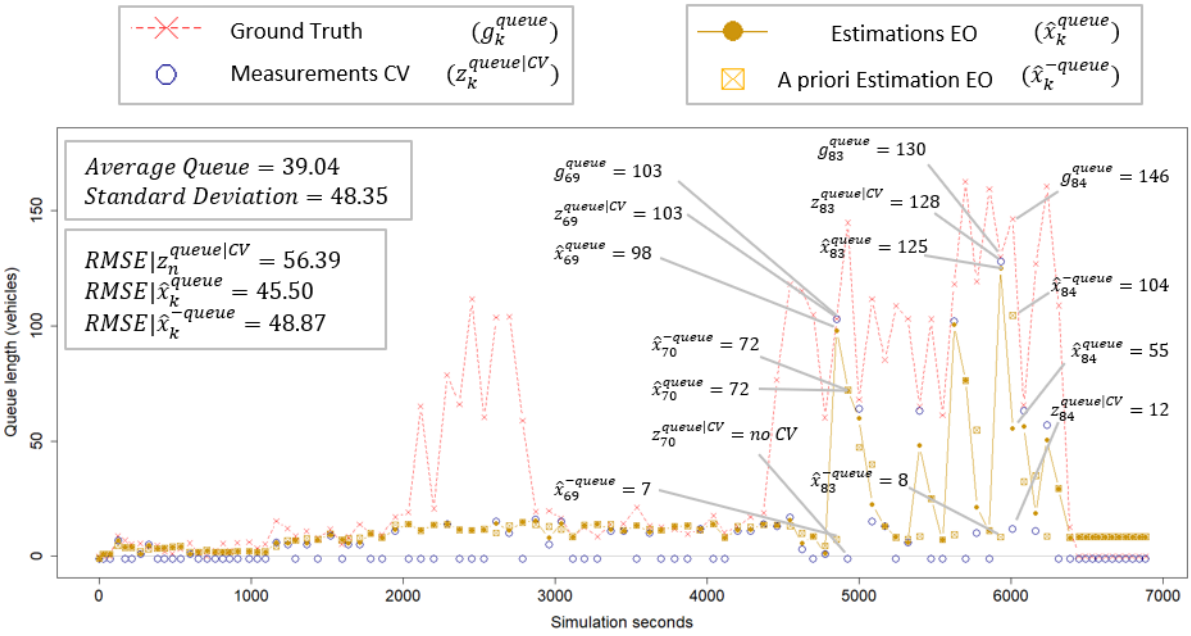

Figure 4.14 Inherent prediction in the Extended Observer

This indicates the instability of the measurements and the high need for filtering in cases of oversaturation. The difference between queue estimation at the end of cycle k and the prediction at the end of cycle k comes from the new measurement during cycle k. The prediction or the a priori estimation (x_k^{-queue}) at the end of cycle k is not the same value that could be possibly available to the UTCS one step ahead ($x_{k|k-1}^{-queue}$), as described with equation (3.17).

4.4.3 Additional Measurements

The process model facilitates the filtering of error-prone and sporadic CV measurements, but has its limitations, independent of possible tuning efforts. For example, the first peak in Figure 4.14 is not detected by the process model alone, because the limited CV measurements are observing very low queues not only for the queues but also for the arrival measurements. As shown in Figure 4.10, additional measurements from other sources can be useful in such circumstances. The abundance of measurements means that the influence of the process model in the fusion process can be relaxed accordingly.

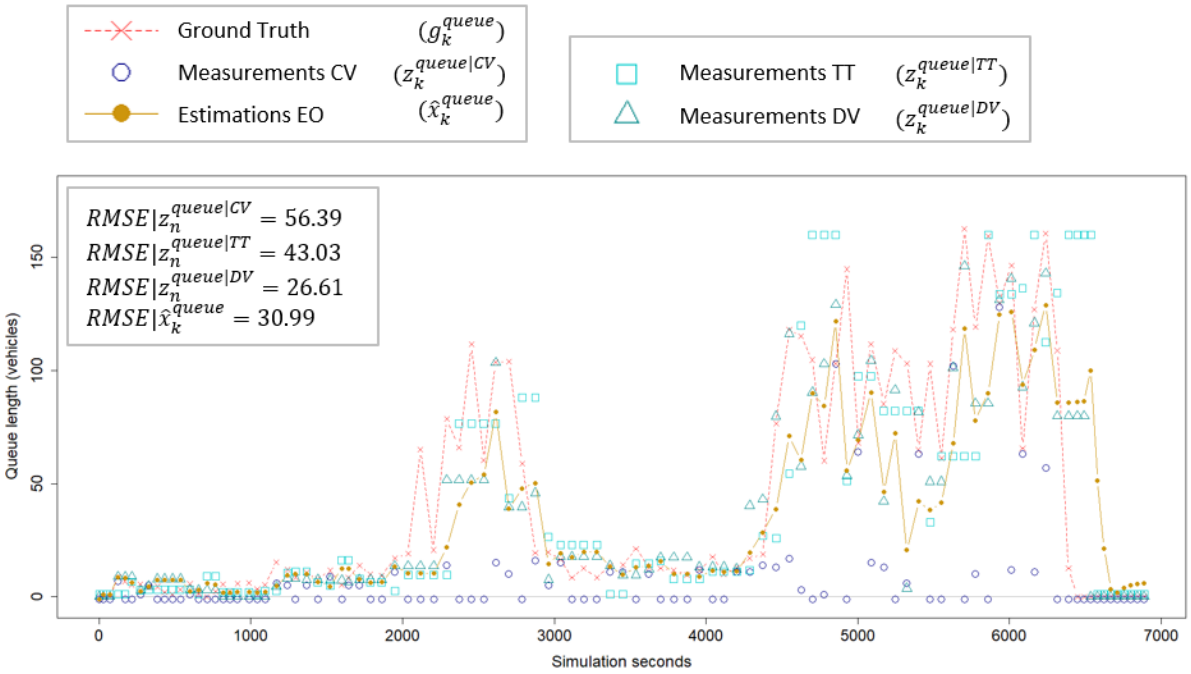

Figure 4.15 Additional measurements in the Extended Observer

Figure 4.15 shows the results of the Extended Observer by including measurements from Aggregated Section data. The process noise covariance is updated every filter step and the CV measurement noise covariance is updated according to equation (4.2). In addition, the noise covariance ratios for the Aggregated Section data is set to a lower value (0.10), in order to rely more on the variety of the measurements in oversaturated conditions (equation (4.3) and equation (4.4)). The Extended Observer can detect now the first peak and handle the errors from the stop-and-go during the second peak. A quick comparison with Figure 4.10, where constant and equal measurement and process noise covariances are implemented, shows the change of performance of the filter.

$$\frac{R_k^{queue|TT}}{Q_{k-1}^{queue}} = \frac{R_k^{queue|DV}}{Q_{k-1}^{queue}} = 0.10 \tag{4.3}$$

$$\frac{R_k^{queue|CV}}{Q_{k-1}^{queue}} = 1.0 \tag{4.4}$$

4.5 Summary

Chapter 4, in combination with chapter 3, answers mainly the first research question, regarding the methodology for diverse measurements with an adaptive formulation. The test intersection is analyzed for various traffic demand and saturation levels, to cover the dynamic traffic flow process at signalized intersections. The wide ranges of queue length, and queue length variance, highlights the need for adaptive process noise covariance (section 4.2).

The magnitude and variance of measurements errors from CV reduces for increasing penetration rates, especially in undersaturated conditions. For mainly oversaturated conditions, the measurement noise covariance remains close to the process noise covariance. Depending on the traffic demand, and resulting saturation degree, the error of the CV measurements fluctuates between cycles. In addition, the average RMSE varies from 5 to 55 vehicles. The choice of measurement noise covariance influences the estimation accuracy.

Measurement errors from Aggregated Sections are naturally error-prone for cycle-to-cycle estimation. They depend mainly on the underlying approximate measurement equations and cannot improve greatly for increasing penetration rates. Their error decreases for long oversaturated conditions. Measurement errors from Connected Sections are low, in the range of their line of sight. The instability of measurement errors calls for adaptive calculation of the process and measurement noise variance ratio.

Data fusion methods for UTCS must consider the operational challenges and requirements. The inclusion of historical models increases the accuracy but introduces a bias in the estimation and reduces the ability to react to unexpected changes. The inherent prediction of the Extended Observer can be used when no measurements are available. It reduces the CV measurement errors in cases of oversaturation. The combination of different measurements has the potential to mitigate their individual disadvantages and utilize their advantages.

The proposed formulation avoids a cumbersome tuning effort and allows an intuitive formulation of fusion for UTCS. It tries to find the balance between correcting the wrong measurements and not discarding the accurate ones, without the need for many ad-hoc rules.

5. Evaluation

The algorithms of the Extended Observer are introduced in chapter 3 and analyzed in chapter 4, with the help of detailed equations and output diagrams. Now the attention is shifted from cycle-to-cycle analysis to a statistical evaluation of the results from multiple simulation runs. In that sense, chapter 5 tries to answer mainly the second research question, regarding the accuracy and potential benefit from the fusion.

Different penetration rates and various data availability scenarios are examined, with the focus on low penetration rates and realistic data availability. This supports a better understanding of the adaptive formulation and robustness of the presented methodology. Two different simulation environments are used. The test intersection, as described in section 4.1, and a real-world intersection from the city of Verona, Italy. The former is used for various simulation scenarios (section 5.2) and the latter for the evaluation of the algorithms under real-world conditions (section 5.3). In section 5.1, the statistical tools are presented.

The evaluation is done in isolated intersections, even though the enhanced traffic estimation is designed to assist UTCS, that typically operate on a network scale. This choice is made to allow a controlled simulation environment for an in-depth analysis and evaluation. In all scenarios, the randomness of the traffic state and signal control is guaranteed by the simulation settings. The Extended Observer works in the same way, independent if the UTCS is working on isolated intersections with a decentralized approach or on a network scale with a centralized configuration, as long as the required input data for each intersection is available. The proposed methodology aims to be applicable with low calibration efforts in all traffic and control conditions, independent of underlying UTCS.

Generally, five main evaluation scenarios can be identified, based on the typical operational states for network applications [PAPAGEORGIOU, 1998A]:

- Low demand (e.g. off-peak).
- Expected, high demand (e.g. peak hour).
- Unexpected, high demand (e.g. unplanned events).
- Unexpected, reduced capacity (e.g. lane blocking).
- Local device failures (e.g. sensor disconnection).

The evaluation under all conditions is practically impossible, even in simple simulation environments for such a dynamic application area, as traffic signal control. To reach a certain level of confidence in the developed formulation, the following simulation scenarios cover all these operational states.

Checking different levels of demands for the different signals (see also Figure 4.2) covers the first three operational states listed above. The unexpected, reduced capacity is simulated in the real-world intersection, with simulation of high percentages of Heavy Good Vehicles (HGV).

They reduce the capacity of the intersection drastically due to lower departure rates and blocking of the right turning lanes. The local device failure is included in all simulated scenarios, with the inclusion of errors in the measurements. Additionally, the examination of very low penetration rates means that for many cycles there is no traffic data communication.

Furthermore, the proposed module is evaluated as part of the UTC loop (see also Figure 1.1). Tab. 5.1 shows the two main parts of the evaluation concept:

- The Extended Observer is evaluated for its data fusion ability by checking the accuracy of the measurements, estimations, and predictions.
- The Extended Observer is evaluated for its ability to support legacy signal control by checking the signal timings and the resulting traffic flow.

Evaluation structure		
Part of the UTC Loop	**Input - Output**	**Key Performance Indicators**
Data Fusion	Extended Observer Input	RMSE Measurements
	Extended Observer Output	RMSE Estimation, RMSE Prediction
Signal Control	Signal Control Input (Signal Timings)	Green Time, Cycle Time, Green Split
	Signal Control Output (Traffic Flow)	Delays, Stops, Clearing Time

Tab. 5.1 Evaluation overview

Data Fusion

The measurements (z_n) from the Connected Environments and the output of the Extended Observer are evaluated, by comparing the Root Mean Square Error (RMSE) of the different simulation scenarios. The RMSE of the measurements ($RMSE|z_n$) and the RMSE of the Extended Observer ($RMSE|\hat{x}_k$) are calculated with the following formulas:

$$RMSE|z_n = \sqrt{\frac{\sum_{i=1}^{n}(z_n - g_n)^2}{n}} \tag{5.1}$$

$$RMSE|\hat{x}_k = \sqrt{\frac{\sum_{i=1}^{k}(\hat{x}_k - g_k)^2}{k}} \tag{5.2}$$

with:

$RMSE|z_n$: RMSE from measurements

$RMSE|\hat{x}_k$: RMSE from Extended Observer

z_n: measurement for signal cycle k

n: the total number of signal cycles with available measurements

$\hat{x}_k$: Extended Observer estimation for signal cycle k

k: the total number of signal cycles

g_n, g_k: ground truth according to the simulation for cycles with measurements, and for all cycles respectively

The ground truth comes from the simulation environment (PTV Vissim, COM interface), by reading the relevant values at the start of green of the relevant signal group. The evaluation focuses on the queue length estimation. It is the most challenging to estimate, due to its instability and signal control-dependency. Moreover, it is calculated based on the parallel estimation of the other state variables. Thus, it can be used as overall performance indicator of the presented methodology. The ground truth of the queue length is calculated by reading the relevant queue counter at the start of green of the relevant signal group. This gives the ground truth of the back-end of the queue at the start of the green.

The RMSE is in the same units as the parameter to be evaluated. It is used typically as an indicator of the accuracy of measurements and estimators. It gives the distance between estimated (or observed) values and the true value. Generally, the accuracy of an estimator includes two main elements: the bias (i.e. systematic error) and the precision (i.e. random error) [EUROPEAN COMMISSION, 2020; WALTHER & MOORE, 2005]. This thesis focuses only on the comparison of the resulting accuracy of the measurements and estimations from the simulations. The theoretical calculation of the bias and precision is not in the scope of this thesis. The presented methodology has no knowledge of the accuracy from the incoming measurements.

Signal Control

To evaluate the influence of the fusion on legacy control systems, two aspects are examined: the utilization and the effectiveness of the legacy signal control, with the replacement of detectors. For the evaluation of the signal control utilization, the green time (G), the cycle time (C), and the green split (G/C) are used. The green split is defined as the green to cycle time ratio. For the evaluation of the signal control effectiveness, the average vehicle delay (D), the average number of stops per vehicle (S) and the time that is required to clear all queues are used. For the latter, the term Queue Clearing Time is used (QCT). It is calculated as the time between the last added vehicle in the simulation and the start of the last signal cycle with no queued vehicles.

5.1 Statistical Considerations

Microscopic simulations are increasingly used for evaluation of new algorithms and comparison of traffic scenarios. The significance of careful design and even more thorough statistical analysis has been well documented and stressed by the research community [FGSV, 2006; DOWLING ET AL., 2004]. In the context of this thesis, extra attention must be drawn to the challenge of evaluating oversaturated traffic conditions. They show an instability during the transition from undersaturation to oversaturation, and vice versa. In addition, comparing different traffic control methods (fixed-time, rule-based, model-based) adds to the variability between simulation scenarios. In the following, the most important statistical considerations for the simulation set-up are presented. They are divided in two main areas: simulation settings and simulation results.

5.1.1 Number of Simulation Runs

The calculation of the minimum number of simulation runs, in order to achieve a certain confidence level of the results, is done based on the recommendations of the German Road and Transportation Research Association [FGSV, 2006] and the U.S. Federal Highway Administration [DOWLING ET AL., 2004]. The average vehicle delay (D) is selected as the parameter to define the minimum number of required simulations runs. After a first series of simulation runs, the sample standard deviation of the average vehicle delay is calculated. The typical 95-perecent level of confidence is then chosen. The desired range is defined as the ratio of the desired confidence interval (CI) divided by the standard deviation of the related parameter. In this thesis we strive to achieve a desired range of 2, with a desired confidence of 95%. This results in a minimum number of simulations runs of 8. The exact calculation is given in [DOWLING ET AL., 2004]:

$$CI_{(1-alpha)\%} = 2 \times t_{(1-alpha/2),N-1} \times \frac{s}{\sqrt{N}} \tag{5.3}$$

with:

$CI_{(1-alpha)\%}$: $(1-alpha)$% confidence interval for the true mean, where alpha equals the probability of the true mean not lying within the confidence interval.

$t_{(1-alpha/2),N-1}$: Student's t-statistic for the probability of a two-sided error summing to alpha with N-1 degrees of freedom, where N equals the number of repetitions.

s: Standard deviation of the simulation results

To be on the safe side, all simulation results stem from 12 simulation runs per scenario. The standard deviation of average vehicle delays (s_d) is chosen as examined simulated output. Practically, this gives an indication of the stability between the different random seeds. High standard deviations of delays are normal in cases of adaptive signal control, especially in

oversaturation. Therefore, it is decided, to fix the level of confidence ($1 - alpha = 0.95$), the number of runs ($N = 12$), the desired range ($\frac{CI}{s} = 2$) and state the resulting standard deviation of average delays in the detailed evaluation tables.

5.1.2 Statistical Significance

The statistical analysis and graphical presentation of the results is done with RStudio, an integrated development environment (IDE) for R [RSTUDIO, 2020]. R is a free software for statistical computing and graphics [THE R FOUNDATION, 2020]. The chosen statistical tests are typical hypothesis tests, where the null hypothesis describes the case of no difference between the scenarios examined. Paired, one-tailed, t-tests are used in this thesis as statistical test for rejecting or accepting the null hypothesis. The calculated p-value is compared with the predefined $alpha$ value. The typical value of 0.05 is used. If the p-value is lower than 0.05, the null hypothesis is rejected and the difference between the two datasets is considered significant. The p-value is defined as the probability of obtaining a result equal to or more extreme than what was observed in the data [MANGIAFICO, 2020]. The statistical significance (or not) is indicated together with the exact p-value for more transparency in the evaluation tables. The Shapiro-Wilk test is used to test if the distribution of the differences of the paired measurements is normally distributed to confirm the suitability of the paired t-test. If the differences are not normally distributed, the Wilcoxon–Mann–Whitney test is used to reject or accept the null hypothesis.

For example, to evaluate the statistical significance of the difference between $RMSE|z_n$ and $RMSE|\hat{x}_k$, a paired t-test is conducted that compares the averages of 12 simulation runs (i.e. 12 pairs of results). In addition, the difference of the averages from all simulation runs is calculated and given along with the results of the hypothesis testing with the following formula:

$$\Delta RMSE\% = \frac{\overline{RMSE|\hat{x}_k} - \overline{RMSE|z_n}}{\overline{RMSE|z_n}} \times 100\% \tag{5.4}$$

5.2 Test Intersection

The simulation settings of the test intersection remain as are presented in section 4.1. Every simulation scenario assures s_d below 5 seconds. In section 5.2.1, the data fusion ability of the Extended Observer is evaluated. In section 5.2.2, the influence on the legacy signal control is evaluated.

5.2.1 Data Fusion

In Part I, the data availability scenario with only CV measurements is examined. In Part II, the combination of multiple data sources is evaluated.

Part I. Connected Vehicles as Single Data Input

In this part, the second research question, regarding the benefits and accuracy of data fusion is answered. The following table gives an overview of the examined research question, the key findings, and the practical interpretation of this part of the evaluation.

Research Question: *What is the benefit and accuracy of the data fusion, when only Connected Vehicles are available as data input?*	
Key findings (benefits)	Practical interpretation (accuracy)
A. The Extended Observer reduces high CV measurement errors in oversaturation. The Extended Observer can be used to improve error-prone and sporadic CV measurements through system knowledge.	• As penetration rate increases, the fused estimations and the CV measurements become more accurate. • Fused estimations have lower RMSE (5-30% RMSE reduction) than the CV measurements for all penetration rates. • The highest and most significant RMSE reduction is observed in the lowest penetration rates (p<20%).
B. The Extended Observer retains low CV measurement errors in undersaturation. The Extended Observer can be used to keep the information between cycles with good CV measurements through system knowledge.	• Higher penetration rates (p>20%) result in systematic and accurate CV measurements. In these cases, direct CV measurements can be used. • RMSE and RMSE reduction is highly related to the number of undersaturated/oversaturated cycles.
C. The Extended Observer retains its performance for various measurement errors, measurement equations and signal control methods.	• Improvements from the fusion are independent of measurement equations. • Simple measurement equations are sufficient. • The presented formulation allows comparison of various measurement equations. • Accuracy of the fusion remains the same for different control methods.
D. The Extended Observer allows inclusion of expected traffic patterns.	• An accurate historical model could improve drastically (35-53% RMSE reduction) the estimations of arrival rate. • There is no statistically significant influence in the estimation of the queue length. Random walk for arrivals is sufficient for queue length estimation. • A historical model introduces a bias and makes the filtering less sensitive to sudden changes.

Tab. 5.2 Key findings and practical interpretation of the evaluation - Part I

A. The Extended Observer reduces high CV measurement errors in oversaturation

As discussed in chapter 4, in cases of oversaturation, measurements from CV are error prone, especially in low penetration rates (see also section 4.3.1, Figure 4.6). It is therefore essential to examine if the Extended Observer can use the error-prone measurements and improve the estimation for various penetration rates with statistical significance. Figure 5.1 shows the RMSE from the CV measurements ($RMSE|z_n^{queue|cv}$) and the fused estimations ($RMSE|\hat{x}_k^{queue}$). Tab. 5.3 presents the statistical evaluation.

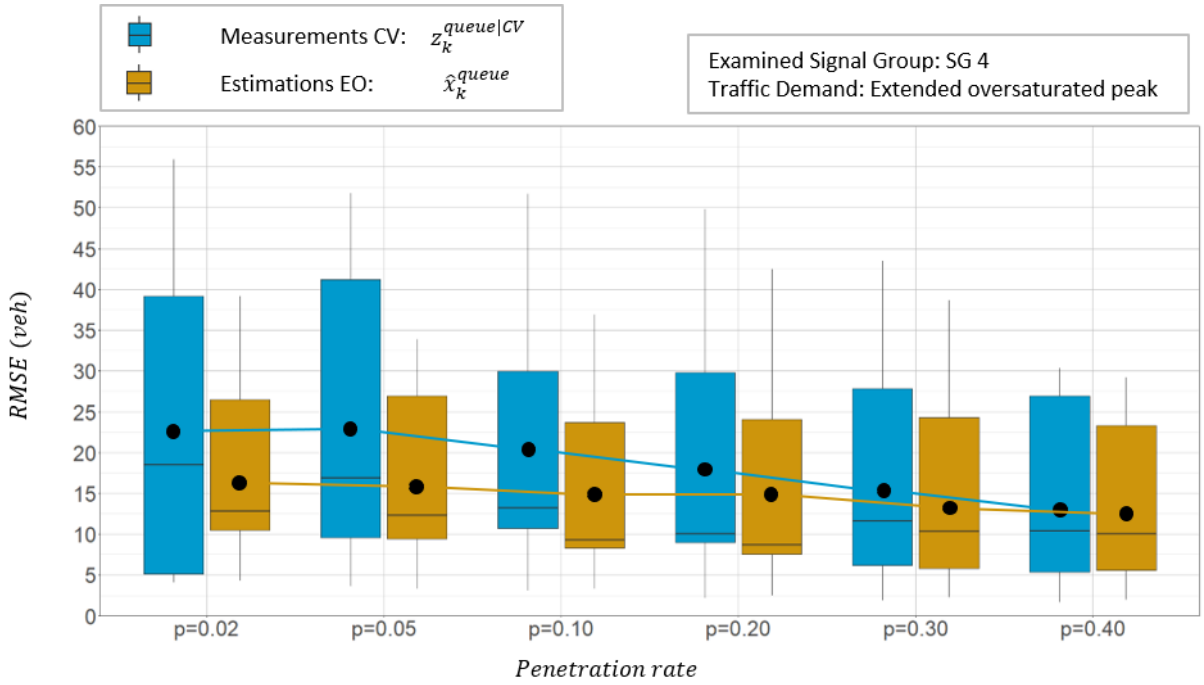

Figure 5.1 Errors in oversaturation - measurements from Connected Vehicles and estimations from the Extended Observer

Penetration rate of CV (p)	RMSE (veh)		Error Reduction		
	$\overline{RMSE\|z_n^{queue\|cv}}$	$\overline{RMSE\|\hat{x}_k^{queue}}$	$\overline{\Delta RMSE\%}$	$\overline{\Delta RMSE}$	p_value
p = 0.02	22.51	16.92	*-24.84%	*-5.59	0.03051
p = 0.05	23.08	16.13	*-30.09%	-6.94	0.00598
p = 0.10	20.21	15.20	*-24.77%	*-5.01	0.00115
p = 0.20	18.15	15.22	*-16.13%	*-2.93	0.00168
p = 0.30	15.87	14.51	*-8.55%	*-1.36	0.00789
p = 0.40	13.86	13.16	-5.12%	-0.71	0.07164

*statistically significant reduction: $N = 12,\ CI_{(1-alpha)\%} = 95\%, {}^{CI}/_{s_d} = 2,\ s_d < 5\ seconds$

Tab. 5.3 Error reduction in oversaturation - measurements from Connected Vehicles and estimations from the Extended Observer

The Extended Observer can utilize the CV measurements and reduce their errors by utilizing the process equation (3.12), providing an improved estimation. Both the CV measurements and the fused estimations improve naturally as the penetration rate increases. The fusion outperforms the CV measurements for all penetration rates. The improvement from the fusion is statistically significant for all penetration rates except for p=0.40. This is an indication that

for penetration rates above 30-40%, the CV measurements start to be reliable and representative of the overall traffic flow. This is consistent with all existing literature on the topic of connected vehicles in signal control. Hence, the rest of the evaluation will focus on the lower penetration rates. The potential improvement is higher for lower penetration rates. Moreover, the fusion avoids, as expected from any filtering method, the extreme errors. Interestingly, for p=0.02, there are simulation runs with very low CV errors, when the scarce CV measurements are representative of the ground truth.

B. The Extended Observer retains low CV measurement errors in undersaturation

In contrast, in cases of mainly undersaturated conditions, the RMSE from the CV measurements remain low because of the low and stable queues. In these cases, it is important that the fusion retains also low errors. Figure A.3 shows how the high errors for the mainly oversaturated signal (SG 4) are reduced. At the same time, the low measurement errors for the mainly undersaturated signal (SG 2) are maintained. Both signals use the same fusion formulation without any prior knowledge or assumptions for the traffic demand. Generally, filtering of good measurements, will slightly reduce the quality. In the case of traffic signal control, good measurements are mostly possible in undersaturation.

C. The Extended Observer retains its performance for various measurement errors, measurement equations and signal control methods

The results in Figure 5.1 and Tab. 5.3 come from simulation with no location error from map matching of the Connected Vehicles. The large errors are due to the stop and go behavior and low penetration rates. A critical point for the robustness of the developed methodology is the ability to deal with various and most importantly unknown errors. Figure A.4 shows the RMSE of the CV measurements for increasing location error ($\varepsilon = 1.50m, 6.00m, 12.00m$) and the resulting RMSE.

The Extended Observer improves the CV measurements for all penetration rates and measurement errors in terms of RMSE reduction as before. The evaluation of the results from Figure A.4, showed no statistically significant dependency between the location error and the performance of the filter regarding RMSE reduction (i.e. with low location error vs. high location error). For the rest of the thesis, a location error of 6 meters is used to emulate a moderate but realistic, for real-world applications, error.

The clear separation of the measurement and process equations allows the integration of different QLE as incoming measurement equations. The evaluation shows that the measurement equation (3.37) performs better than the simpler measurement equation (3.36), especially for lower penetration rates. This is consistent with the results from [COMERT, 2013; COMERT, 2016]. However, the straightforwardness and simplicity of (3.36) is very attractive for real-world implementations. The Extended Observer can utilize any of the measurement variations, for all penetration rates. It reduces the RMSE in both cases, consistently [PAPAPANAGIOTOU & BUSCH, 2020]. This flexibility can be advantageous for testing different

algorithms for CV measurements in real-world applications. In this thesis the measurement equation (3.37) is used for all scenarios to obtain the queue measurement equations from CV.

Furthermore, in [PAPAPANAGIOTOU & BUSCH, 2020], the algorithms are evaluated with fixed-time control, rule-based and model-based control. The fusion reduces the RMSE for all control methods, as expected, since the formulation includes the signal timings of the current signal cycle and not aggregated or average signal timings. However, the performance in terms of error reduction, is even higher for fixed-time control. The reason is, that there are more oversaturated cycles and thus higher measurement errors. Practically, the measurements are of lower quality and thus the potential of improvement is higher.

D. The Extended Observer allows inclusion of expected traffic patterns despite cycle-to-cycle formulation

There are many cases where a certain historical pattern of the traffic demand might be recognized at signalized intersections. The integration of historical models for the arrival, turning, departure and penetration rate is possible with the respective process equations. Because of the queue dynamics, there is no historical model consideration for the queue length process equation. Theoretically, the historical model adds a historical bias to the estimation that should be avoided. Practically, this might be useful in cases of very low penetration rates when for many cycles no new information (measurements) is coming. The integration of the historical pattern allows the improvements of the CV measurements significantly (35-53%) [PAPAPANAGIOTOU & BUSCH, 2020]. The big improvements should be however attributed to the assumed accurate knowledge of the historical pattern and the high measurement errors for low penetration rates.

Nonetheless, the improvements in the arrival rate estimation resulted in no significant change in the respective average RMSE of the queue length estimations. That means that if only the queue length estimation is of interest, a simple random walk implementation for the arrivals with no knowledge of historical patterns might be sufficient. In fact, the inclusion of a historical model reduces naturally the ability of the filter to react to sudden changes. All presented evaluation results in this thesis use typical random walk processes with no assumption of previous knowledge of traffic patterns for all parallel filters.

Part II. Connected Environments as Multiple Data Input

In the following, different data availability scenarios are examined. The following table gives an overview of the specific research question, the key findings, and the practical interpretation of the second part of the evaluation.

Research Question: *What is the benefit and accuracy of the data fusion, when multiple Connected Environments are available as data input?*	
Key findings - benefits	Practical interpretation - accuracy
A. The fused estimations outperform mobile sensors for all penetration rates. The Extended Observer can be used to improve sporadic CV measurements through the inclusion of Aggregated Section data.	• Fused estimation reduces the average RMSE from CV measurement from 16-26 vehicles to 10-15 vehicles. • In cases of very low queues and high penetration rates (p>20), the CV measurements remain slightly better than the fusion (ΔRMSE<1 vehicle). • Measurements based on speed differences (RMSE=15-20) outperform measurements from travel times (RMSE=12-17) in oversaturation for all penetration rates. • The prediction errors are marginally higher than the estimation errors for all penetration rates (<0.5 vehicles difference). • The prediction accuracy stems from the inclusion of the signal timings in the process equation and the cycle-to-cycle correction.
B. The fused estimations outperform infrastructure-based sensors if the queue extends beyond their range. The Extended Observer can be used to improve infrastructure-based sensors through the inclusion of Aggregated Section data.	• For oversaturation, fusion (RMSE=10-15) outperforms the loop-based detection (RMSE=18-28) for all penetration rates. • For low queues, infrastructure-based sensors (RMSE<1 vehicle) outperform the fused estimation (RMSE<5 vehicles). • For oversaturation, fusion can improve camera measurements even for very low penetration rates (ΔRMSE= 5 vehicles).

Tab. 5.4 Key findings and practical interpretation of the evaluation - Part II

A. The Extended Observer improves CV measurements through Aggregated Section measurements

In the case of low penetration rates, that is the focus of this thesis, it must be guaranteed that the traffic state estimation avoids high errors and sporadic information. The Extended Observer can fuse CV and Aggregated Section measurements to provide an enhanced traffic state estimation. Figure 5.2 shows the RMSE from the individual data inputs (measurements) and the respective fused estimation for the extended oversaturated peak (SG 4).

The estimation and all measurements improve for increasing penetration rates. The measurements based on the travel time ($z_n^{queue|TT}$) are improving only slightly with increasing penetration rates. This is expected, as the errors from the travel times are mostly due to approximate calculation of the queue based on (3.45). The measurements based on the difference in velocities ($z_n^{queue|DV}$) gives measurements with low RMSE. This shows that simplified formulas for measurements without sophisticated analytical methods can be useful in data fusion for signal control with a predict and correct formulation.

The fusion outperforms the measurements for all penetration rates. Tab. 5.5 shows the statistical evaluation of the estimation in comparison to the initial CV measurements. The reduction is statistically significant for all penetration rates and more drastic in comparison to Tab. 5.3. This is due to the correction from the added measurements from the Aggregated

Section data. For penetration rates p=0.05 and p=0.30 the differences are not normally distributed and therefore the Wilcoxon–Mann–Whitney is used for the calculation of the p-value.

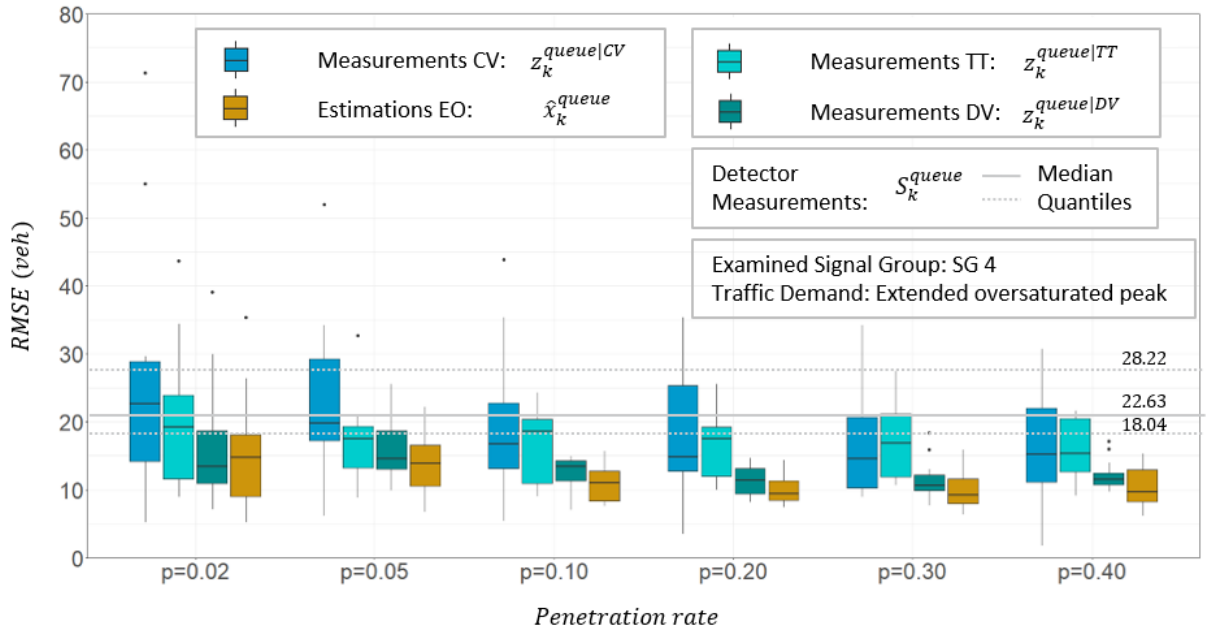

Figure 5.2 Fused estimations from the Extended Observer for various penetration rates - SG 4 extended oversaturated peak

Penetration rate of CV (p)	RMSE (veh)		Error Reduction		
	$\overline{RMSE\|z_n^{queue\|CV}}$	$\overline{RMSE\|\hat{x}_k^{queue}}$	$\overline{\Delta RMSE\%}$	$\overline{\Delta RMSE}$	p_value
p = 0.02	25.80	15.47	*-40.04%	*-10.33	0.00568
p = 0.05	23.71	14.12	*-40.45%	*-9.59	0.00049
p = 0.10	19.69	11.00	*-44.15%	*-8.69	0.00364
p = 0.20	18.56	9.98	*-46.23%	*-8.58	0.00407
p = 0.30	17.00	10.27	*-39.61%	*-6.73	0.00073
p = 0.40	16.47	10.34	*-37.25%	*-6.14	0.00369

*statistically significant reduction: $N = 12,\ CI_{(1-alpha)\%} = 95\%, {}^{CI}/_{s_d} = 2,\ s_d < 5\ seconds$

Tab. 5.5 Error reduction in oversaturation - Measurements from Connected Vehicles and fused estimations from the Extended Observer

For the same simulation scenario, the evaluation of SG 1 (Figure A.5) shows that for low demand and undersaturation, CV measurements have the lowest errors and Aggregated

Section measurements have now the higher errors. This shows clearly that a formulation is needed with no predefined measurement errors. The fused estimation remains very close to the very accurate CV measurements for all penetration rates. For high penetration rates (p>0.20), the fusion shows slightly higher error (around 0.5 vehicles) than the CV measurements.

This indicates that the decision to set the noise covariance ratios for the Aggregated Section data to a lower value (equation (4.3)), in comparison to the noise covariance ratio for the CV data (equation (4.4)) as described in section 4.4.3 has the desired influence. In practice, this can be explained as a decision to potentially lose a $DRMSE$ of 0.5-1.0 vehicles in undersaturation and potentially gain a $DRMSE$ of 5.0-10.0 vehicles in oversaturation.

The presented formulation has the advantage of the inherent prediction (a priori estimation) that comes along with any Kalman filter implementation ($\hat{x}_k^{-queue}$). The difference between the a priori estimation and the a posteriori estimation ($\hat{x}_k^{queue}$) in the cycle-to-cycle formulation remains always below 1 vehicle [PAPAPANAGIOTOU & BUSCH, 2020]. This is due to the knowledge of the signal timings ($u_k^{utilized\ green}, u_k^{red}$) and the low possible state changes between signal cycles. The a priori estimation has typically larger RMSE than the a posteriori estimation for all penetration rates. The difference between queue estimation for cycle k ($\hat{x}_k^{queue}$) and prediction for cycle k ($\hat{x}_k^{-queue}$) stems from the new measurement during cycle k (z_k^{queue}).

In practice, only the prediction ($\hat{x}_{k|k-1}^{-queue}$) that is known one cycle in advance can potentially be used to feed an UTCS. This has naturally a larger uncertainty (see also equation (3.17)). The evaluation shows that there is no statistically significant difference between $\hat{x}_{k|k-1}^{-queue}$ and $\hat{x}_k^{-queue}$. The absolute difference remains below 0.5 vehicles with no statistically significant difference for all penetration rates. That is because the formulation of the arrival and departure filters follows a random walk and the signal timings do not present huge jumps between cycles.

A reduction of the prediction accuracy is expected if the signal control is forced to have consecutives cycles with large signal timing and traffic demand differences. A typical example is absolute public transport prioritization in short intervals that are conflicting and interrupting the major flows. The a posteriori estimation however is not expected to be influenced by this, since the measurements are correcting the predictions at the beginning of the current signal cycle (i.e. the signal timings that were applied are known). The confirmation of this needs however further thorough analysis and goes beyond the scope of this thesis.

B. The Extended Observer outperforms infrastructure-based sensors in cases of oversaturation

Figure 5.2 shows also the RMSE from the model-based UTCS Spot/Utopia with the horizontal light grey lines (median and lower/upper quantiles). The fusion outperforms the loop detectors when the queue extends beyond the fixed-location detection point. In all other cases (i.e. SG1,

SG2, SG3) the queue length estimation from Spot outperforms all measurements and the estimation. The detectors are placed 300m away from the stop-line and can capture the complete queue for the other signals. A less ideal distance (i.e. 100m) would result naturally to reduced performance of the loop-based estimation.

Figure A.6, Tab. A.3, Tab. A.4 of the Appendix show the difference between the queue length estimation from Spot (S_k^{queue}) based on loop detectors and the fused estimation ($\hat{x}_k^{queue}$). The fusion outperforms Spot for the extended oversaturated peak of SG 4 for all penetration rates. The average RMSE of the Extended Observer ranges around 16-18 vehicles, while the average RMSE from Spot is around 21-28 vehicles. Spot outperforms the fusion consistently for SG 2. The average RMSE of Spot is around 2.0 vehicles while the average RMSE of the fusion of mobile sensors is around 5.0 vehicles, for all penetration rates. The results are statistically significant for all penetration rates.

Figure A.7 and Figure A.8 in the Appendix show two cycle-to-cycle simulation runs for SG 4 and SG 2. The main advantages of the Spot measurements are the high accuracy in low queues and the ability to capture zero queues perfectly. The main disadvantage is the inability to capture high queues beyond its range. These characteristics are valid for any infrastructure-based estimation.

In contrast, the main advantage of the Extended Observer is the ability to capture long queues and avoid extreme errors. The main disadvantage is the inability to capture zero queues if no infrastructure-based sensors are used.

This limitation can be overcome by including infrastructure-based sensors in the Extended Observer. Figure A.9 in the Appendix shows an indicative simulation run where Connected Section (CS) data are fused with Aggregated Section data (only travel times). The Extended Observer utilizes the accuracy of the camera measurements in low queues and the ability of the travel times to correct the estimation in cases of oversaturation. On one hand, the Extended Observe practically extends the range of the camera. On the other hand, the Extended Observe can still capture the zero queues through the camera measurements.

Figure 5.3 shows the RMSE for CS measurements, Aggregated Section measurements and fused estimations. For all penetration rates, the fused estimations have lower error as expected. Tab. 5.6 shows the statistical evaluation that confirms the significant reduction of the camera errors through the fusion with travel times. The evaluation for the other signals shows no statistically significant difference between the camera measurements and the fusion. This confirms that the fusion manages to retain the extremely low measurement errors from the camera. Both RMSE remain below 1 vehicle independent of penetration rates.

The different RMSE for the cameras for different penetration rates is only a result of stochasticity from the microscopic simulation environment. The cameras are simulated to capture all vehicles in their range (10 vehicles) with stochastic error (standard deviation of 1 vehicle).

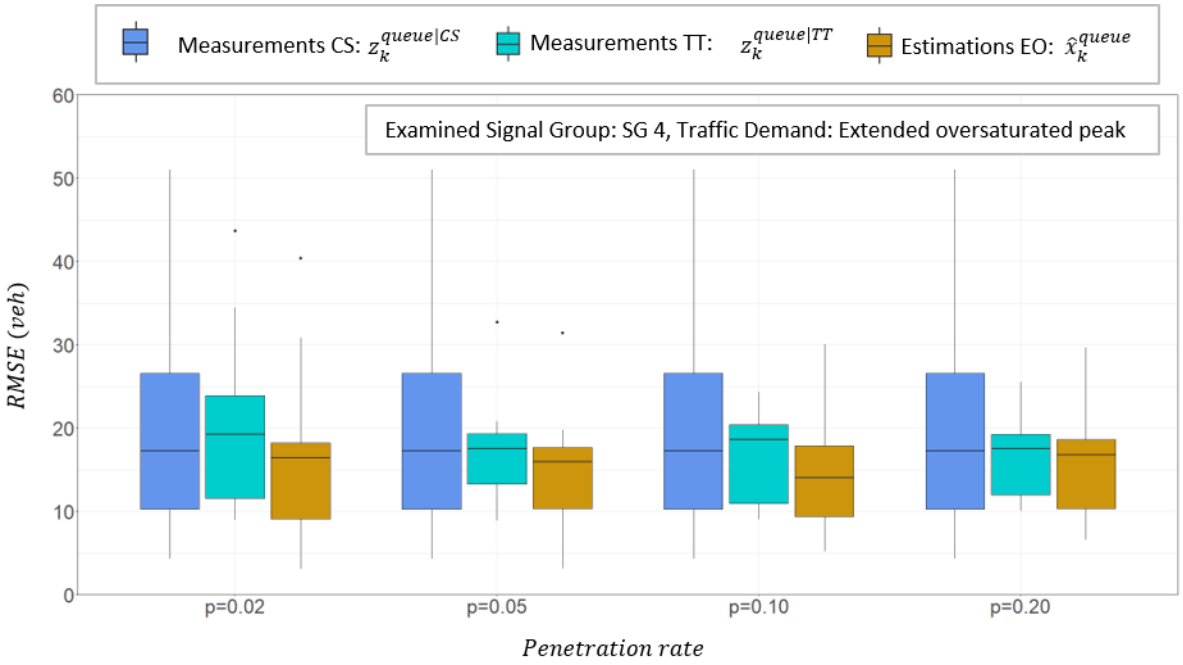

Figure 5.3 Fused estimations from the Extended Observer with camera and travel times

Penetration rate of CV (p)	RMSE (veh)		Error Reduction		
	$\overline{RMSE\|z_n^{queue\|CV}}$	$\overline{RMSE\|\hat{x}_k^{queue}}$	$\overline{\Delta RMSE\%}$	$\overline{\Delta RMSE}$	p_value
p = 0.02	19.66	16.80	*-14.57%	*-2.86	0.04614
p = 0.05	20.40	15.21	*-25.43%	*-5.19	0.00024
p = 0.10	19.90	14.46	*-27.34%	*-5.44	0.01050
p = 0.20	21.85	15.45	*-29.25%	*-6.39	0.00049

*statistically significant reduction: $N = 12,\ CI_{(1-alpha)\%} = 95\%, {}^{CI}/_{s_d} = 2,\ s_d < 5\ seconds$

Tab. 5.6 Error reduction in oversaturation - Measurements Connected Vehicles and fused estimations EO

5.2.2 Signal Control

Part III. Feeding the test intersection with the Extended Observer

After the evaluation of the data fusion, the focus moves to the potential influence on the existing signal control. Tab. 5.7 gives the overview of Part III of the evaluation. The key benefits and indicative numbers try to give some answers to the respective research question. Detailed evaluation is presented after the overview table for each finding.

Research Question: *What is the benefit and accuracy of the data fusion when it feeds an existing signal control?*	
Key findings - benefits	Practical interpretation - accuracy
A. The improved estimation results in improved signal control input (i.e. signal timings), by recognizing oversaturation.	• The fused estimation (CV and Aggregated Section) results in signal timings closer to the legacy control with full detection, in comparison to estimation only based on CV measurements (delay reduction 23-34% and stop reduction 19-45%). • The higher the penetration rate, the higher the green and cycle times: i.e. tendency to serve oversaturated streams. • For low penetration rates (p<0.20), relying solely on CV measurements results in lower green times, cycle times and green splits.
B. The impact of the Extended Observer on the signal control output (i.e. traffic flow) starts from very low penetration rates, by recognizing oversaturation and facilitating its clearance.	• Fused estimations (CV and Aggregated Section) result in reduced delays and stops for all penetration rates and control methods, in comparison to using the Extended Observer only with CV measurements. • Already for extremely low penetration rates (p=0.2), the Extended Observer reduces the delays from 66 to 32 seconds, in comparison to fixed-time control. • For extremely low penetration rates (p=0.2), the Extended Observer increases the delays from 25 to 32 in comparison to legacy control with full detection. • Better queue estimation cannot guarantee reduction of delays or stops for the complete intersection. • The potential improvements on the signal control output (i.e. traffic flow) depends on the underlying signal control method. • The benefits from the fusion are higher for model-based control than for rule-based control. They start additionally from low penetration rates.

Tab. 5.7 Key findings and practical interpretation of evaluation - Part III

The set-up of the simulation environment allows the communication between the fusion and the signal control. The Extended Observer can feed two implemented signal control methods. A rule-based control that measures the time gaps at all approaches and a fully adaptive model-based control (Spot/Utopia). When the feeding is activated, the signal control ignores all loop detectors and gets only information from the fusion, which in turn also ignores all loop detectors. The rule-based control simple extends the green time to cover the estimated queues. The model-based control uses all estimations: turning rates, (predicted) arrivals, departure rates and the queue length estimations. In practice, all detectors are deleted from the simulation environment and Spot gets values only from the Extended Observer.

A. The improved estimation from the Extended Observer results in improved signal control input

Figure 5.4 shows how the green time, cycle time and green split change for the with increasing penetration rates in comparison to the rule-based legacy control with full loop detection coverage $(G_L, C_L, (G/C)_L)$. Firstly, only CV measurements are used for the queue length estimation $(G_{EO}^{CV}, C_{EO}^{CV}, (G/C)_{EO}^{CV})$. Then, additional Aggregated Section measurements are

included to evaluate if the improvements in estimation shown in the previous section turn into improvements in signal control input ($G_{EO}^{CV+AS}, C_{EO}^{CV+AS}, (G/C)_{EO}^{CV+AS}$) and output (Figure 5.5).

The reference point for the evaluation is the signal timings from the legacy control: i.e. the difference between the resulting timings and the baseline is evaluated. The fused estimation results into statistically significant higher green times and green splits that are closer to the ones from the control with full detection (see also Figure 5.4.a, Figure 5.4.c and Tab. A.5). However, the enhanced estimation results also into higher cycles times that are drifting further away from the reference point (Figure 5.4.b). This behavior has been observed for both rule-based and model-based control.

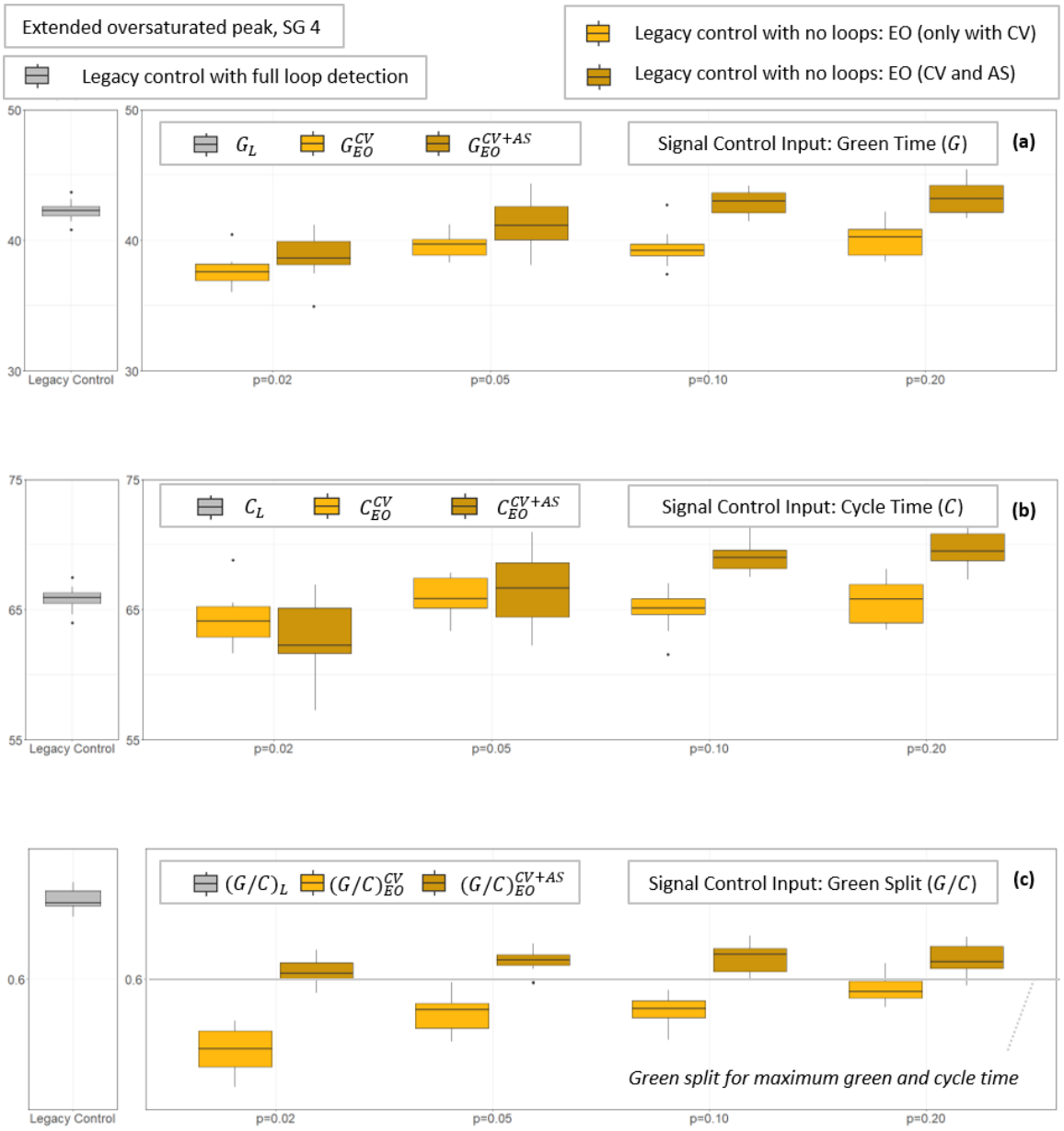

Figure 5.4 Legacy signal control input with fused estimations from the Extended Observer

B. The impact of the Extended Observer on the signal control output starts from very low penetration rates

Figure 5.5 and shows what is the resulting signal control output (i.e. traffic flow) in terms of average vehicle delays. On the left side of the diagram, the light grey boxplot (Spot) gives the lower reference point for the delays and the dark grey boxplot (fixed-time) gives an indication of the higher reference point. The fixed-time control is as shown in Figure 4.2 ,with green times that would theoretically cover the saturated peaks of both signal stages (i.e. calculation based on peak arrivals). Tab. A.6-Tab. A.11 of the Appendix show the complete statistical evaluation of the average number of stops and average vehicle delays.

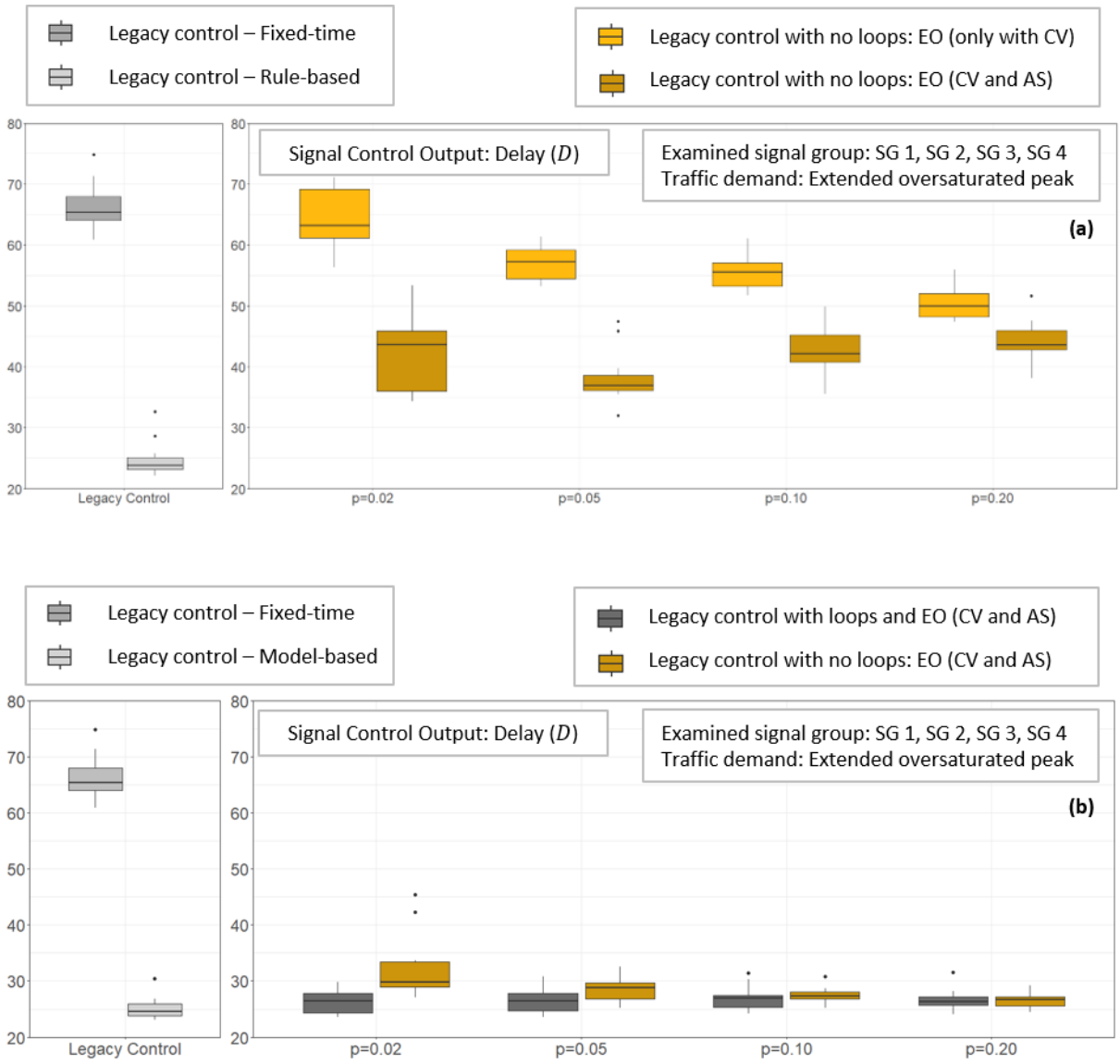

Figure 5.5 Legacy signal control output with fused estimations from the Extended Observer

The fusion reduces the average delays (6-22 seconds) and stops (0.60-2.10) for all penetration rates (Figure 5.5.a, Tab. A.6, Tab. A.7) consistently (i.e. with statistical significance). The biggest improvements are observed for the lower penetration rates. Figure 5.5.b shows how the fused estimation (dark-gold boxplot) gets much closer to the respective legacy control in comparison to Figure 5.5.b. This is expected, since the model-based control can utilize easier the state estimation. The delays from the EO-based control are 1-7 seconds higher (Tab. A.8) than the one from the legacy control, whereas the stops are only 0.05-0.5 higher (Tab. A.9). The respective difference from the EO-based control and the fixed-time control is considerably higher. The delays fall from 66 seconds to 26-32 seconds (Tab. A.10) and the stops from 4.7 to 1.0 (Tab. A.11).

This indicates that low penetration rates might never outperform full loop detection but can provide an alternative to traffic-dependent signal plan selection that usually takes place in real-systems in longer intervals (e.g. 30-120 minutes). This needs further investigation and goes beyond the scope of this thesis. The dark-grey boxplot shows a test scenario where the model-based control runs with full loop detection and just uses the queue estimation from the Extended Observer for queue correction. Even though the provided queue estimation is more accurate in comparison to only loop detection, there is no improvement in the control output. In fact, the performance of the control slightly decreases. This shows that queue correction towards the ground truth does not guarantee optimal control overall. However, it can be effectively used for targeted improvements of oversaturated approaches, especially in cases of missing or faulty detection.

In [PAPAPANAGIOTOU & BUSCH, 2020] the queue correction from the Extended Observer has shown to reduce the delays (15-27%) for the oversaturated signal and the overall intersection (2-15%), in comparison to legacy control with one missing detector on the main oversaturated approach. Furthermore, in [PAPAPANAGIOTOU & BUSCH, 2020], camera measurements are utilized for low queues and CV for higher queue values. The improvements in the control are not as big as the improvements in queue length estimation. The controller is limited by maximum green times and must consider the other directions too. Hence, it cannot always fully serve very long queues, even if they are correctly estimated.

5.3 Real-world Intersection

In this section the performance of the Extended Observer is evaluated with the help of microscopic simulations of an intersection in the city of Verona, Italy, where the UTCS Spot/Utopia is operating (Figure A.11). First the simulation settings are presented with brief description of the implementation, calibration, and validation efforts. Then, the evaluation results are presented for realistic low penetration rates. In section 5.4, it is described how the formulation is validated as a Proof of Concept (PoC) for real-world implementation. The developed technical architecture in the case of feeding Spot/Utopia is presented and some recommendations for potential future implementations are given.

5.3.1 Settings

Implementation

The Extended Observer gets the measurements from the simulation environment through COM API and feeds the simulated Spot controller through the Spot/Utopia communication protocol. All algorithms are developed in C++ based on a free variable-dimension EKF library [ZALZAL, 2006] and run parallel with the simulation (runtime always below 1 sec). Even though the development is purely scientific, it's applicability has been proven in real-world conditions (see section 5.4).

The duration of each simulation run is 2 hours with 12 simulation runs per scenario and cool down phase until all vehicles leave the network (at least 15 minutes). Four days (Monday-Thursday) of a typical week (April 2017) are taken and each is repeated with three different random seeds to reach 12 simulation runs that cover sufficiently stochastic variations. The fusion ignores all loop detectors and makes no use of historical traffic patterns. There is no tuning of the algorithms in comparison to the test intersection implementation described before.

The only needed recalculation is the parameters α and β of the approximate power function for the travel time measurements, exactly as described for the test intersection (see also Figure A.2). To calculate α and β two random historical days (March 2017) were simulated to get the minimum travel time (approximates the free flow travel), maximum travel times and maximum queue length. The power function gives only an approximation of the congestion and hence there is no need for extra tuning efforts. In fact, these random days are simulated with a different control method (rule-based) to guarantee no fitting of the power function to the Spot control. The travel time measurement locations are identical to the real road sections of a certain traffic data provider.

Calibration and Validation

For the calibration, real detector data from Spot/Utopia are used to get the traffic demand and the turning movements. The traffic signal control is emulated in the microscopic simulation by running Spot/Utopia locally and communicating with the simulation environment (PTV Vissim) in real-time. The validation is done by comparing the average travel times from the simulation with data from traffic data providers. The validation is by no means perfect but is considered sufficient for the comparative evaluation of scenarios that is aimed here. Figure A.12 shows indicative datasets used for the calibration and validation.

Many traffic data providers have been examined in the scope of this work for the specific intersection and in general, regarding traffic data format, coverage, and resolution. The exact penetration rate of Connected Vehicles is not published, and varies greatly between countries, cities and even intersections. A real-world penetration rate of 5-15% is considered realistic from all traffic data experts that were interviewed for this thesis. However, the hands-on data analysis indicated much lower penetration rates.

5.3.2 Results

Part IV. Feeding the real-world intersection with the Extended Observer

The results of this section focus on the signal control output. The data fusion evaluation shows that all key findings remain valid for multiple lanes and signal stages and is therefore not repeated here. Tab. 5.8 gives the overview of the last part of the evaluation that examines the performance of the EO-based control under realistic conditions.

Research Question: *What is the benefit and accuracy of the data fusion when it feeds a real-world signal control?*	
Key findings - benefits	Practical interpretation - accuracy
A. The Extended Observer provides a reliable alternative to loop detectors.	• The Extended Observer can accelerate the clearing of the queues up to 41% in comparison to model-based control. • The Extended Observer retains similar level of performance regarding delays and stops, in comparison to loop detectors, with slight decrease of delays (-4 seconds) and insignificant increase of stops. • The benefits start from very low penetration rates 2-5%. • The benefits do not increase significantly as the penetration rate increases.
B. The Extended Observer is robust against unexpected extreme changes in demand and capacity.	• As duration of oversaturation increases, the reduction of the clearing time increases too. • The Extended Observer can be used with minimum filter tuning to improve any fixed-time control. • The Extended Observer can be used as basis for adaptive control with minimum signal configuration efforts • Adaptive control with ideal loop detection topology and good signal configuration is always superior in low penetration rates.

Tab. 5.8 Key findings and practical interpretation of evaluation - Part IV

A. The Extended Observer provides a reliable alternative to loop detectors

Figure 5.6 and Tab. 5.9 depict the evaluation results for penetration rate p=0.05 for the early morning peak 06:15-08:00. An overview of all parameters are contained in Tab. A.12. Four control scenarios are presented:

- *Fixed-time*: The fixed-time control that is based on the maximum configured green times for all signals.
- *Spot-faulty detection:* The real Spot as runs on the field, where the entry detector for SG-3050-1 and the exit detector for the respective free right turners are not working.
- *Spot-full detection:* The planned Spot as if the two detectors were working.
- *Spot-EO:* The control where the Extended Observer feeds Spot with turnings, departures, arrivals, and queue length estimation.

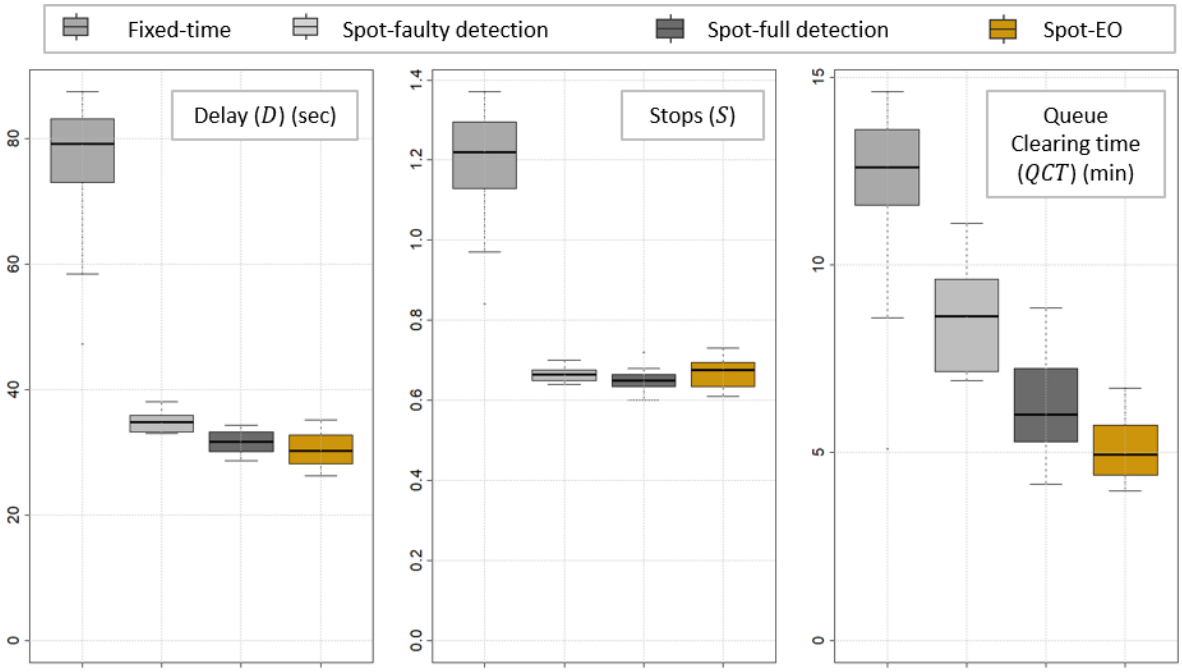

Figure 5.6 Signal control output for real-world intersection, Spot with Extended Observer.

p=0.05, 06:15-08:00			Spot with EO vs. Spot with faulty detection			Spot with EO vs. Spot with full detection		
Delay (sec)			**Delay reduction**			**Delay reduction**		
$\overline{D_{Spot}^{faulty}}$	$\overline{D_{Spot}^{full}}$	$\overline{D_{Spot}^{EO}}$	$\overline{\Delta D\%}$	$\overline{\Delta D}$	p_value	$\overline{\Delta D\%}$	$\overline{\Delta D}$	p_value
34.87	31.59	30.55	*-12.38%	*-4.32	6.3e-05	-3.29%	-1.04	0.1101
Stops			**Stops increase**			**Stops increase**		
$\overline{S_{Spot}^{faulty}}$	$\overline{S_{Spot}^{full}}$	$\overline{S_{Spot}^{EO}}$	$\overline{\Delta S\%}$	$\overline{\Delta S}$	p_value	$\overline{\Delta S\%}$	$\overline{\Delta S}$	p_value
0.66	0.65	0.67	+0.75%	+0.005	0.2895	*+2.69%	*+0.0175	0.0361
Queue Clearing time (min)			**Queue Clearing time reduction**			**Queue Clearing time reduction**		
$\overline{QCT_{Spot}^{faulty}}$	$\overline{QCT_{Spot}^{full}}$	$\overline{QCT_{Spot}^{EO}}$	$\overline{\Delta QCT\%}$	$\overline{\Delta QCT}$	p_value	$\overline{\Delta QCT\%}$	$\overline{\Delta CT}$	p_value
8.6	6.3	5.1	*-41.02%	*-3.5	3.3e-06	*-19.45%	*-1.2	0.0145

*statistically significant reduction: $N = 12,\ CI_{(1-alpha)\%} = 95\%, {}^{CI}/_{s_d} = 2,\ s_d < 3\ seconds$

Tab. 5.9 Signal control output for Verona intersection, Spot with and without Extended Observer

The signal control configuration (i.e. stage sequence, minimum and maximum stage duration) remains identical for all above scenarios. In the highest demand peak, the maximum green times are reached for all controls.

In comparison to the fixed-time control, the Extended Observer reduces the average vehicle delay to 30 seconds (from 75 seconds), the average number of stops to 0.67 (from 1.18) and the clearing time to 5 minutes (from 12 minutes). In comparison to the real Spot control, the delay reduction from the fusion is -12% and the clearing time reduction reaches -41% (both statistically significant). The increase in stops is trivial and not statistically significant. In comparison to the planned Spot control, the delay and clearing time reduction are -3% and -19% respectively (both statistically significant). The increase in stops is +3% and statistically significant with p=0.0361.

Overall, the Spot-EO achieves lower delays and faster clearing of the queue, in comparison to both the real (i.e. faulty detection) and planned (i.e. full detection) control. The slight increase in terms of stops and the high reduction in terms of clearing time indicates the change in behaviour of Spot through the feeding of the Extended Observer. The lack of knowledge of exact individual vehicle arrivals is balanced out by the recognition of the oversaturation. Note that the planned Spot-control (detector distance from stop line around 100m) is not an ideal topology, where longer distances are needed. This lower than optimal distance is however extremely typical for real-world implementations for reduction of cabling and digging costs.

B. The Extended Observer is robust against unexpected extreme changes in demand and capacity

The following simulation results aim to test the robustness of the filtering. It is examined if the influence on the control remains the same in extreme demand, and capacity discrepancies, even if the signal configuration is of low quality. For that, an even lower penetration rate is chosen (p=0.02). Moreover, the simulation starts directly in the peak hour (7:00-09:00 and 17:00-19:00). This adds an extra challenge, because of the abrupt and lengthy oversaturation. Furthermore, extreme percentage of HGV (20%) is introduced. In the previous presented results (Part V-A), an assumption of a moderate 5% HGV is made due to the lack of detailed classification data for the specific intersection.

Another configuration is introduced for the following results (Part IV-B): *Spot*-EO*. Here, the control is configured with increased maximum stage length for serving SG-3050-7 (south→west movement). To put this in perspective, the *Spot-loops* (full detection) allows green times for SG-30-50-7 between 12-21 seconds that fit greatly the traffic demand, whereas the *Spot*-EO* is configured to allow green times for SG-30-50-7 between 12-48 seconds. This way, any overestimation would lead to extreme reduction of performance. The maximum signal timings for the other decisive signal groups (SG-30-50-1 and SG-30-50-2) remain the same for both *Spot*-EO* and *Spot-loops.* Their range is already high (27-63 seconds and 36-72 seconds respectively). *Spot*-EO* should be regarded as a control that has very low need for configuration and allows high signal timing variations (or degraded adaptive control).

Figure A.13 and Tab. A.13 show the results of the described extreme scenario. The jump in delays, stops and clearing time is observed for all signal control methods due to the reduction of capacity from the high number of HGV. As before, the *Spot*-EO* results in increased delays (from 43-56 sec to 46-67 sec) and stops (from 0.75-0.85 to 0.83-1.0), in comparison to the full detection. They both remain much lower than the respective delays (142-161 sec) and stops (2.0-2.15) of the fixed-time control. The *Spot*-EO* achieves again lower clearing times (5.8-18.9 minutes) in comparison to the full detection (6.8-20.7 minutes). This shows that the Extended Observer supports a faster clearing of the queues in extreme conditions even if the configuration is far from optimal. The results were confirmed for both peak hours. Figure A.14 shows additionally the results for the moderate HGV percentage (5%) for both peak hours. The performance of the fusion remains similar for both peak hours despite the different traffic demand combination.

5.4 Proof of Concept

Technical Architecture

The algorithms of the Extended Observer do not require microscopic simulations. Microscopic simulations (PTV Vissim) are used in this thesis for systematic analysis and evaluation (chapters 4 and 5 respectively) in absence of enough real-world Connected Vehicles. At the same time, a Proof of Concept (PoC) is developed for verification of the applicability of the Extended Observer in a real-world environment. Figure 5.7 illustrates all the necessary modules and interfaces that are developed and tested in the scope of this thesis.

The Extended Observer is extended with an interface that fetches the Connected Environments data. The most prominent traffic data providers (Here, Inrix, TomTom) are integrated thought REST API and provide the Aggregated Section (AS Server-Client) measurements. A mobile app is developed to provide Connected Vehicle (CV Server-Client) measurements through AMQP (Advanced Message Queuing Protocol). The Connected Environments Interface is part of the Extended Observer but can be used without the data fusion just for monitoring purposes. The last part to complete the PoC is the remote communication with the existing traffic signal control (Spot client-server communication). This is developed and tested in the chair of Traffic Engineering and Control with the support of Swarco AG.

Recommendations

The PoC is completely developed and validated but not tested on the field. The minimum input requirements are typical real-time signal data and real-time traffic data. The signal data must be available at least every cycle, optimally every 1-3 seconds. The minimum traffic data required are aggregated travel times and/or speeds. Optimally, individual Connected Vehicles should be available. Of course, the available loop detectors can be integrated to the fusion.

The Extended Observer integrates measurements for each intersection separately. Therefore, it can be used to feed adaptive intersections locally or centrally. It is tested in this thesis at isolated intersections to examine in detail its data fusion potential and influence on the control. However, if in the real-world the incoming data are predominately Aggregated Section data (as expected in the transition phase with low penetration rates), it is reasonable to consider the data fusion as part of an UTCS that uses a macroscopic view of the traffic flow. In that case, the Extended Observer can provide enhanced traffic state estimation and prediction both at the intersection level and at the link level. The output of the data fusion can easily find implementations in many traffic flow modelling approaches.

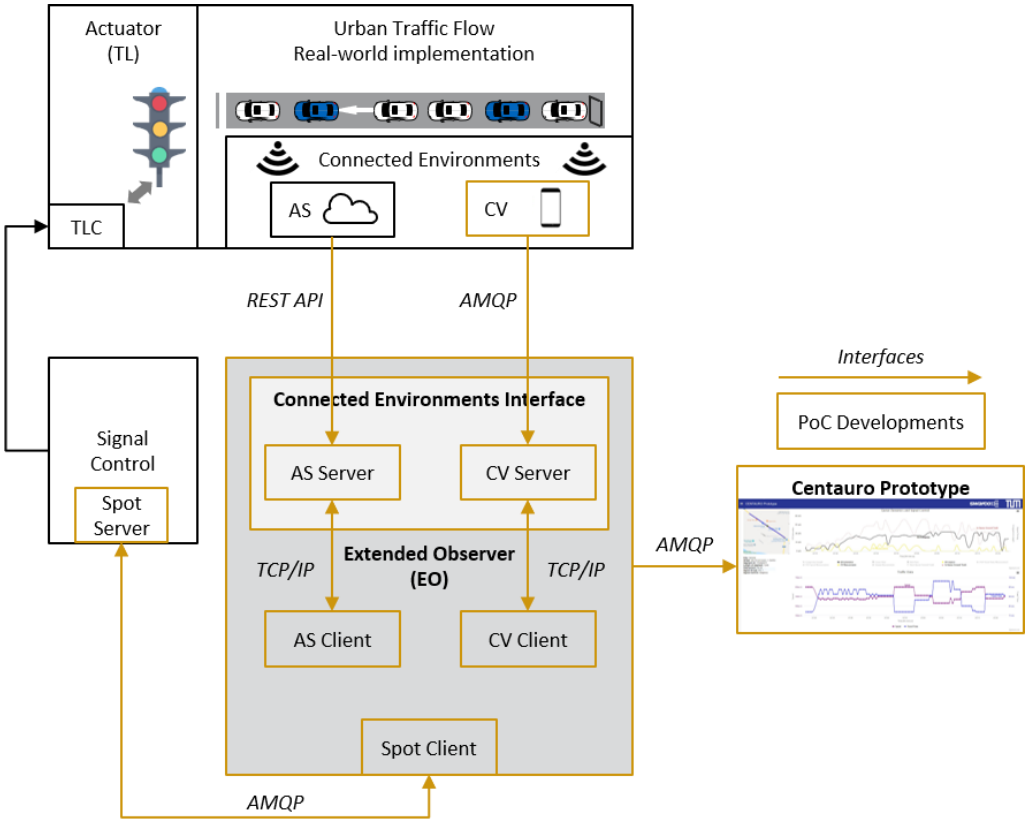

Figure 5.7 Extended Observer Proof of Concept - backend developments

Even though the Extended Observer is designed to work without any knowledge of the accuracy of the measurements, it is vital to provide transparency to the cities before, during and after the implementation. The quality of the measurements from low penetration rates not only varies greatly between intersections, cities, and countries, but also varies during the day. The analysis of the input (measurements) and output (estimations, predictions) should not be underestimated for real-world implementations. This should allow clear Service Level Agreements (SLA) between traffic data providers, traffic signal control providers and cities. Figure 5.8 illustrates the developed software modules for the PoC. In the scope of this work a web-application is also developed, to assist the state-of-the-art analysis, the developments and the implementation of the PoC [NOACK, 2018; NOACK ET AL., 2019]. The algorithms of the

PoC are the same as the algorithms analyzed and evaluated in the simulation environment (chapters 4 and 5 respectively). The input can be switched from simulation input to real-world input, or use both at the same time. Furthermore, the Extended Observer can use for example Aggregated Section measurements from the real-world and CV measurements from the simulation environments as input. This flexibility opens additionally the possibility to tune the algorithms based on simulations before implementation.

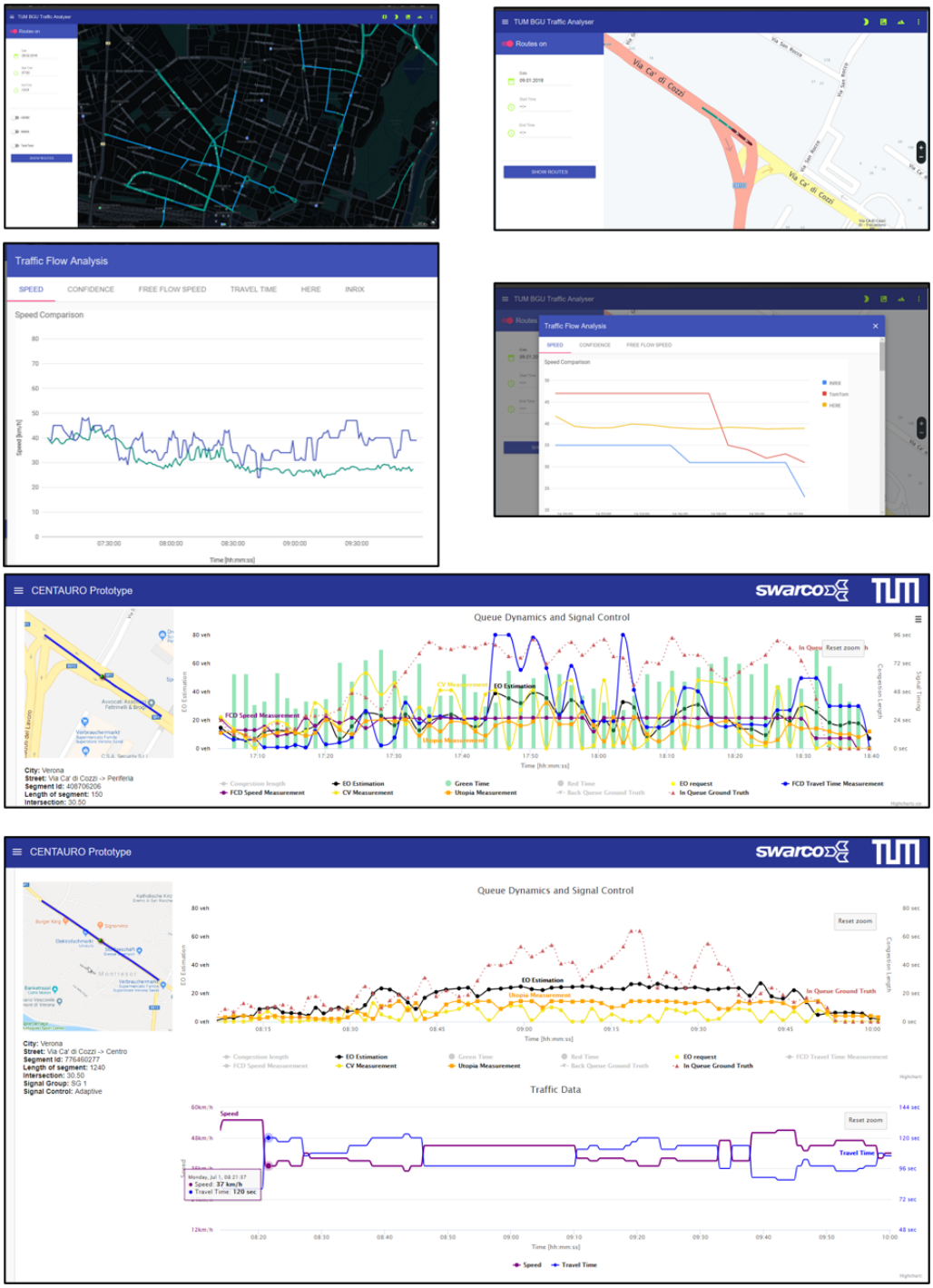

Figure 5.8 Extended Observer Proof of Concept - frontend developments

5.5 Summary

The Extended Observer combines the sporadic measurements from Connected Vehicles with the process equation to keep a robust estimation, under varying traffic conditions. In oversaturation, the fusion reduces the high CV measurements errors, while in undersaturation avoids filter deviations. The highest benefit is observed for lower penetration rates ($p<20\%$) and oversaturation. For higher penetration rates in undersaturation, the fusion cannot improve the already very good CV measurements but keeps the quality until the next measurement is available. The performance of the data fusion module is independent of the signal control method, measurement errors and underlying measurement equations. Simple formulas can be used and compared easily through the predictor-corrector formulation. In addition, historical models can be utilized to improve arrival rate estimation. This however introduces a bias to the estimation and reduces the ability to adapt to abrupt changes (Tab. 5.2 - Part I).

Introducing multiple measurements allows the Extended Observer to improve its performance. Aggregated Section data (travel times and speeds) can be used to improve CV measurements in oversaturation even further. The fusion outperforms infrastructure-based sensors for oversaturation that extends beyond their range. The example of fusion from camera and travel time measurements shows the potential of combining infrastructure and mobile sensors (Tab. 5.4 - Part II).

The enhanced fused estimation, with Aggregated Section data, results in an improved signal control, in comparison to a control based solely on filtering of CV. The fused estimation pushes the legacy control to account for the oversaturated approaches. This however leads to higher green and cycle times. The improvements from the fusion can be seen also in the resulting traffic flow. The Extended Observer not only recognizes congestion but accelerates its clearance too. The effects are significant even for very low penetration rates, where delays and stops are reduced in comparison to fixed time drastically. As expected, mobile sensors cannot make the legacy control work better than it is configured for. The model-based legacy control can utilize the fusion significantly better than the rule-based control, as it utilizes more information from it, such as arrivals and departures (Tab. 5.7 - Part III).

The evaluation of the real-world intersection shows that the Extended Observer can easily be used for topologies with multiple lanes, more complicated signal group stages, real traffic demand, and typical signal configuration. The control based on the Extended Observer outperforms the legacy control in terms of queue clearing time for realistic low penetration rates (5%). The fusion reduces slightly the delays, while the stops increase marginally. Furthermore, the fusion shows robustness when tested with extreme demand and supply unpredictability (Tab. 5.8 - Part IV).

The applicability in the real-world has been validated with the development of a PoC for the UTCS Spot/Utopia for the same intersection that is used for the simulations in Verona, Italy.

6. Conclusions and Outlook

The term *adaptive* has been established in the domain of signal control to describe different levels of Urban Traffic Control Systems. It refers to adapting signal timings, based on real-time measurements. This thesis suggests that the notion of adaptivity should not be restricted to signal timings. In future urban environments, it will be essential to adapt the data input, based on diverse sensors and communication technologies.

The emerging Connected Environments in urban areas promise great benefits for Urban Traffic Control Systems. However, the available data vary greatly in resolution and accuracy, especially for the currently low penetration rates (1-15%). Trajectories of individual Connected Vehicles are very scarce. Typically, only Aggregated Section measurements, such as travel times, speeds, and delays from Floating Car Data are available. According to simulation studies, higher penetration rates (25-40%) are needed to achieve tangible benefits for the state estimation and control. Current Urban Traffic Control Systems are designed to work with measurements from all incoming vehicles and not only from a small sample size. Therefore, uncertain measurements from Connected Vehicles are hard to integrate in the control. This leaves a new range of sensors outside of the perspective of the signal control.

The analysis of different data sources shows that Connected Vehicles measurements vary greatly in different locations and times of the day. Especially in low penetration rates, their potential lies in their range, and not in their accuracy. Data fusion methods facilitate enhanced traffic state estimation from multiple sensors, and can accelerate the integration of Connected Environments in Urban Traffic Control Systems. Therefore, a module for sensor and data fusion for signal control is introduced in this thesis. Its development builds on robust algorithms, that capture the highly dynamic problem of traffic state estimation and control. The goal is to provide a formulation that is not only independent of the varying data availability, but also independent of the underlying signal control method.

State-space formulation of dynamic controlled systems allows a straightforward and extendable problem formulation. The Extended Kalman Filter estimates the state of a controlled process and allows the integration of measurements from multiple sensors. Direct and indirect measurements, with different errors, are fused via a predictor-corrector formulation. The prototypical data fusion module developed in this thesis, the Extended Observer, builds on the Extended Kalman Filter, to estimate the queue length, arrival, departure, turning and penetration rate. The main process equation for queue length estimation is developed based on the conservation law and the signal timings. The design of the Extended Observer allows the combination of multiple filters for robust estimation. Practical measurement equations for various sensor types, that can be used for cycle-to-cycle correction of the a priori estimation, are presented. Furthermore, a detailed description of the adaptive formulation shows how to update the measurement vector and measurement noise covariance

at every filter step. This allows a generic formulation with variable-dimension measurement vector and adaptive noise covariances.

The cycle-to-cycle analysis confirms the high instability of queues around saturation. It also validates the increasing queue variance for increasing queues. This emphasizes the need for a dynamic calculation of the process noise covariance. Regarding the measurement errors, the penetration rate is shown to influence the errors from Connected Vehicles, mainly for undersaturated conditions. In oversaturated conditions, the main source of uncertainty is the stop-and-go behavior of the vehicles and therefore the measurement errors are significantly higher for all penetration rates. This high variability of the measurement errors indicates that the measurement noise covariance from mobile sensors should not be set as a fixed value. It is proposed to reduce the measurement noise covariance for increasing penetration rates. At the same time, it is proposed to increase the measurement noise covariance for higher queues. Aggregated Section measurements recognize oversaturated conditions, even though they can only offer a rough approximation of the queue. Connected Section measurements from cameras are very good in their range, but unable to capture longer queues. Overall, this variability und unpredictability of measurement and process errors confirms the need for adaptive data fusion formulation.

The suggested formulation of the Extended Observer considers additionally the operational requirements. The operators emphasize the need not only for accuracy and coverage, but also for transparency, simplicity, and flexibility. The proposed algorithms are designed to work with uncertainty in measurement errors. Moreover, the Extended Observer requires low computational resources, without the need to store historical data. Nevertheless, the possibility of historical data inclusion is also given with the proposed formulation. Furthermore, the Extended Observer supports an intuitive tuning, by adjusting only the measurement to process covariance ratio. This should allow the operators to adjust the weighting of the measurements, depending on the local availability and accuracy. This way, the Extended Observer can be used to enhance existing infrastructure sensors in oversaturation or even replace them. The Proof of Concept developments for the state-of-the-art Urban Traffic Control System Spot/Utopia validate the feasibility of the prototypical module.

The evaluation results from the test intersection show that the highest benefit from the fusion of isolated measurements from Connected Vehicles occurs for oversaturated conditions for low penetration rates (<20%). The fusion reduces the high Root Mean Square Error from the measurements between 16-30%. The measurements are combined with the process equation and improve the estimation through system knowledge. Fusion of CV measurements becomes obsolete in undersaturated conditions and high penetration rates (>20%). The benefit in that case is the retaining of the quality for cycles with no measurements. Moreover, it is shown that simple measurement equations are sufficient with a predictor-corrector formulation due to the regular updates. At the same time, the fusion performance is independent of the signal control and measurement error.

Enhanced fusion of measurements from Aggregated Section data with measurements from Connected Vehicles reduces the Root Mean Square Error even further (37-46%). The fused estimation shows lower errors than the individual data sources. In comparison to control based solely on Connected Vehicles, the fused estimation reduces the average delay and number of stops between 23-34% and 19-45% respectively. Aggregated Section data improve the estimations that go beyond the infrastructure range. For example, fusion of travel times with camera measurements improves the measurements from cameras between 14-29%. The results suggest that the fused estimation leads to dramatically lower average delays and number of stops, in comparison to fixed-time control, even for very low penetration rates (2%). The average delays reduce from 66 to 32 seconds and the average number of stops reduce from 4.7 to 1.5. However, legacy control with full detection performs better than a control based on fused estimation of mobile sensors. The average delays and number of stops with full detection are 25 seconds and 1.0 respectively.

The evaluation results from the real intersection indicate that replacing entirely infrastructure-based sensors with mobile sensors in low penetration rates, changes the behavior of the control. The control favors oversaturated approaches, since mobile sensors observe higher queues than infrastructure sensors. This leads to higher green times for the oversaturated approach and higher cycle times. The overall performance of the control, in terms of average delays and number of stops, remains similar. Hence, data fusion methods are considered a reliable alternative to infrastructure-based sensors for oversaturated conditions. Mobile sensors have the advantage to accelerate the clearance of queues even for very low penetration rates (<5%). It is also shown that the proposed predictor-corrector formulation is robust in cases of unpredictable extreme conditions. High traffic demand peaks and high truck rates are examined. The performance of the fusion and the control remains consistent, without any prior knowledge of historical demand or vehicle composition.

The control in low penetration rates is bound to be less efficient in terms of stops and delays, since the exact arrival or platooning of vehicles is not known. This is the biggest shortcoming from low penetration rates in signal control that is not covered in this thesis. In addition, on-demand phases cannot be served with the accuracy achieved from infrastructure-based sensors for low penetration rates. The detection and prediction of the exact arrival of individual vehicles is more important for the control, in comparison to the cycle-to-cycle estimation of queues and arrivals, especially in undersaturated conditions.

To fill this gap, extending the state vector to capture vehicles in shorter segments, and following individual vehicles, should be further investigated. The presented second-by-second formulation can be the basis for such extension. Furthermore, the measurements from Connected Vehicles shall be expanded to include more detailed information from the ego-vehicle (e.g. vehicle type, headways), as well as information from Vehicle-to-Vehicle communication (e.g. relative acceleration). The use of Extended Kalman Filter as basis, opens the door to tracking of Connected and Automated Vehicles. This flexibility of the Extended

Observer to cover a wide range of sensor types might be its greatest asset, not only for legacy but also for future systems.

Even though the proposed methodology is designed for Urban Traffic Control Systems, traffic state estimation and prediction might be equally valuable to other Dynamic Traffic Management applications. For example, travel time prediction, route recommendation, signal performance analytics and control of individual vehicle trajectories (e.g. Green Light Optimal Speed Advisory, platooning of Connected and Automated Vehicles) would benefit from the Extended Observer. Other future work includes examining further the robustness of the fusion module, in relation to other critical aspects of signal control, such as Public Transport prioritization, vehicle fleet composition, signal coordination, pedestrians, and bicyclists.

In the short-term, mobile sensors are expected to assist current Urban Traffic Control Systems to identify long queues, warn for upcoming congestion and evaluate the performance of the signal control. As the penetration rates increases, strategic inductive loop detectors, that are utilized for macroscopic traffic flow estimation, might be gradually replaced from mobile sensors. In the long-term, Vehicle-to-Infrastructure and Vehicle-to-Vehicle communication should reduce the number of infrastructure-based sensors even further. Still, inductive loop detectors are considered in many cases necessary, to ensure safe intersection crossing and might be necessary even in very high penetration rates. The robust development of the existing systems, in a way that allows multiple sensor types to be integrated, is very important for safe and effective signalized intersections.

Last but not least, there is an increased interest in light Urban Traffic Control Systems, with low installation and maintenance costs, by cities internationally. A predictor-corrector data fusion formulation could be used for estimation and prediction, with minimum sensor requirements. The expectations from the mobile sensors, in the transition phase of Urban Traffic Control Systems, should not be to outperform full infrastructure-based detection. Yet, this thesis indicates that appropriate data fusion methods will achieve stable and adequate level of service, even in low penetration rates.

References

AKCELIK, R. [1980]: Time-Dependent Expressions for Delay, Stop Rate and Queue Length at Traffic Signals. Internal Report AIR 367–1. Australian Road Research Board, Vermont South, Australia, pp.1–19.

ALBINO, V.; BERARDI, U. & DANGELICO, R.M. [2015]: Smart Cities : Definitions, Dimensions, Performance, and Initiatives. Journal of Urban Technology, 22(1), pp.2–21.

AMINI, S.; PAPAPANAGIOTOU, E. & BUSCH, F. [2016]: Traffic Management for Major Events. Digital Mobility Platforms and Ecosystems State of the Art Report, (July), pp.186–196.

ARGOTE-CABAÑERO, J.; CHRISTOFA, E. & SKABARDONIS, A. [2015]: Connected vehicle penetration rate for estimation of arterial measures of effectiveness. Transportation Research Part C: Emerging Technologies, 60, pp.298–312.

ASTROM, J.K. & MURRAY, R.M. [2010]: Feedback Systems An Introduction for Scientists and Engineers, Princeton University Press.

BARTONOVA, A.; CASTELL, N.; COLETTE, A.; SCHNEIDER, P.; VIANA, M.; VOOGT, M.; WEIJERS, E.; WESSELING, J.; BLOKHUIS, C.; MALHERBE, L.; SPINELLE, L. & GONZALEZ-ORTIZ, A. [2019]: Eionet Report - ETC/ACM 2018/21 - Low Cost Sensors. , (April).

BRAUN, R.; BUSCH, F.; KEMPER, C.; HILDEBRANDT, R.; WEICHENMEIER, F.; MENIG, C.; PAULUS, I. & PREßLEIN-LEHLE, R. [2009]: TRAVOLUTION – Netzweite Optimierung der Lichtsignalsteuerung und LSA-Fahrzeug-Kommunikation. Straßenverkehrstechnik, 6, pp.365–374.

BRIGNOLO, R. [2014]: Advances in harmonizing the Deployment Approach for C-ITS in Europe. COMeSafety 2 Deliverable 3.5.

BUSCH, F. & KRUSE, G. [2001]: MOTION for SITRAFFIC - a modern approach to Urban Traffic Control. In 2001 IEEE Intelligent Transportation Systems. pp. 61–64.

CELIKKAYA, N.; FULLERTON, M. & FULLERTON, B. [2019]: Use of Low-Cost Air Quality Monitoring Devices for Assessment of Road Transport Related Emissions. Transportation Research Procedia, 41(2018), pp.762–781.

CELIKKAYA, N.; PAPAPANAGIOTOU, E. & BUSCH, F. [2016]: Eco-Sensitive Traffic Management. Digital Mobility Platforms and Ecosystems State of the Art Report, (July), pp.171–185.

CHANDRA, R. & GREGORY, C. [2011]: Insync adaptive traffic signal technology: Real-time artificial intelligence delivering real-world results. 18th World Congress on Intelligent Transport Systems and ITS America Annual Meeting 2011, 2(March), pp.1686–1698.

CHENG, Y.; QIN, X.; JIN, J.; RAN, B. & ANDERSON, J. [2011]: Cycle-by-Cycle Queue Length Estimation for Signalized Intersections Using Sampled Trajectory Data. Transportation Research Record: Journal of the Transportation Research Board, No. 2257, pp.87–94.

COMERT, G. [2016]: Queue length estimation from probe vehicles at isolated intersections: Estimators for primary parameters. European Journal of Operational Research, 252(2), pp.502–521.

COMERT, G. [2013]: Simple analytical models for estimating the queue lengths from probe vehicles at traffic signals. Transportation Research Part B: Methodological, 55, pp.59–74.

DOWLING, R.; SKABARDONIS, A. & ALEXIADIS, V. [2004]: Traffic Analysis Toolbox Volume III : Guidelines for Applying Traffic Microsimulation Modeling Software. Rep. No. FHWA-HRT-04-040, U.S. DOT, Federal Highway Administration, Washington, D.C, III(July), p.146.

DYNNIQ [2020]: ImFlow. verfügbar unter: https://dynniq.com/products-and-services/imflow/ [Accessed 5. June 2020].

ETSI [2009A]: ETSI EN 302 637-2, Intelligent Transport Systems (ITS), Vehicular Communications; Basic Set of Applications; Part 2: specification of cooperative awareness basic service. , 2, pp.1–44.

ETSI [2009B]: ETSI EN 302 637-3, Intelligent Transport Systems (ITS), Vehicular Communications; Basic Set of Applications; Part 3: specifications of decentralized environmental notification basic service. , 3.

EUROPEAN COMMISSION [2016]: C - ITS Platform, Final Report.

EUROPEAN COMMISSION [2019A]: EU regional and urban development, Smart cities. verfügbar unter: https://ec.europa.eu/info/eu-regional-and-urban-development/topics/cities-and-urban-development/city-initiatives/smart-cities_en [Accessed 10. August 2019].

EUROPEAN COMMISSION [2019B]: European Commission, Intelligent transport systems. verfügbar unter: https://ec.europa.eu/transport/themes/its_en [Accessed 10. August 2019].

EUROPEAN COMMISSION [2020]: Root mean square error (RMSE). verfügbar unter: https://ec.europa.eu/eurostat/cros/content/root-mean-square-error-rmse_en [Accessed 14. May 2020].

FAOUZI, N.E. EL & KLEIN, L.A. [2016]: Data Fusion for ITS: Techniques and Research Needs. Transportation Research Procedia, 15, pp.495–512.

FAOUZI, N.E. EL; LEUNG, H. & KURIAN, A. [2011]: Data fusion in intelligent transportation systems: Progress and challenges - A survey. Information Fusion, 12(1), pp.4–10.

FARAGHER, R. [2012]: Understanding the Basis of the Kalman Filter Via a Simple and Intuitive Derivation [Lecture Notes]. IEEE Signal Processing Magazine, 29(5), pp.128–132.

FENG, Y.; HEAD, K.L.; KHOSHMAGHAM, S. & ZAMANIPOUR, M. [2015]: A real-time adaptive signal control in a connected vehicle environment. Transportation Research Part C: Emerging Technologies, 55, pp.460–473.

FGSV [2006]: Hinweise zur mikroskopischen Verkehrsflusssimulation: Grundlagen und Anwendung.

FGSV [2011]: Hinweise zur Strategieanwendung im dynamischen Verkehrsmanagement.

FGSV [2003]: Hinweise zur Strategieentwicklung im dynamischen Verkehrsmanagement.

FGSV [2015]: Richtlinien für Lichtsignalanlagen - Lichtzeichenanlagen für den Straßenverkehr.

FHWA [2013]: Measures of Effectiveness and Validation Guidance for Adaptive Signal Control

Technologies. Fhwa-Hop-13-031, (July).

FHWA [2015]: Signal Timing Manual. NCHRP Report, (812), p.317p.

FHWA [2006]: Traffic Detector Handbook. U.S. Department of Transportation, Federal Highway Administration, I–II(October), p.462.

FISCHER, H.-J. [2015]: Standardization and Harmonization Activities Towards a Global C-ITS. In Vehicular ad hoc networks - Standards, Solutions, and Research. Springer, pp. 29–35.

FRIEDRICH, B. [1999]: Ein verkehrsadaptives Verfahren zur Steuerung von Lichtsignalanlagen. Dissertation. Technische Universität München.

FRIEDRICH, B.; MATSCHKE, I.; ALMASRI, E. & MÜCK, J. [2002]: Data Fusion Techniques for Adaptive Traffic Signal Control.

FU, L.; HELLINGA, B. & ZHU, Y. [2001]: An adaptive model for real-time estimation of overflow queues on congested arterials. IEEE Conference on Intelligent Transportation Systems, Proceedings, ITSC, (February), pp.219–226.

GARTNER [2020]: Gartner Hype Cycle. verfügbar unter: https://www.gartner.com/en/newsroom/press-releases/2019-29-08-gartner-identifies-five-emerging-technology-trends-with-transformational-impact [Accessed 6. June 2020].

GIFFINGER, R.; FERTNER, C.; KRAMAR, H.; KALASEK, R.; PICHLER-MILANOVIC, N. & MEIJERS, E. [2007]: Smart cities - Ranking of European medium-sized cities,

GOODALL, N.J. [2013]: Traffic Signal Control with Connected Vehicles. Dissertation. University of Virginia.

GOOGLE DEVELOPERS [2020]: Protocol buffers. verfügbar unter: https://developers.google.com/protocol-buffers/ [Accessed 30. May 2020].

HAMAD, K. & ABUHAMDA, H. [2015]: Estimating Base Saturation Flow Rate for Selected Signalized Intersections in Doha, Qatar. Journal of Traffic and Logistics Engineering, 3(2), pp.168–171.

HE, Q.; HEAD, K.L. & DING, J. [2014]: Multi-modal traffic signal control with priority, signal actuation and coordination. Transportation Research Part C: Emerging Technologies, 46, pp.65–82.

HEAD, L. [2016]: The Multi Modal Intelligent Traffic Signal System (MMITSS): A Connected Vehicle Dynamic Mobility Application.

IBM GLOBAL BUSINESS SERVICES [2010]: Smarter cities for smarter growth. verfügbar unter: https://www.ibm.com/downloads/cas/3OO2WQJA [Accessed 10. August 2019].

IETF [2016]: The GeoJSON Format. Internet Engineering Task Force. verfügbar unter: https://tools.ietf.org/html/rfc7946 [Accessed 30. May 2020].

ILGIN GULER, S.; MENENDEZ, M. & MEIER, L. [2014]: Using connected vehicle technology to improve the efficiency of intersections. Transportation Research Part C: Emerging Technologies, 46, pp.121–131.

ISO [2017]: ISO/TS 19091:2017, Intelligent transport systems — Cooperative ITS — Using V2I

and I2V communications for applications related to signalized intersections.

JING, P.; HUANG, H. & CHEN, L. [2017]: An adaptive traffic signal control in a connected vehicle environment: A systematic review. Information (Switzerland), 8(3).

JOHNSTON, D. [2017]: Learnings arising from the fusion of traffic data from multiple sources. In ITS World Congress 2017 Montreal. pp. 1–8.

JUNIPER RESEARCH FOR INTEL [2017]: Smart Cities-What's in it for citizens. verfügbar unter: https://newsroom.intel.com/wp-content/uploads/sites/11/2018/03/smart-cities-whats-in-it-for-citizens.pdf [Accessed 10. August 2019].

KALMAN, R.E. [1960]: A New Approach to Linear Filtering and Prediction Problems 1. Transactions of the ASME-Journal of Basic Engineering, 82(Series D), pp.35–45.

KATHS, H.J. [2017]: Kooperative Lichtsignalsteuerung Integration von Fahrzeugen in die Steuerung vernetzter Verkehrssysteme. Dissertation. Technische Universität München.

KINRA, A.; KASHI, S.B.; PEREIRA, F.C.; COMBES, F. & ROTHENGATTER, W. [2019]: Textual Data in Transportation Research: Techniques and Opportunities. In C. Antoniou, L. Dimitriou, & F. Pereira, eds. Mobility Patterns, Big Data and Transport Analytics. Elsevier, pp. 173–197.

KLEIN, L.A. [2018]: ITS sensors and architectures for traffic management and connected vehicles / Lawrence A. Klein., CRC Press.

KUHNE, R. & MICHALOPOULOS, P. [2001]: Continuum Flow Models. Traffic-flow theory, pp.5-1-5–51.

LÄMMER, S. [2007]: Reglerentwurf zur dezentralen Online-Steuerung von Lichtsignalanlagen in Straßennetzwerken. Dissertation. Technische Universität Dresden.

LANGDON, S.; DAY, C.M.; STEVANOVIC, A.; TANAKA, A. & LEE, K. [2019]: Traffic Signal Systems Research: Past, Present, and Future Trends. 100 YEARS TRB, CENTENNIAL PAPERS, Standing Committee on Traffic Signal Systems (AHB25).

LEE, J.B. [2013]: A Kalman filter based Queue Estimation Algorithm using Time Occupancies for Motorway On-ramps. , (January), pp.13–17.

LEE, S.; WONG, S.C. & LI, Y.C. [2015]: Real-time estimation of lane-based queue lengths at isolated signalized junctions. IEEE Transactions on Intelligent Transportation Systems, 16(3), pp.1549–1558.

LINDLEY, D. V. [1952]: The theory of queues with a single server. Mathematical Proceedings of the Cambridge Philosophical Society, 48(2), pp.277–289.

LINT, H. VAN & DJUKIC, T. [2012]: Applications of Kalman Filtering in Traffic Management and Control. Tutorials in Operations Research INFORMS 2012, (2), pp.59–91.

LIU, H. [2016]: Next Generation Traffic Control with Connected and Automated Vehicles. Automated Vehicle Symposium 2016.

LIU, H.; VAN LINT, H.; VAN ZUYLEN, H. & VITI, F. [2006]: Urban travel time prediction based on queue estimation. IFAC Proceedings Volumes (IFAC-PapersOnline), 11(PART 1), pp.484–490.

MANGIAFICO, S.S. [2020]: Summary and Analysis of Extension Program Evaluation in R. verfügbar unter: https://rcompanion.org/handbook/D_01.html [Accessed 15. May 2020].

MAU, S. [2005]: What is the Kalman Filter and How can it be used for Data Fusion? Robotics Math, (December 2005), pp.16–811.

MAURO, V. & TARANTO, C. DI [1989]: UTOPIA. IFAC Control, Computers, Communications in Transportation, pp.245–252.

MAYBECK, P.S. [1979]: Stochastic models, estimation, and control, Vol. 1, New York: ACADEMIC PRESS, INC.

MERTZ, J. [2001]: Ein mikroskopisches Verfahren zur verkehrsadaptiven Knotenpunktsteuerung mit Vorrang des öffentlichen Verkehrs. Dissertation. Technical University of Munich.

MILLER, A.J. [1963]: Settings for Fixed-Cycle Traffic Signals. Journal of the Operational Research Society, 14(4), pp.373–386.

MIRCHANDANI, P. & HEAD, L. [2001]: A real-time traffic signal control system: Architecture, algorithms, and analysis. Transportation Research Part C: Emerging Technologies, 9(6), pp.415–432.

MIUCIC, R. [2018]: Connected Vehicles R. Miucic, ed., Springer Nature Switzerland AG 2019.

MOBILEYE [2020]: Mobileye. verfügbar unter: https://www.mobileye.com/ [Accessed 30. May 2020].

MÜCK, J. [2002]: Estimation methods for the state of traffic at traffic signals using detectors near the stop-line. Traffic Engineering and Control.

NOACK, F. [2018]: Comparative Analysis of Real-Time Traffic Data for Integration in Urban Traffic Control Systems. Master Thesis, Chair of Traffic Engineering and Control, Technical Universtiy of Munich.

NOACK, F.; PAPAPANAGIOTOU, E. & COCONEA, L. [2019]: A web application for analysing real-time traffic data. In 13th ITS European Congress, Brainport, the Netherlands, 3-6 June 2019. pp. 3–6.

PAPAGEORGIOU, M. [1998A]: Automatic Control Methods in Traffic and Transportation. Proceedings of the NATO Advanced Study Institute on Operations Research and Decision Aid Methodologies in Traffic and Transportation Management, pp.46–83.

PAPAGEORGIOU, M. [1998B]: Some remarks on macroscopic traffic flow modelling. Transportation Research Part A: Policy and Practice, Volume 32(5), pp.323–329.

PAPAPANAGIOTOU, E. & BUSCH, F. [2020]: Extended Observer for Urban Traffic Control Based on Limited Measurements from Connected Vehicles. IEEE Transactions on Intelligent Transportation Systems, 21(4), pp.1664–1676.

PELED, I.; RODRIGUES, F. & PEREIRA, F.C. [2019]: Model-Based Machine Learning for Transportation. In C. Antoniou, L. Dimitriou, & F. Pereira, eds. Mobility Patterns, Big Data and Transport Analytics. Elsevier, pp. 145–171.

PETERSON, A.; BERGH, T. & STEEN, K. [1986]: LHOVRA - a new traffic signal control strategy

for isolated junctions. IEE Conference Publication Second int. conf. on road traffic control;, pp.98–101.

PROJECT CONSORTIUM TUM LIVING LAB CONNECTED MOBILITY [2016]: Digital Mobility Platforms and Ecosystems State of the Art Report. , (July).

RAMEZANI, M. & GEROLIMINIS, N. [2015]: Queue Profile Estimation in Congested Urban Networks with Probe Data. Computer-Aided Civil and Infrastructure Engineering, 30(Issue 6), pp.414–432.

REED, T. & KIDD, J. [2019]: Global Traffic Scorecard. INRIX Research, (February).

ROBERTSON, I.D. [1886]: Methods of Signal Coordination. ITE, pp.36–40.

ROSTAMI SHAHRBABAKI, M.; SAFAVI, A.A.; PAPAGEORGIOU, M. & PAPAMICHAIL, I. [2018]: A data fusion approach for real-time traffic state estimation in urban signalized links. , 92, pp.525–548.

ROUPHAIL, N.; TARKO, A. & JING, L. [2001]: Traffic Flow at Signalized Intersections. Traffic-flow theory, (March 2016), pp.9-1-9–28.

RSTUDIO [2020]: RStudio. https://rstudio.com/. verfügbar unter: https://rstudio.com/ [Accessed 15. May 2020].

RUSSO, F.; RINDONE, C. & PANUCCIO, P. [2014]: The process of smart city definition at an EU level. WIT Transactions on Ecology and The Environment, 191, pp.979–989.

SIMS, A.G. & DOBINSON, K.W. [1980]: The Sydney coordinated adaptive traffic (SCAT) system philosophy and benefits. IEEE Transactions on Vehicular Technology, 29(2), pp.130–137.

STEINBERG, A. & BOWMAN, C. [2001]: Revisions to the JDL Data Fusion Model. In Handbook of Multisensor data fusion. CRC Press.

STEVANOVIC, A. [2010]: Adaptive Traffic Control Systems: Domestic and Foreign State of Practice A Synthesis of Highway Practice Transportation Research Board, ed., WASHINGTON: NCHRP.

SWARCO INTERNAL WORKSHOP [2020]: Swarco Internal Presentation.

SWARM ANALYTICS [2020]: Swarm Analytics. verfügbar unter: https://www.swarm-analytics.com/urban-traffic/ [Accessed 30. May 2020].

TAMPÈRE, C.M.J. & IMMERS, L.H. [2007]: An extended Kalman filter application for traffic state estimation using CTM with implicit mode switching and dynamic parameters. IEEE Conference on Intelligent Transportation Systems, Proceedings, ITSC, pp.209–216.

THE R FOUNDATION [2020]: The R Project for Statistical Computing. https://www.r-project.org/. verfügbar unter: https://www.r-project.org/ [Accessed 15. May 2020].

TISCHLER, K. [2016]: Neue Ansätze zur Nutzung von Induktionsschleifen-Daten an Lichtsignalanlagen : Minimierung von Fahrzeughalten und Schätzung von Kfz-Wartezeiten. Dissertation.

TOMTOM INTERNATIONAL B.V. [2012]: OpenLR: White Paper. , pp.1–156.

U.S. DEPARTMENT OF DEFENCE, D.F.S. OF THE J.D. OF L. [1991]: Data fusion lexicon. In JDL. U.S. Department of Defence, Data Fusion Subpanel of the Joint Directors of Laboratories, Technical Panel for C3.

UNITED NATIONS ED. [2019]: World Urbanization Prospects 2018: Highlights ST/ESA/SER., New York: United Nations.

UNIVERSITÄT BONN [2020]: Definitions of Sensor and Data Fusion in the Literature. Institute of Computer Science-Security and Netwoked Systems-Universität Bonn. verfügbar unter: https://net.cs.uni-bonn.de/de/wg/sdf/what-is-it/sdf-definitions/ [Accessed 31. May 2020].

VELOSO, M.; BENTO, C. & PEREIRA, F.C. [2009]: Multi-Sensor Data Fusion on Intelligent Transport Systems. MIT Portugal, Transportation Systems, Working Paper Series (Paper# ITS-CM-09-02), (March).

VERKEHRS-SYSTEME AG [2020]: VS-PLUS. verfügbar unter: http://www.vs-plus.com/documents/VS-PLUS_Produktblatt_DE.pdf [Accessed 5. June 2020].

VIGOS, G.; PAPAGEORGIOU, M. & WANG, Y. [2008]: Real-time estimation of vehicle-count within signalized links. Transportation Research Part C: Emerging Technologies, 16(1), pp.18–35.

VITI, F. [2006]: The Dynamics and the Uncertainty of Delays at Signals. Dissertation. Delft University of Technology.

VITI, F. & VAN ZUYLEN, H. [2004]: Modeling Queues at Signalized Intersections. Transportation Research Record, 1883(1), pp.68–77.

VITI, F. & VAN ZUYLEN, H.J. [2009]: The Dynamics and the uncertainty of queues at fixed and actuated controls: A probabilistic approach. Journal of Intelligent Transportation Systems: Technology, Planning, and Operations, 13(1), pp.39–51.

WALTHER, B.A. & MOORE, J.L. [2005]: The concepts a literature with of species richness the performance estimators , of estimator review performance precision. Ecography, 28(July), pp.815–829.

WELCH, G. & BISHOP, G. [2001]: An Introduction to the Kalman Filter. SIGGRAPH 2001, Los Angeles, CA, August 12-17, p.80.

WRIGHT, J.; GARRETT, J.K.; HILL, C.J. & KRUEGER, G.D. [2014]: National Connected Vehicle Field Infrastructure Footprint Analysis, Washington.

ZALZAL, V. [2006]: KFilter - Free C++ Extended Kalman Filter Library. http://kalman.sourceforge.net/. verfügbar unter: http://kalman.sourceforge.net/ [Accessed 22. May 2020].

List of Abbreviations

AI	Artificial Intelligence
ANPR	Automatic Number Plate Recognition
API	Application Programming Interface
AS	Aggregated Section
ATCS	Adaptive Traffic Control Systems
ATMS	Adaptive Traffic Management Systems
AV	Automated Vehicles
BD	Big Data
BSM	Basic Safety Message
CAM	Cooperative Awareness Message
CAV	Connected and Automated Vehicles
CS	Connected Section
CV	Connected Vehicles
DENM	Decentralized Environmental Message
DTM	Dynamic Traffic Management
EKF	Extended Kalman Filter
EO	Extended Observer
EPICS	Enhanced Public Transport Intersection Control Strategy
FCD	Floating Car Data
HGV	Heavy Good Vehicles
ICT	Information and Communication Technologies
IDE	Integrated Development Environment
IoT	Internet of Things

ITS	Intelligent Transportation Systems
KF	Kalman Filter
ML	Machine Learning
MOTION	Method for the Optimization of Traffic Signals in Online Controlled Networks
OD	Origin-Destination
PVD	Probe Vehicle Data
QLE	Queue Length Estimators
REST	Representational State Transfer
RHODES	Real-time, Hierarchical, Optimized, Distributed, and Effective System
RiLSA	Richtlinien für Lichtsignalanlagen
RSU	Roadside Unit
SCATS	Sydney Coordinated Adaptive Traffic System
SCOOT	Split, Cycle and Offset Optimisation Technique
SPAT	Signal Phase And Timing
SPOT	Signal Progression Optimization Technology
TL	Traffic Light
TLC	Traffic Light Controller
TMC	Traffic Message Channel
UTC	Urban Traffic Control
UTCS	Urban Traffic Control Systems
UTOPIA	Urban Traffic OPtimization by Integrated Automation
V2I	Vehicle-to-Infrastructure
VDS	Video Detection Systems
WLAN	Wireless Local Area Network

Table of Figures

List of Tables

Appendix

I. Emerging Technologies for Urban Traffic Control Systems

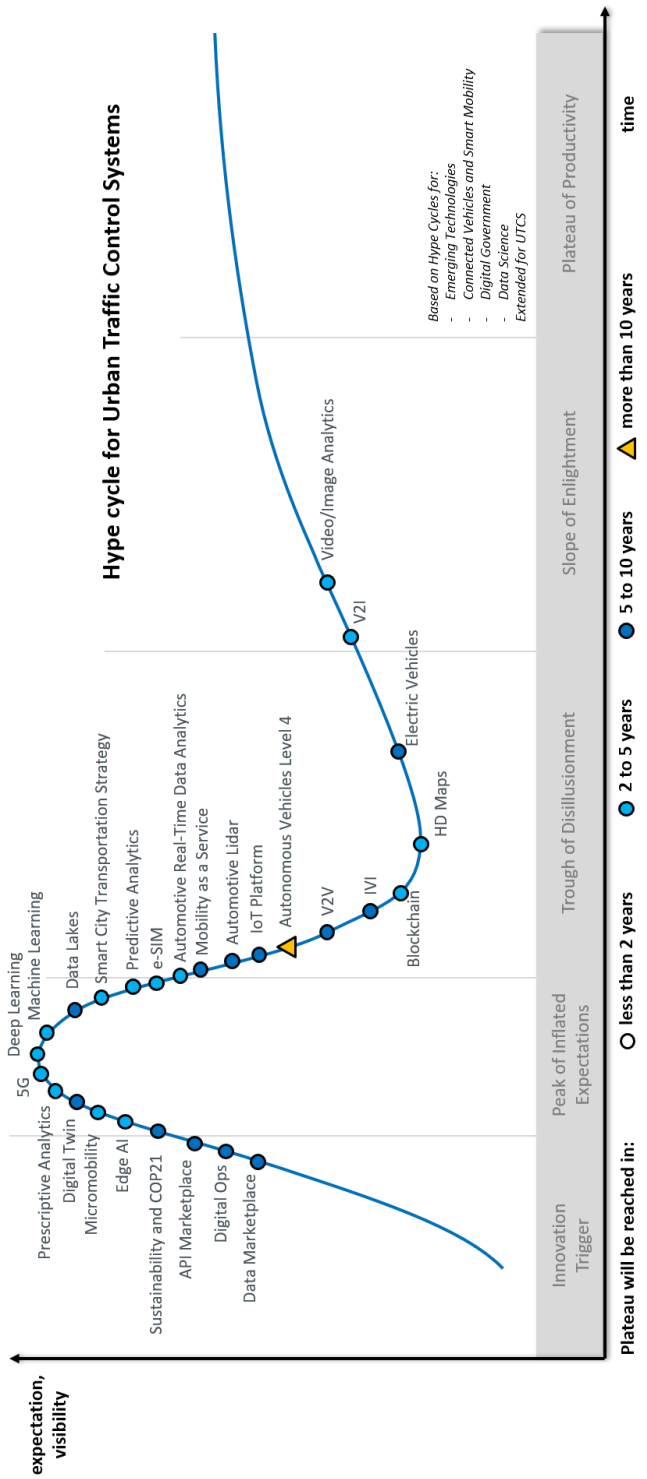

Figure A.1 Hype cycle for Urban Traffic Control Systems

II. Notation Overview

Symbol	Description	Vector/Matrix/Unit:	Definition in:
$\hat{x}_k^-$	A priori estimate	vector	Figure 3.1
$\hat{x}_k$	A posteriori estimate	vector	Figure 3.1
n	Number of state variables	#	Figure 3.1
m	Number of measurements	#	Figure 3.1
x_k	Actual states (never known)	vector	Equation (3.1)
z_k	Actual measurements	vector	Equation (3.2)
k	Current time step	#	Equation (3.1)
$k-1$	Previous time step	#	Equation (3.1)
$f()$	Process vector function	vector	Figure 3.1
u_k	Control input	vector	Equation (3.1)
w_{k-1}	Process noise	vector	Equation (3.1)
Q_k	Process noise covariance	matrix	Figure 3.1
$h()$	Measurement vector function	vector	Figure 3.1
v_k	Measurement noise	vector	Equation (3.2)
R_k	Measurement noise covariance	matrix	Figure 3.1
$A_{k[i,j]}$	Jacobian matrix of $f()$ with respect to x	matrix	Equation (3.3)
$W_{k[i,j]}$	Jacobian matrix of $f()$ with respect to w	matrix	Equation (3.4)
$H_{k[i,j]}$	Jacobian matrix of $h()$ with respect to x	matrix	Equation (3.5)
$V_{k[i,j]}$	Jacobian matrix of $h()$ with respect to v	matrix	Equation (3.6)
$\hat{x}_0$	Initial estimation	vector	Figure 3.1
P_0	Initial error covariance	matrix	Figure 3.1

Symbol	Description	Vector/Matrix/Unit:	Definition in:
P_k^-	A priori estimate error covariance	matrix	Figure 3.1
P_k	A posteriori estimate error covariance	matrix	Figure 3.1
K_k	Kalman gain	matrix	Figure 3.1
x_k^{queue}	Actual queue length (maximum queue at beginning of green)	vehicles	Tab. 3.1
x_k^{arr}	Actual arrival rate	vehicles/second	Tab. 3.1
x_k^{dep}	Actual departure rate	vehicles/second	Tab. 3.1
x_k^{turn}	Actual turning rate	%	Tab. 3.1
x_k^{pen}	Actual penetration rate	%	Tab. 3.1
$z_k^{queue\|CE}$	Queue measurements from all Connected Environments	vector	Tab. 3.2
$z_k^{arr\|CE}$	Arrival rate measurements from all Connected Environments	vector	Tab. 3.2
$z_k^{dep\|CE}$	Departure rate measurements from all Connected Environments	vector	Tab. 3.2
$z_k^{turn\|CE}$	Turning rate measurements from all Connected Environments	vector	Tab. 3.2
$z_k^{pen\|CE}$	Penetration rate measurements from all Connected Environments	vector	Tab. 3.2
z_k^{CS}	Measurements from Connected Section (e.g. camera)	vector	Tab. 3.2
$z_k^{queue\|CS}$	Queue measurements from Connected Section (e.g. camera)	vehicles	Tab. 3.2
$z_k^{arr\|CS}$	Arrival rate measurements from Connected Section (e.g. camera)	vehicles/second	Tab. 3.2
$z_k^{dep\|CS}$	Departure rate measurements from Connected Section (e.g. camera)	vehicles/second	Tab. 3.2
$z_k^{turn\|CS}$	Turning rate measurements from Connected Section (e.g. camera)	%	Tab. 3.2

Symbol	Description	Vector/Matrix/Unit:	Definition in:
z_k^{CV}	Measurements from Connected Vehicles (e.g. V2I)	vector	Tab. 3.2
$z_k^{queue\|CV}$	Queue measurements from Connected Vehicles (e.g. V2I)	vehicles	Tab. 3.2
$z_k^{arr\|CV}$	Arrival rate measurements from Connected Vehicles (e.g. V2I)	vehicles/second	Tab. 3.2
$z_k^{dep\|CV}$	Departure rate measurements from Connected Vehicles (e.g. V2I)	vehicles/second	Tab. 3.2
$z_k^{turn\|CV}$	Turning rate measurements from Connected Vehicles (e.g. V2I)	%	Tab. 3.2
$z_k^{pen\|CV}$	Penetration rate measurements from Connected Vehicles (e.g. V2I)	%	Tab. 3.2
z_k^{DV}	Measurements (from Difference in Velocities) from Aggregated Section (e.g. aggregated FCD), only for queue, as below	vector	Tab. 3.2
$z_k^{queue\|DV}$	Queue measurements (from Difference in Velocities) from Aggregated Section (e.g. aggregated FCD)	vehicles	Tab. 3.2
z_k^{TT}	Measurements (from Travel Time) from Aggregated Section (e.g. aggregated FCD), only for queue, as below	vector	Tab. 3.2
$z_k^{queue\|TT}$	Queue measurements (from Travel Time) from Aggregated Section (e.g. aggregated FCD)	vehicles	Tab. 3.2
CV_k^q	Last queued Connected Vehicle at the start of signal cycle k	-	Figure 3.5
T_k^q	Timestamp from CV_k^q	seconds	Figure 3.5
S_k^q	Location of CV_k^q	meters	Figure 3.5
V_k^q	Speed of CV_k^q	km/h	Figure 3.5
L_k^q	Position of CV_k^q in the queue	#	Figure 3.5
M_k^q	Total number of Connected Vehicles in the queue at the start of signal cycle k	#	Figure 3.5

Symbol	Description	Vector/Matrix/Unit:	Definition in:
$T_k^{crossing}$	Time duration from start of signal cycle k until CV_k^q crosses the stop line	seconds	Figure 3.5
CV_k^j	Last Connected Vehicle that joined the queue during signal cycle k	-	Figure 3.5
T_k^j	Timestamp from CV_k^j	seconds	Figure 3.5
S_k^j	Location of CV_k^j	meters	Figure 3.5
V_k^j	Speed of CV_k^j	km/h	Figure 3.5
L_k^j	Position of CV_k^j in the queue	#	Figure 3.5
M_k^j	Total number of Connected Vehicles in the queue at the end of signal cycle k	#	Figure 3.5
$T_k^{joining}$	Time duration from start of red time of cycle k until CV_k^j joins the queue	seconds	Figure 3.5
CSV_k^q	Last queued vehicle detected by the Connected Section at the start of signal cycle k	-	Figure 3.6
D_k^q	Total number of vehicles in range departing the queue	#	Figure 3.6
C_k^{CS}	Coverage (range) of Connected Section	#	Figure 3.6
CSV_k^j	Last vehicle detected by the Connected Section that joined the queue during signal cycle k	-	Figure 3.6
A_k^j	Total number of vehicles in range, joining the queue	#	Figure 3.6
S_k^{DV}	The distance between the end of the congested section and the stop line	meters	Figure 3.7
L_k^{DV}	The number of vehicles in queue, based on the deviations in speed	#	Figure 3.7
G	Green time duration of the examined signal.	seconds	pp.78
C	Cycle time duration.	seconds	pp.78

Symbol	Description	Vector/Matrix/Unit:	Definition in:
G/C	Green split of the examined signal: ration of G/C	%	pp.78
D	Average vehicle delay	seconds	pp.78
S	Average number of stops	#	pp.78
QCT	Queue clearing time	minutes	pp.78
$CI_{(1-alpha)\%}$	Confidence interval for minimum number of simulation runs	%	Equation (5.3)
s_d	Standard deviation of average vehicle delays from simulation runs	sec	Equation (5.3)
$t_{(1-alpha/2),N-1}$	Student's t-statistic	%	Equation (5.3)
N	Number of simulation runs	#	pp.78
CI/s_d	Desired confidence range	#	pp.78

Tab. A.1 Basic notation overview

III. Test intersection

EKF Parameter	EO Starting values and adaptive configuration with minimum assumptions				
	Departure Rate (vehicles/sec)	**Arrival Rate (vehicles/sec)**	**Queue Length (vehicles)**	**Turning Rate**	**Penetration Rate**
$\hat{x}_0$	0.50	0.20	3.00	0.50	0.01
P_0	0.10^2	0.10^2	1.00^2	0.10^2	0.10^2
$\hat{x}_k$	Equation (3.9)	Equation (3.10)	Equation (3.12)	Like equation (3.9)	Like equation (3.9)
Q_k	0.10^2	0.10^2	Equation (4.1): $Q_{k-1}^{queue} = \hat{x}_{k-1}^{queue}$ (4.2)	0.10^2	0.10^2
R_k	0.10^2	0.10^2	Equation (4.2): $R_k^{queue\|CV} = Q_{k-1}^{queue\|CV}(1 - \hat{x}_{k-1}^{pen})$ Equation (4.3): $R_k^{queue\|TT} = Q_{k-1}^{queue} * 0.10$ $R_k^{queue\|DV} = Q_{k-1}^{queue} * 0.10$ $R_k^{queue\|CS} = \begin{cases} 1.00^2 & , in\ range \\ QueueCapacity^2 & , out\ of\ range \end{cases}$	0.10^2	0.10^2

Tab. A.2 Starting values and adaptive configuration of the EO for the test intersection

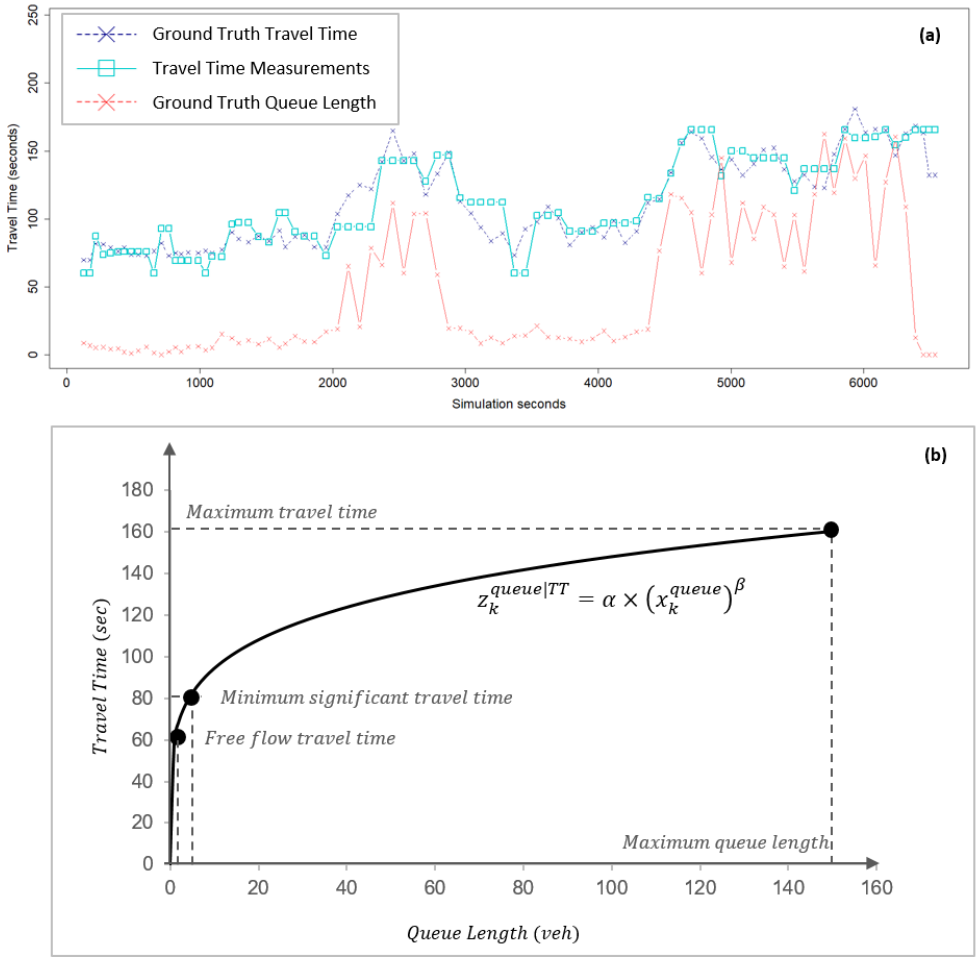

Figure A.2 Approximate travel time and queue length correlation

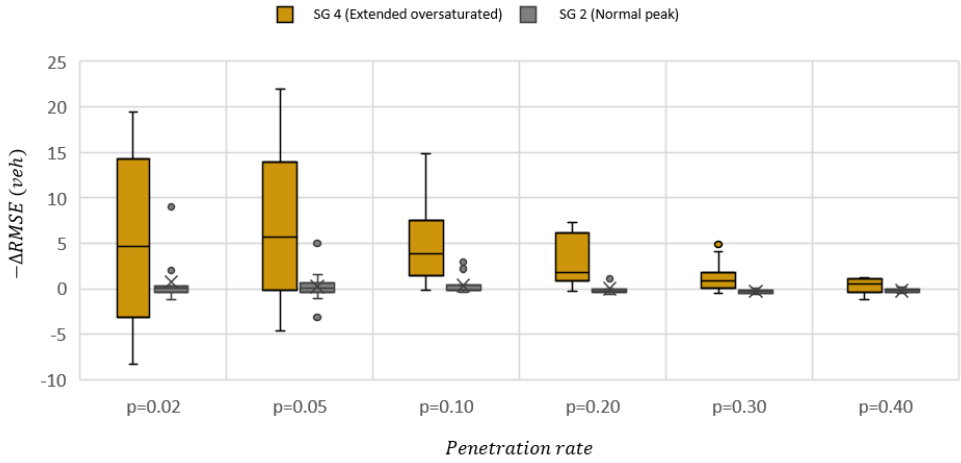

Figure A.3 Error reduction - SG 4 extended oversaturated and SG 2 normal peak

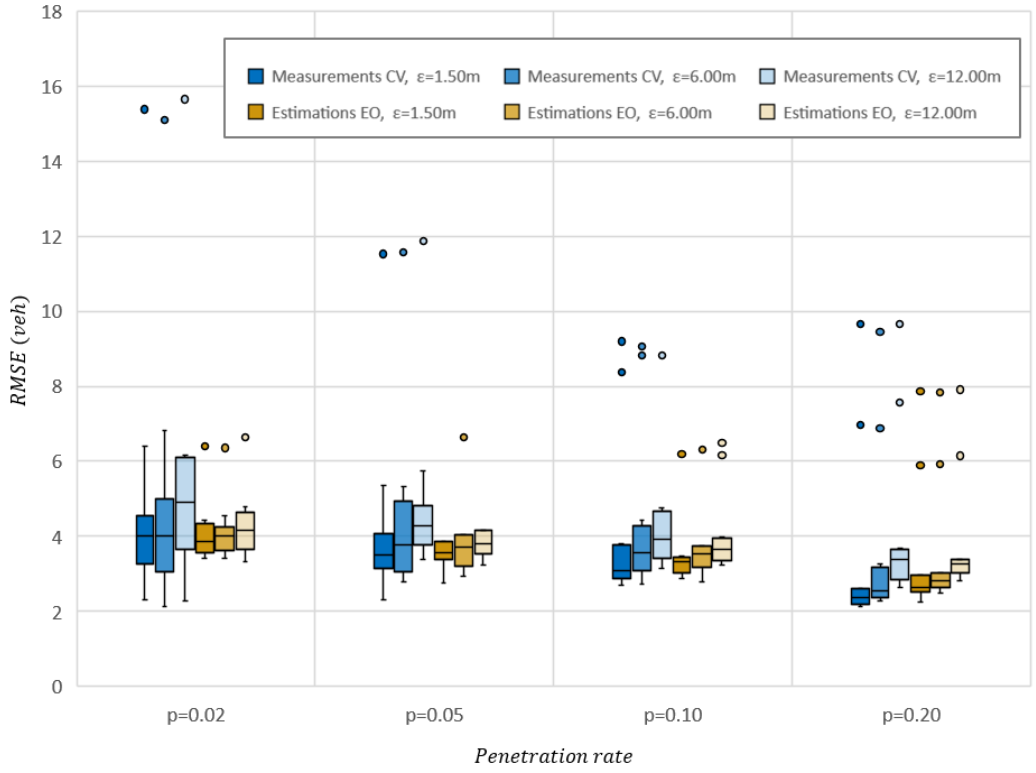

Figure A.4 Error reduction - Measurements with additional errors - SG 4

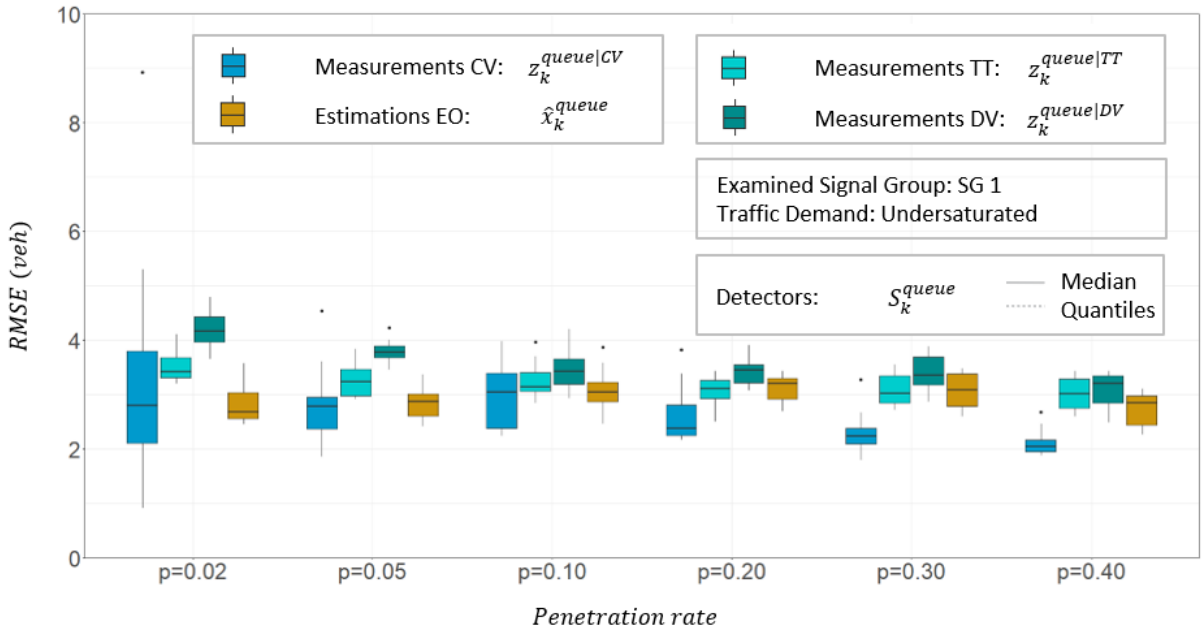

Figure A.5 Fused estimations for various penetration rates - SG 1

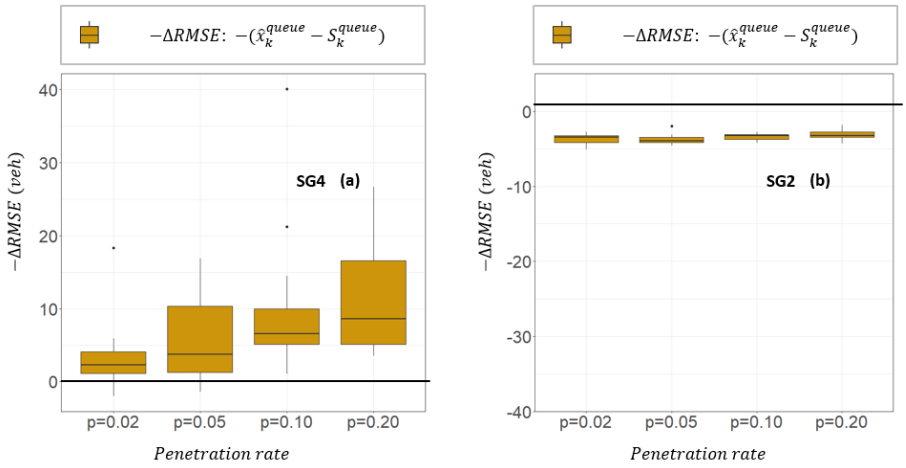

Figure A.6 Comparison of Extended Observer with estimation from inductive loop detection

Penetration rate of CV (p)	RMSE (veh)		Error Reduction	
	$\overline{RMSE \mid z_n^{queue\mid CV}}$	$\overline{RMSE \mid \hat{x}_k^{queue}}$	$\overline{\Delta RMSE}$	p_value
p = 0.02	21.65	18.05	*-3.60	0.00342
p = 0.05	22.99	17.68	*-5.31	0.00583
p = 0.10	26.75	16.42	*-10.33	0.00024
p = 0.20	28.02	16.42	*-11.60	0.00027

*statistically significant reduction: $N = 12,\ CI_{(1-alpha)\%} = 95\%, {}^{CI}/_{s_d} = 2,\ s_d < 5\ seconds$

Tab. A.3 Comparison of Extended Observer with inductive loop detection - SG 4 extended oversaturated peak

Penetration rate of CV (p)	RMSE (veh)		Error Reduction	
	$\overline{RMSE \mid z_n^{queue\mid CV}}$	$\overline{RMSE \mid \hat{x}_k^{queue}}$	$\overline{\Delta RMSE}$	p_value
p = 0.02	1.69	5.38	*+3.68	2.16e-09
p = 0.05	1.88	5.63	*+3.76	8.65e-10
p = 0.10	1.50	4.90	*+3.40	1.30e-11
p = 0.20	2.10	5.21	*+3.11	6.78e-09

*statistically significant reduction: $N = 12,\ CI_{(1-alpha)\%} = 95\%, {}^{CI}/_{s_d} = 2,\ s_d < 5\ seconds$

Tab. A.4 Comparison of Extended Observer with inductive loop detection - SG 2 normal peak

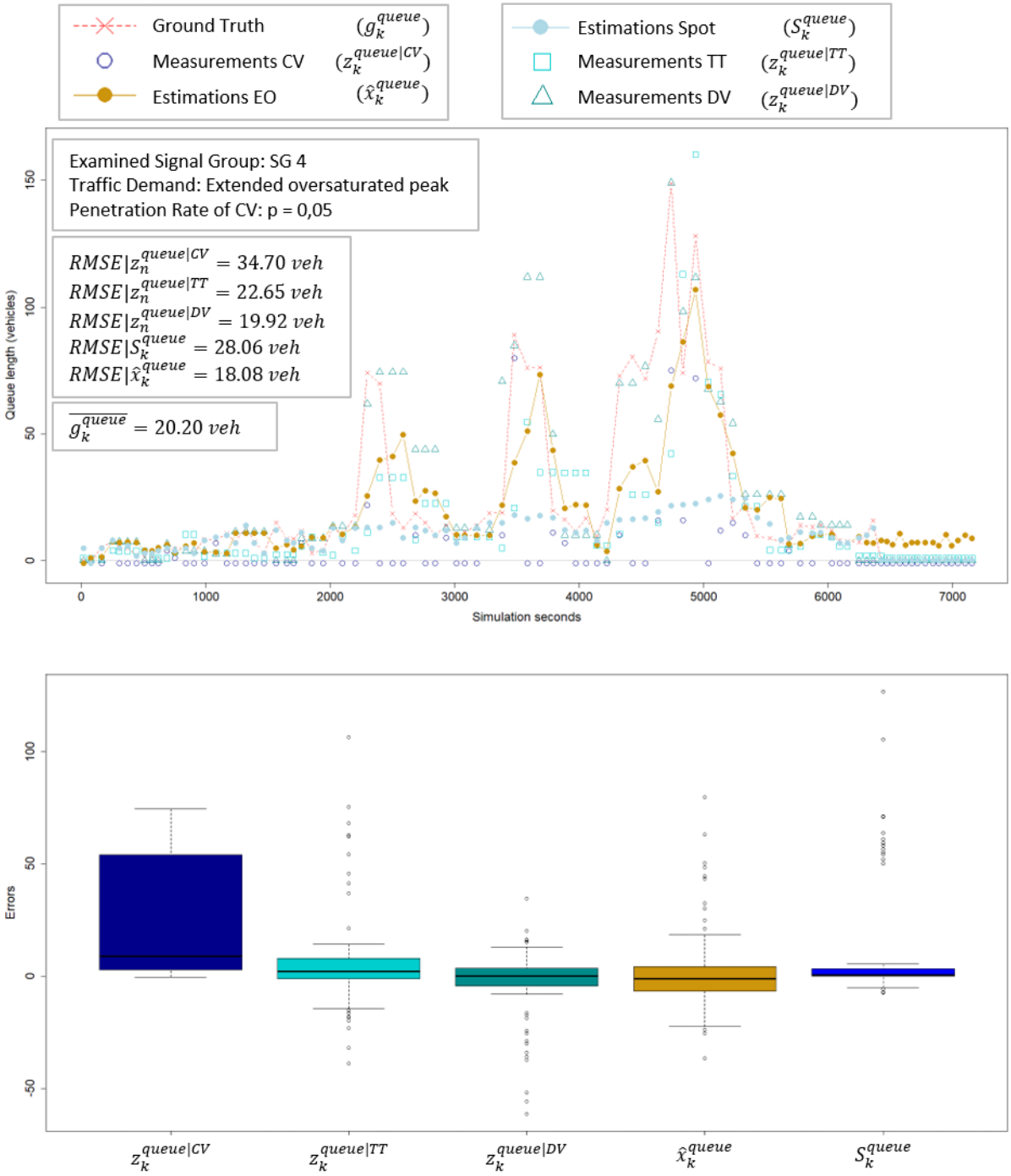

Figure A.7 Fused estimation from Extended Observer, mobile measurements and loop-based measurements - SG 4 extended oversaturated peak

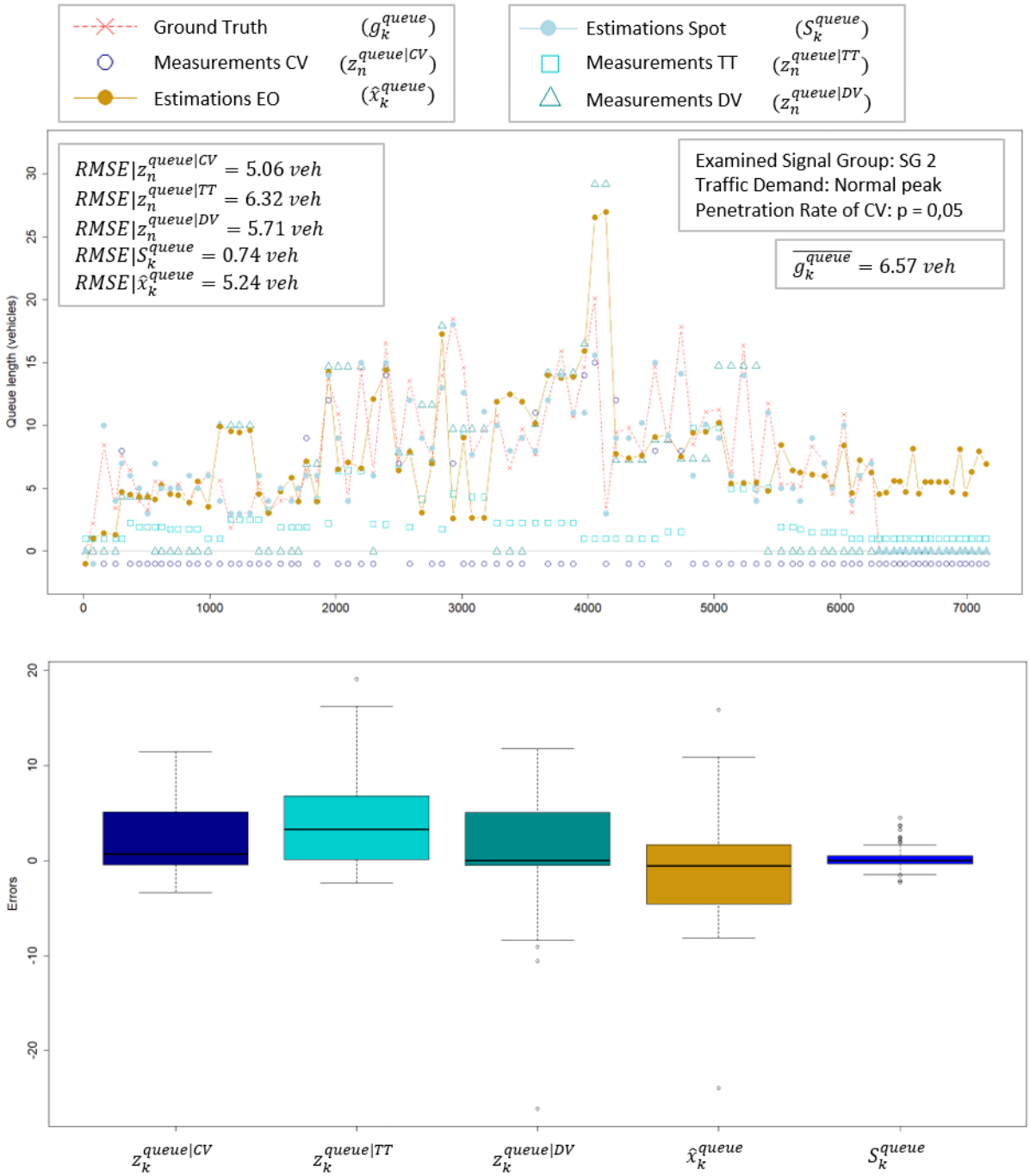

Figure A.8 Fused estimation from Extended Observer, mobile measurements and loop-based measurements - SG 2 normal peak

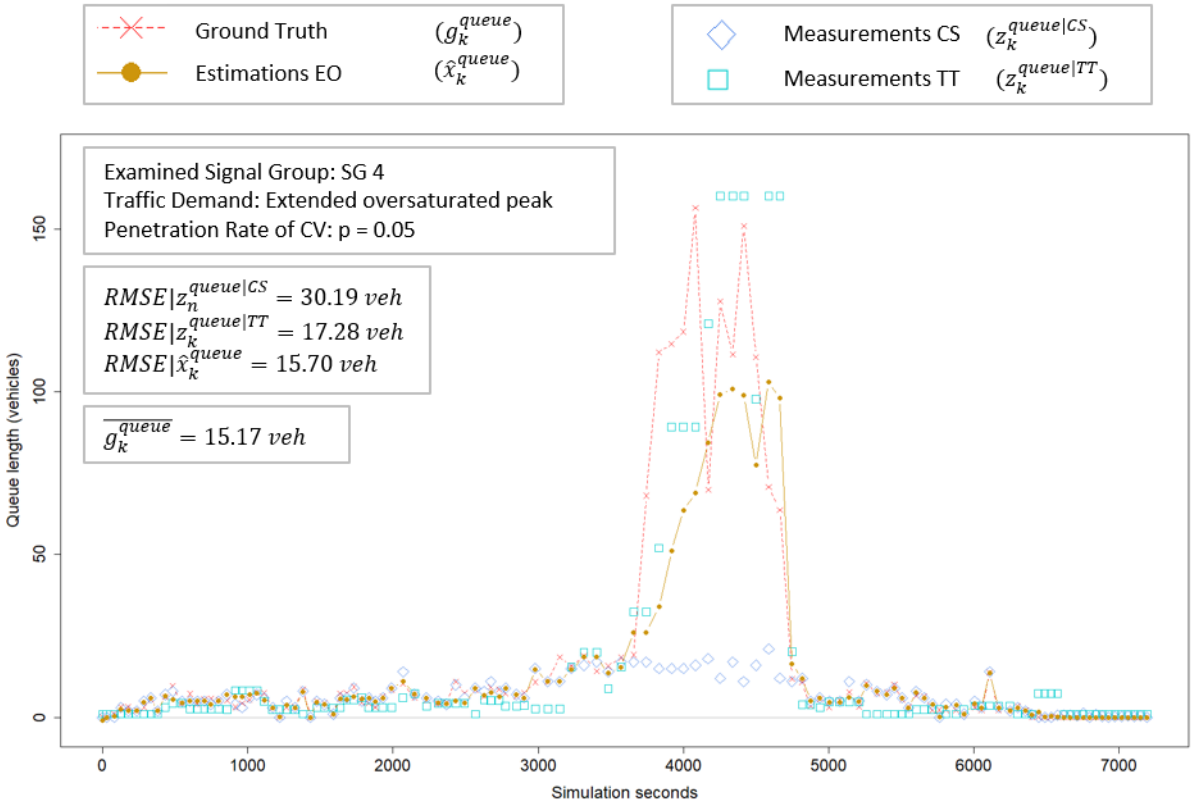

Figure A.9 Fused estimations from the Extended Observer based on camera and travel times

Penetration rate of CV (p)	Legacy signal control			EO feeding the legacy signal control						Difference from legacy signal control input		
				$\hat{x}_k^{queue(CV)}$			$\hat{x}_k^{queue(CV+AS)}$					
	(sec)	(sec)	(%)	(sec)	(sec)	(%)	(sec)	(sec)	(%)	p_value	p_value	p_value
	$\overline{G_L}$	$\overline{C_L}$	$\overline{G/C_L}$	$\overline{G_{EO}^{CV}}$	$\overline{C_{EO}^{CV}}$	$\overline{(G/C)_{EO}^{CV}}$	$\overline{G_{EO}^{CV+AS}}$	$\overline{C_{EO}^{CV+AS}}$	$\overline{(G/C)_{EO}^{CV+AS}}$	$\overline{\Delta G}$	$\overline{\Delta C}$	$\overline{\Delta(G/C)}$
p = 0.02	42	66	63	38	**64	57	*39	63	*60	0.0181	0.0359	3.9e-09
p = 0.05				40	**66	59	*41	67	*61	0.0040	0.0261	7.0e-07
p = 0.10				39	**65	59	*43	69	*61	0.0002	0.0109	1.1e-08
p = 0.20				40	**66	60	*43	70	*61	0.0202	0.0002	2.5e-06

*statistically significant reduction of difference to legacy: $N = 12,\ CI_{(1-alpha)\%} = 95\%, {}^{CI}/_{s_d} = 2,\ s_d < 5\ seconds$

**statistically significant increase of difference to legacy: $N = 12,\ CI_{(1-alpha)\%} = 95\%, {}^{CI}/_{s_d} = 2,\ s_d < 5\ seconds$

Tab. A.5 Improved legacy signal control input through additional measurements

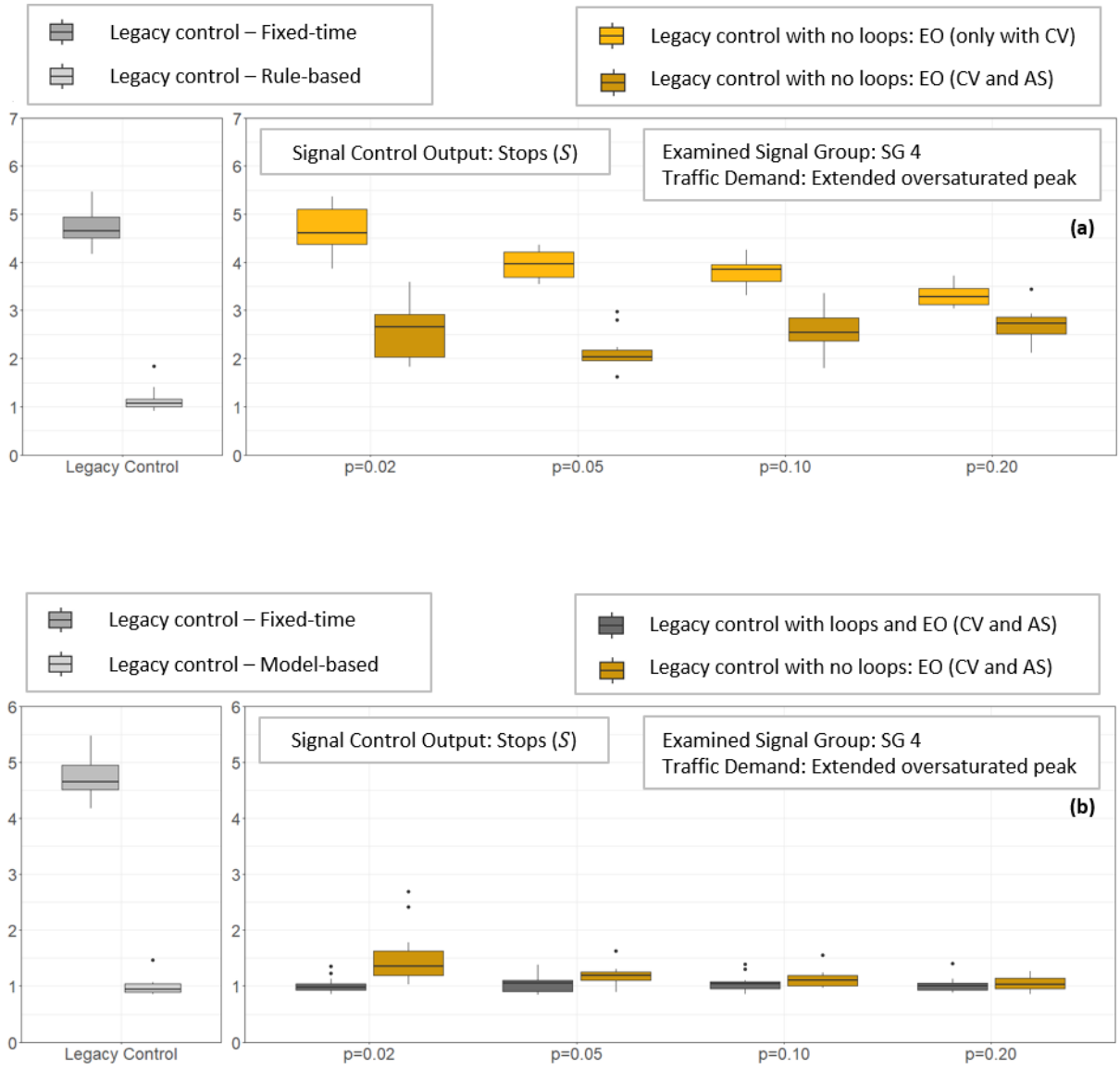

Figure A.10 Legacy signal control output with fused estimations from the Extended Observer - stops

Penetration rate of CV (p)	Delay (sec)		Delay Reduction		
	$\overline{D_{EO}^{CV}}$	$\overline{D_{EO}^{CV+AS}}$	$\overline{\Delta D\%}$	$\overline{\Delta D}$	p_value
p = 0.02	64.26	42.35	*-34.11%	*-21.92	1.19e-06
p = 0.05	57.10	38.22	*-33.06%	*-18.88	1.08e-09
p = 0.10	55.49	42.83	*-22.81%	*-12.66	4.00e-07
p = 0.20	50.47	44.07	*-22.81%	*-6.40	0.00022

*statistically significant reduction: $N = 12,\ CI_{(1-alpha)\%} = 95\%, {CI}/{s_d} = 2,\ s_d < 5\ seconds$

Tab. A.6 Signal control output with fused estimations from the Extended Observer - comparison with Connected Vehicles - delays

Penetration rate of CV (p)	Stops		Stops Reduction		
	$\overline{S_{EO}^{CV}}$	$\overline{S_{EO}^{CV+AS}}$	$\overline{\Delta S\%}$	$\overline{\Delta S}$	p_value
p = 0.02	4.67	2.57	*-45.10%	*-2.10	1.09e-06
p = 0.05	3.98	2.15	*-46.05%	*-1.83	1.09e-09
p = 0.10	3.79	2.59	*-31.57%	*-1.20	1.23e-06
p = 0.20	3.32	2.69	*-19.11%	*-0.64	0.00267

*statistically significant reduction: $N = 12,\ CI_{(1-alpha)\%} = 95\%, {CI}/{s_d} = 2,\ s_d < 5\ seconds$

Tab. A.7 Signal control output with fused estimations from the Extended Observer - comparison with Connected Vehicles - stops

Penetration rate of CV (p)	Delay (sec) $\overline{D_L^M}$	$\overline{D_{EO}^{CV+AS}}$	Delay Increase $\overline{\Delta D\%}$	$\overline{\Delta D}$	p_value
p = 0.02	25.15	32.15	*+27.85%	*+7.00	0.0005
p = 0.05		28.38	*+12.86%	*+3.32	4.711e-05
p = 0.10		27.43	*+9.06%	*+2.28	1.326e-05
p = 0.20		26.50	*+5.40%	*+1.36	0.0046

*statistically significant increase: $N = 12,\ CI_{(1-alpha)\%} = 95\%, {CI}/{s_d} = 2,\ s_d < 5\ seconds$

Tab. A.8 Signal control output with fused estimations from the Extended Observer - comparison with full detection model-based - delays

Penetration rate of CV (p)	Stops $\overline{S_L^M}$	$\overline{S_{EO}^{CV+AS}}$	Stops Increase $\overline{\Delta S\%}$	$\overline{\Delta S}$	p_value
p = 0.02	1.00	1.53	*+53.35%	*+0.53	0.0064
p = 0.05		1.19	*+19.26%	*+0.19	0.0003
p = 0.10		1.13	*+13.40%	*+0.13	0.0002
p = 0.20		1.04	*+4.94%	*+0.05	0.1098

*statistically significant increase: $N = 12,\ CI_{(1-alpha)\%} = 95\%, {CI}/{s_d} = 2,\ s_d < 5\ seconds$

Tab. A.9 Signal control output with fused estimations from the Extended Observer - comparison with full detection model-based - stops

Penetration rate of CV (p)	Delay (sec) $\overline{D_L^F}$	$\overline{D_{EO}^{CV+AS}}$	Delay Reduction $\overline{\Delta D\%}$	$\overline{\Delta D}$	p_value
p = 0.02	66.16	32.15	*-51.41%	*-34.01	2.415e-10
p = 0.05		28.38	*-57.11%	*-37.78	1.302e-12
p = 0.10		27.43	*-58.55%	*-38.74	6.563e-13
p = 0.20		26.50	*-59.94%	*-39.66	9.342e-14

*statistically significant reduction: $N = 12,\ CI_{(1-alpha)\%} = 95\%, {}^{CI}/_{S_d} = 2,\ s_d < 5\ seconds$

Tab. A.10 Signal control output with fused estimations from the Extended Observer - comparison with fixed-time - delays

Penetration rate of CV (p)	Stops $\overline{S_L^F}$	$\overline{S_{EO}^{CV+AS}}$	Stops Reduction $\overline{\Delta S\%}$	$\overline{\Delta S}$	p_value
p = 0.02	4.72	1.53	*-67.67%	*-3.19	3.056e-10
p = 0.05		1.19	*-74.86%	*-3.53	2.47e-12
p = 0.10		1.13	*-76.09%	*-3.59	1.322e-12
p = 0.20		1.04	*-77.88%	*-3.68	1.307e-13

*statistically significant reduction: $N = 12,\ CI_{(1-alpha)\%} = 95\%, {}^{CI}/_{S_d} = 2,\ s_d < 5\ seconds$

Tab. A.11 Signal control output with fused estimations from the Extended Observer - comparison with fixed-time - stops

IV. Real-world intersection

EKF Parameter	EO Starting values and adaptive configuration with minimum assumptions					
	Approach Departure Rate (vehicles/sec)			Lane Arrival Rate (vehicles/sec)	Queue Length (vehicles)	Turning Rate	Penetration Rate
$\hat{x}_0$	0.50			0.20	3.00	0.50	0.01
P_0	0.10^2			0.10^2	1.00^2	0.10^2	0.10^2
$\hat{x}_k$	Equation (3.9)			Equation (3.10) and equation (3.25)	Equation (3.12)	Like equation (3.9)	Like equation (3.9)
${}^*x_k^{hist}$	**SG 1**	**SG 2**	**SG 7**	-	-	-	-
	0.79	0.78	0.86				
Q_k	0.10^2			0.10^2	Equation (4.1): $Q_{k-1}^{queue} = \hat{x}_{k-1}^{queue}$ (4.2)	0.10^2	0.10^2
R_k	0.10^2			0.10^2	Equation (4.2): $R_k^{queue\|CV} = Q_{k-1}^{queue\|CV}(1 - \hat{x}_{k-1}^{pen})$ Equation (4.3): $R_k^{queue\|TT} = Q_{k-1}^{queue} * 0.10$ $R_k^{queue\|DV} = Q_{k-1}^{queue} * 0.10$ $R_k^{queue\|CS} = \begin{cases} 1.00^2 & , in\ range \\ QueueCapacity^2 & , out\ of\ range \end{cases}$	0.10^2	0.10^2

Tab. A.12 Starting values and adaptive configuration of the Extended Observer for real-world intersection.

${}^*x_k^{hist}$: Historical values for departure rate are according to the Spot/Utopia real configuration and only according to topology. Historical values for turning rates of 0.50 are used as baselines to emulate no previous knowledge of turning rates.

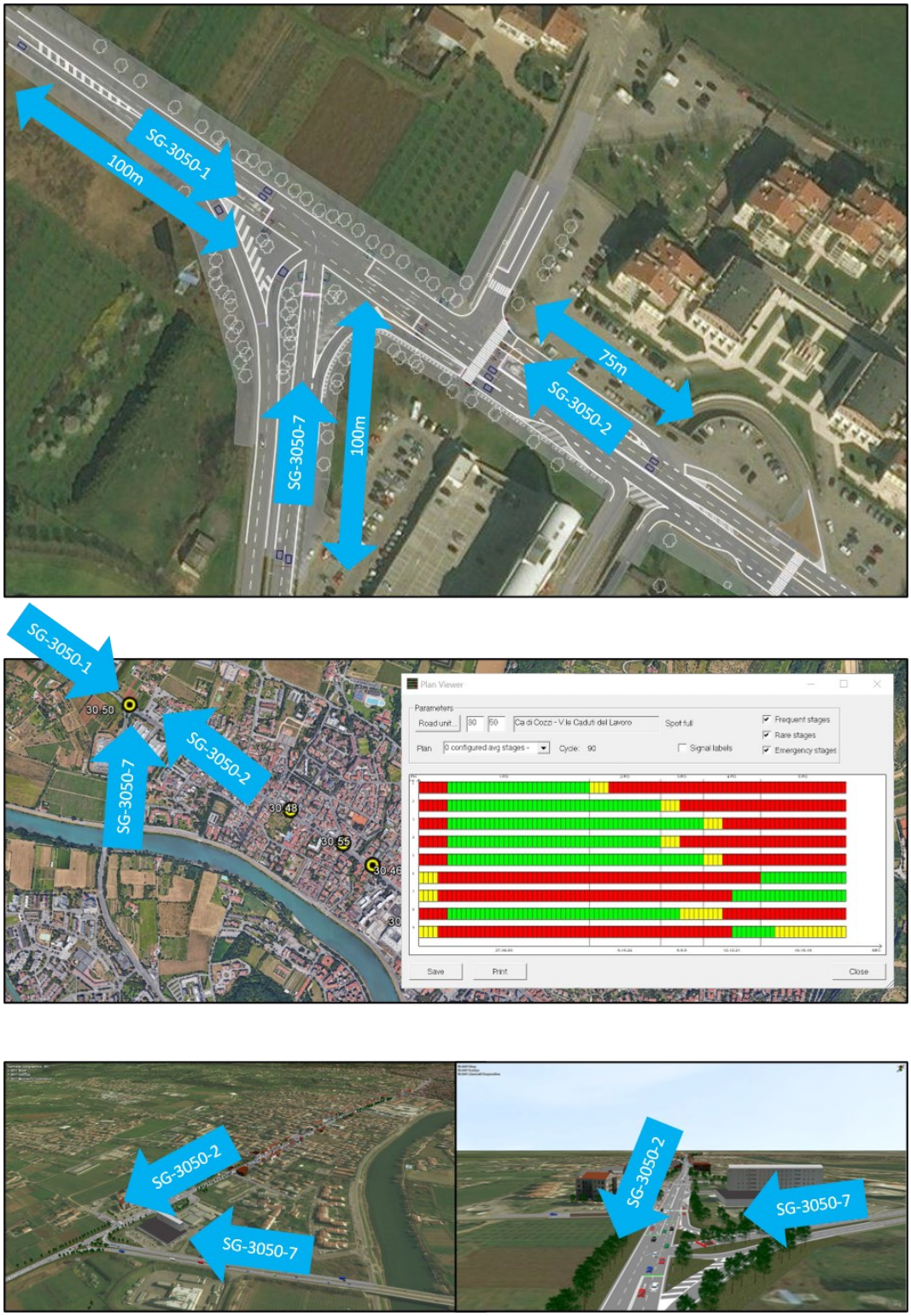

Figure A.11 Topology and configuration for real-world intersection

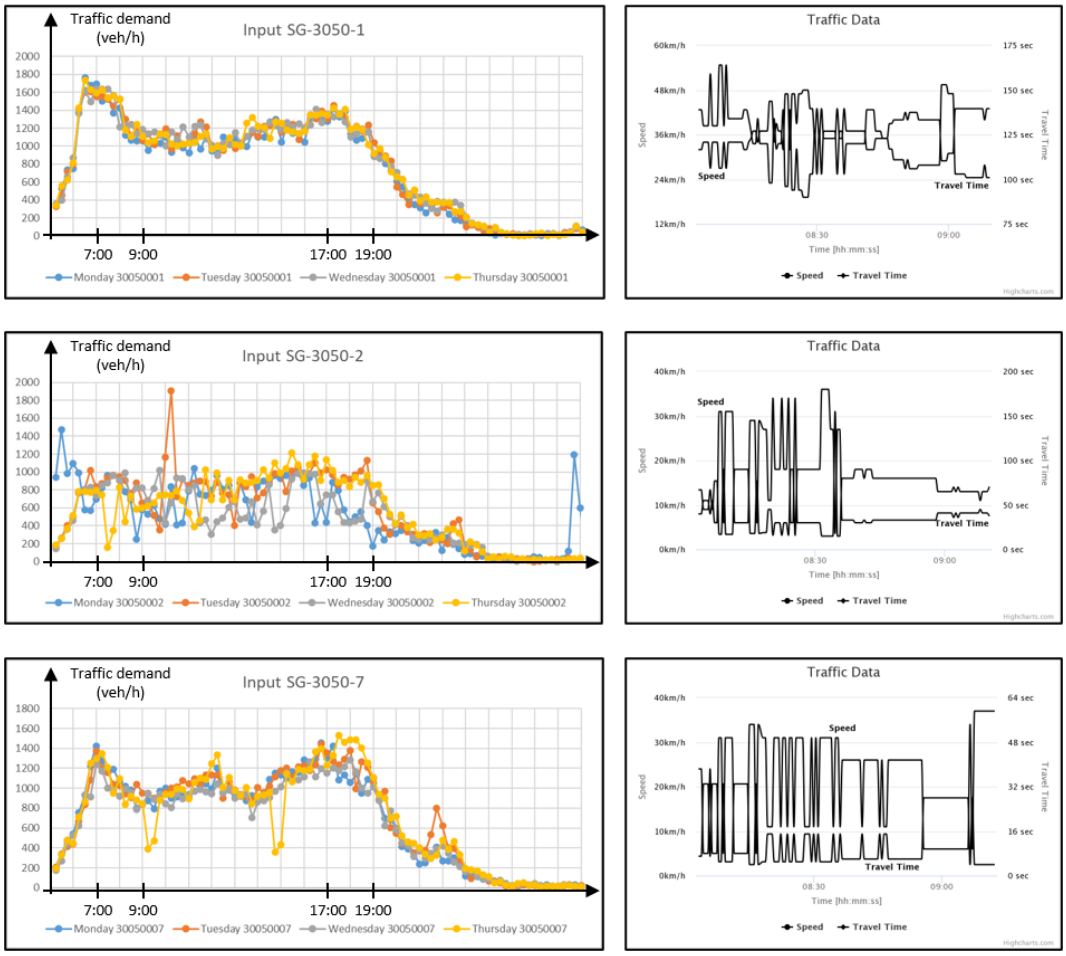

Figure A.12 Indicative data sets for the calibration and validation

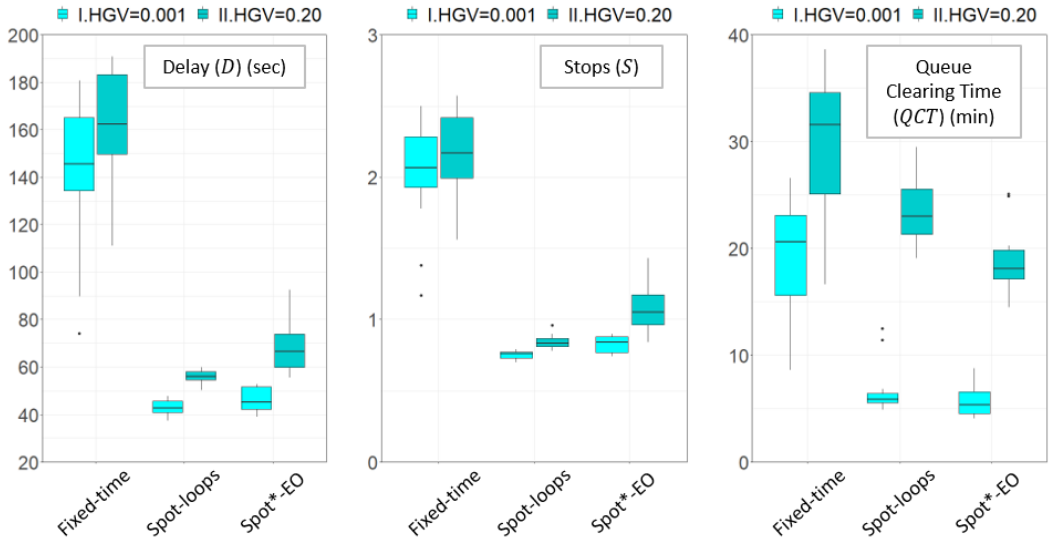

Figure A.13 Signal control output for real-world intersection - Spot with Extended Observer - extreme truck percentage

p=0.02, 07:00-8:45				Spot with full detection		Spot with EO and extended maximum green	
Delay (sec)				**Delay increase from HGV**		**Delay increase from HGV**	
$\overline{D_{Spot}^{HGV\_0.001}}$	$\overline{D_{Spot}^{HGV\_0.20}}$	$\overline{D_{Spot\|EO}^{HGV\_0.001}}$	$\overline{D_{EO}^{HGV\_0.20}}$	$\overline{\Delta D\%}$	$\overline{\Delta D}$	$\overline{\Delta D\%}$	$\overline{\Delta D}$
43.01	55.78	45.84	67.78	*+29.68%	*+12.77	*+47.88%	*+21.95
Stops				**Stops increase from HGV**		**Stops increase from HGV**	
$\overline{S_{Spot}^{HGV\_0.001}}$	$\overline{S_{Spot}^{HGV\_0.20}}$	$\overline{S_{Spot\|EO}^{HGV\_0.001}}$	$\overline{S_{EO}^{HGV\_0.20}}$	$\overline{\Delta S\%}$	$\overline{\Delta S}$	$\overline{\Delta S\%}$	$\overline{\Delta S}$
0.75	0.85	0.83	1.08	*+12.92%	*+0.10	*+30.21%	*+0.25
Queue Clearing Time (min)				**Queue Clearing Time increase from HGV**		**Queue Clearing Time increase from HGV**	
$\overline{CT_{Spot}^{HGV\_0.001}}$	$\overline{CT_{Spot}^{HGV\_0.20}}$	$\overline{CT_{Spot\|EO}^{HGV\_0.001}}$	$\overline{CT_{EO}^{HGV\_0.20}}$	$\overline{\Delta D\%}$	$\overline{\Delta D}$	$\overline{\Delta D\%}$	$\overline{\Delta D}$
6.8	20.7	5.8	18.9	*+203%	13.8	*+224%	13.1

*statistically significant reduction: $N = 12,\ CI_{(1-alpha)\%} = 95\%, {}^{CI}/_{s_d} = 2,\ s_d < 11\ seconds$

Tab. A.13 Signal control output for real-world intersection - Spot with Extended Observer - extreme truck percentage

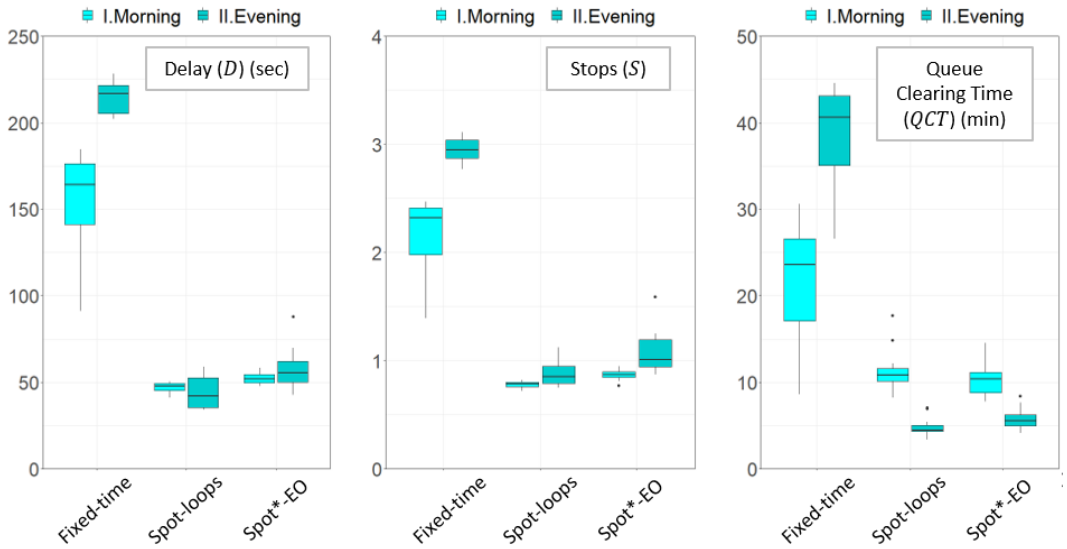

Figure A.14 Signal control output for real-world intersection - Spot with Extended Observer - extreme peaks